

The copyright of this thesis vests in the author. No quotation from it or information derived from it is to be published without full acknowledgement of the source. The thesis is to be used for private study or non-commercial research purposes only.

Published by the University of Cape Town (UCT) in terms of the non-exclusive license granted to UCT by the author.

# The Optimal Placement of Phasor Measurement Units and Their Effects on State Estimation

Prepared for

**Dr S. Chowdhury**

**A/Prof S.P. Chowdhury**

**The University of Cape Town**

Prepared by

**William Yuill**

**YLLWIL001**



**Dissertation submitted to the Faculty of Electrical Engineering at the University of Cape  
Town in fulfilment of the requirements for the degree of**

**Master of Science**

**In**

**Electrical Engineering**

**31 August, 2011**

**Key Words: Phasor Measurement Unit, Integer Linear Programming, State Estimation**

## Declaration

I know the meaning of plagiarism and declare that all the work in the document, save for that which is properly acknowledged, is my own.

This work is submitted to the Department of Electrical Engineering, University of Cape Town, in fulfilment of the requirements for the degree: Masters of Science in Electrical Engineering, and has not been submitted for any other academic purposes.

William Yuill

University of Cape Town

Rondebosch

Cape Town

31 August 2011

University of Cape Town

## Acknowledgements

I would like to thank the following people who assisted me throughout the course of this project:

To Professor Chowdhury and Doctor Chowdhury, thank you for your guidance, interest, open door policy and financial support. Thank you for giving me the platform to travel to conferences and develop my research, networking and presenting skills.

To Dad and Mom, thank you for always supporting, listening and guiding me when the chips are down. I always appreciate it. To Pete and Bob, thanks for being awesome.

To Grace, thank you for your support and for putting up with me while I have been working and listening to me talk about PMUs for extended lengths of time.

University of Cape Town

## Abstract

The electric power system is on the verge of a significant transformation. Modern technology is providing many improved and new options for operation, monitoring and control of the power system. Phasor measurement units (PMUs) are a key technology to be used for as a backbone for sensing and measurement and to improve interface and decision support by utilising instantaneous PMU data. This data will drive faster simulations and advanced visualisation tools that will help system operators assess dynamic challenges to system stability. Therefore, the number of PMUs placed in a system should be minimized so that the PMU deployment is the most cost effective. However there should be a significant enough number of PMUs to maintain full system observability of all the buses in the system. This brings about a trade off between a minimum number of PMUs and the observability of system buses.

Due to the fact that PMUs directly measure voltage and current magnitude and phase angle creates the possibility of improving conventional state estimation (CSE) techniques. The incorporation of PMU measurement data is expected to bring about benefits to applications of the energy management system (EMS) such as: Post-disturbance analysis; inter-area oscillation monitoring, analysis and control; state estimation and improved observability; power plant monitoring and integration; bad data detection and real-time monitoring and control.

Therefore, this work consists of two main objectives. The first objective is to investigate and develop a method for the algorithmic placement of a minimum number of PMUs into a system to ensure full observability. The second objective is to investigate and develop a conventional, hybrid and linear state estimation techniques to incorporate and utilize PMU measurement data to perform state estimation and to study the effects that differing PMU placement positions have on the accuracy of the resultant state estimator solution. The developed methods are to be tested on IEEE 14, 30 and 57 test bus systems. The accuracy of the state estimator solution will be assessed using complex power flow and voltage errors.

This work was able to find minimum PMU placement numbers that correspond to previous best results of minimum placement in the literature for various IEEE test bus systems. The PMU placement positions were used as optimal locations for investigating the impact that PMUs have on the accuracy of state estimation. The results indicate that complex power flow and voltage errors improve as the number of PMUs increase. A linear state estimator converges to a solution in the shortest time and gives the lowest complex power flow and voltage errors for the test systems used in this work. Some placement positions and PMU phasing schemes are more beneficial than others, and this work found the placement and phasing schemes that best improved the accuracy of state estimation.

# Table of Contents

Declaration.....	i
Acknowledgements.....	ii
Abstract.....	iii
List of figures.....	vii
List of graphs.....	viii
List of tables.....	ix
Nomenclature.....	xi
1. Chapter 1: Phasor measurement unit pertinence and placement.....	1
1.1. Introduction.....	1
1.1.1. South Africa’s plan to utilize PMUs.....	1
1.1.2. Phasor measurement unit historical overview.....	2
1.1.3. Phasor measurement unit definition.....	2
1.1.4. Importance of PMU technology.....	4
1.1.5. PMU equipped system compared to SCADA equipped system.....	5
1.1.6. The basics of a generic phasor measurement unit.....	6
1.1.7. Hierarchy for phasor measurement unit systems.....	7
1.1.8. Communication link options for phasor measurement units.....	8
1.2. Phasor measurement unit placement in a power system networks.....	9
1.2.1. Observability.....	10
1.2.2. Minimum PMU placement.....	10
1.2.3. Redundancy.....	10
1.2.4. Zero-injection buses.....	11
1.2.5. Phasing.....	12
1.2.6. Outage of a PMU and/or communication line.....	12
1.2.7. Depth of unobservability.....	12
1.2.8. Test bus systems.....	13
2. Chapter 2: PMU Placement literature review.....	15
2.1. Meta-Heuristic Methods.....	15
2.1.1. Genetic Algorithm.....	15
2.1.2. Tree search and topology.....	19
2.1.3. Particle Swarm Optimization.....	21
2.1.4. Binary search.....	23
2.2. Deterministic techniques.....	25

2.2.1.	Integer linear programming.....	25
2.3.	Summary of literature review.....	28
3.	Chapter 3: Integer linear programming method.....	31
3.1.	Integer programming method development.....	31
3.1.1.	Dealing with zero-injection buses.....	33
3.1.2.	Loss of measurement.....	34
3.1.3.	Placement results for test bus positions.....	36
4.	Chapter 4: Utilising PMU measurement data to improve state estimation:.....	38
4.1.	Process of State Estimation.....	38
4.2.	Component modelling and assumptions.....	39
4.2.1.	Transmission lines.....	39
4.2.2.	Transformers.....	40
4.2.3.	Shunt capacitors or reactors.....	41
4.2.4.	Generators and loads.....	41
4.2.5.	Expression of current in rectangular co-ordinates.....	41
4.2.6.	The bus-admittance matrix.....	42
4.3.	The mathematical modeling of state estimation.....	43
4.3.1.	Measurement functions $\mathbf{h}(\mathbf{x})$ and $\mathbf{Hx}$ .....	45
4.4.	Controlled test metrics.....	47
4.4.1.	Accuracy metrics.....	48
4.4.2.	Convergence criteria.....	49
4.5.	Literature review of incorporating PMU measurements into state estimators.....	50
4.5.1.	Summary of state estimator literature review.....	51
4.6.	Hybrid and linear state estimation models.....	52
4.6.1.	Standard State Estimator combined with PMUs (Hybrid state estimator).....	52
4.6.2.	Polar to Cartesian co-ordinate transformation.....	53
4.6.3.	Linear state estimation model.....	54
4.6.4.	Measurement errors.....	54
4.7.	Model applied to a 4 bus test scenario.....	56
4.7.1.	Conventional state estimator.....	56
4.7.2.	Hybrid state estimator.....	61
4.7.3.	Linear state estimator.....	64
5.	Chapter 5: Results of state estimation using optimal placement positions from ILP algorithm ..	69
5.1.	Algorithm applied to the IEEE 14 bus system.....	69

5.2.	Algorithm applied to the IEEE 30 bus system .....	72
5.3.	Algorithm applied to the IEEE 57 bus system .....	75
5.4.	Comparison of computational time for CSE, HSE and LSE .....	78
5.5.	Linear state estimator applied to IEEE 57 bus system .....	78
5.6.	Variation of resulting errors within specific bus test systems .....	82
5.7.	Phasor measurement unit phasing .....	82
6.	Chapter 6: Conclusions and future work .....	84
6.1.	Conclusions .....	84
6.2.	Future work.....	85
6.2.1.	Bettering the ILP placement algorithm .....	85
6.2.2.	Synergy of theory and implementation .....	85
6.2.3.	Improvement of the state estimator .....	85
6.2.4.	Theoretical system shortcomings .....	86
	References .....	87
	Bibliography .....	90
	Appendix A.....	91

University of Cape Town

## List of figures

Figure 1: Representation of a sinusoidal signal .....	3
Figure 2: Representation of a sinusoidal phasor component.....	4
Figure 3: EMS/SCADA system configuration layout block diagram .....	5
Figure 4: Generic PMU capturing major components .....	7
Figure 5: Hierarchy of the phasor measurement unit system .....	8
Figure 6: IEEE 14 bus system diagram.....	9
Figure 7: Partitioned IEEE 14 bus system indicating PMU placed at bus 2.....	10
Figure 8: PMU placement for full observability and redundancy level of at least 1 .....	11
Figure 9: Partitioned diagram of bus 7 as a zero-injection bus .....	12
Figure 10: Concepts of depth of unobservability.....	13
Figure 11: Chromosome crossover .....	17
Figure 12: Chromosome mutation.....	17
Figure 13: Tree search PMU placement technique .....	20
Figure 14: 6-Bus test system for ILP application.....	26
Figure 15: Algorithm adaptability assessment.....	30
Figure 16: 6-Bus test system for ILP application.....	32
Figure 17: Minimum PMU placement number for full observability for the base case .....	33
Figure 18: Minimum PMU placement number for full observability considering zero-injections .....	34
Figure 19: Minimum PMU number required for system redundancy of two.....	35
Figure 20: PMU device failure at bus 3 .....	36
Figure 21: Equivalent circuit for a transmission line.....	40
Figure 22: Equivalent circuit for an off-nominal tap transformer .....	40
Figure 23: Equivalent circuit of an in-phase tap transformer .....	40
Figure 24: Two-port $\pi$ -model of a network branch .....	41
Figure 25: Four bus example topology .....	42
Figure 26: Traditional nonlinear hybrid state estimator.....	52
Figure 27: Two pass approach incorporating linear and nonlinear state estimation.....	52
Figure A-1: Line diagram of IEEE 14-bus system.....	91
Figure A-2: Line diagram of IEEE 30-bus system.....	93
Figure A-3: Line diagram of IEEE 57 bus system .....	96

## List of graphs

Graph 1: Sum of complex power flow error for 4 bus system.....	66
Graph 2: Sum of complex voltage error for 4 bus system .....	67
Graph 3: Effect of individual PMUs on complex power flow error for 4 bus system .....	68
Graph 4: Effect of individual PMUs on complex voltage error for IEEE 14 bus system .....	68
Graph 5: Sum of complex power flow error for IEEE 14 bus system.....	70
Graph 6: Sum of complex voltage error for IEEE 14 bus system .....	70
Graph 7: Effect of individual PMUs on complex power flow error for IEEE 14 bus system .....	71
Graph 8: Effect of individual PMUs on complex voltage error for IEEE 14 bus system .....	71
Graph 9: Sum of complex power flow error for IEEE 30 bus system.....	73
Graph 10: Sum of complex voltage error for IEEE 30 bus system .....	73
Graph 11: Effect of individual PMUs on complex power flow error for IEEE 30 bus system .....	74
Graph 12: Effect of individual PMUs on complex voltage error for IEEE 30 bus system.....	74
Graph 13: Sum of complex power flow error for IEEE 57 bus system.....	76
Graph 14: Sum of complex voltage error for IEEE 57 bus system .....	76
Graph 15: Effect of individual PMUs on complex power flow error for IEEE 57 bus system .....	77
Graph 16: Effect of individual PMUs on complex voltage error for IEEE 57 bus system.....	77
Graph 17: Effect that an increasing number of PMUs have on the LSE complex power flow error ....	79
Graph 18: Effect that an increasing number of PMUs have on the LSE complex voltage error.....	80
Graph 19: LSE computation time for an increasing number of PMU .....	80
Graph 20: Effect of individual PMUs on complex power flow error for IEEE 57 bus system .....	81
Graph 21: Effect of individual PMUs on complex voltage error for IEEE 57 bus system.....	81
Graph 22: Complex voltage error for different phasing schemes .....	82

## List of tables

Table 1: South Africa’s national utility road map for power system development.....	1
Table 2: Comparisons of PMU and SCADA data sets from [8].....	6
Table 3: Optimal PMU locations obtained by [13].....	17
Table 4: Optimal PMU locations obtained by [14].....	19
Table 5: Required number of PMU placements for incomplete observability [16].....	20
Table 6: Number of PMUs needed for full system observability [17] .....	21
Table 7: Optimal number of PMUS needed for full system observability [18].....	21
Table 8: Minimum number of PMUs required for complete observability .....	23
Table 9: Minimum number of PMUs to make the system observable under normal operating conditions.....	24
Table 10: Minimum number of PMUs to make the system observable under single line outages.....	25
Table 11: Minimum PMU placement for [27].....	27
Table 12: Number of PMU placement for observability without zero-injections .....	27
Table 13: Number of PMU placement for observability including zero-injections .....	27
Table 14: Minimum number of PMUs for complete observability .....	28
Table 15: PMU placement for IEEE standard test systems in different states .....	28
Table 16: PMU placement for IEEE standard test systems for the base case.....	28
Table 17: Minimum PMU placement comparison for reviewed methods .....	29
Table 18: Optimal minimum number of PMUs for full system observability .....	29
Table 19: Results of optimal placement positions for ILP algorithm .....	36
Table 20: Four bus network data .....	42
Table 21: Current phasor standard deviation.....	55
Table 22: Voltage phasor standard deviation.....	55
Table 23: PMU voltage and current phasor standard deviations.....	55
Table 24: Conventional measurements standard deviations .....	55
Table 25: Quantified standard deviations for conventional measurements and PMU measurements .....	56
Table 26: 4-bus system properties.....	57
Table 27: Bus voltages of 4 bus system .....	57
Table 28: Measurement type and associated covariance for 4-bus system.....	59
Table 29: Iteration number and time taken for convergence for 4-bus system.....	67
Table 30: 14-bus system properties.....	69
Table 31: Iteration number and time taken for convergence for 14-bus system .....	72
Table 32: 30-bus system properties.....	72
Table 33: Iteration number and time taken for convergence for 30-bus system .....	75
Table 34: 57-bus system properties.....	75
Table 35: Iteration number and time taken for convergence for 57-bus system .....	78
Table 36: Comparison of computational time for CSE, HSE and LSE .....	78
Table 37: Optimal phasing schemes for best PFE and VE .....	83
Table A-1: IEEE 14-bus system bus data .....	91
Table A-2: IEEE 14-bus system branch data.....	92
Table A-3: IEEE 30-bus system bus data .....	93

Table A-4: IEEE 30-bus system branch data.....	94
Table A-5: IEEE 57-bus system bus data .....	96
Table A-6: IEEE 57-bus system branch data.....	98

University of Cape Town

## Nomenclature

Symbols for PMU placement:

$X_m$	peak amplitude of sinusoidal signal
$\omega$	Frequency in radians per second
$\phi$	Phase angle of sinusoid in radians
$Z_{line}$	Line impedance
$\theta_{line}$	Phase angle of the line impedance
$\Delta$	Load angle
$N_H$	Number of unobserved buses
$N_{PMU}$	Number of PMUs
$v_i^k$	Current velocity of particle $i$ at iteration $k$
$v_i^{k+1}$	Modified velocity of particle $i$
$x_i^k$	Current position of particle $i$ at iteration $k$
$w_i$	Weighting function for velocity of particle $i$
$c_i$	Acceleration co-efficient
$N$	Total number of candidate PMU placement buses
$N_{PMU}^{ub}$	Upper bound of minimum number of PMUs
$x$	State vector
$W_i$	Cost of PMU installed at <i>bus</i> $i$
$x_L$	Lower bound of state vector binary limitation
$x_U$	Upper bound of state vector binary limitation
$b_L$	Lower bound of state vector solution redundancy
$b_U$	Upper bound of state vector solution redundancy
$A$	Binary connectivity matrix

Symbols for state estimation:

$I_{ij}$	Branch current from <i>bus</i> $i$ to <i>bus</i> $j$
$B$	Susceptance
$y_{ij}$	Admittance between <i>bus</i> $i$ and <i>bus</i> $j$
$y_{i0}$	Shunt admittance connected to <i>bus</i> $i$
$V_i$	Voltage phasor at <i>bus</i> $i$
$a$	Transformer tap ratio
$V_{i\_re}$	Real voltage at <i>bus</i> $i$
$V_{i\_im}$	Imaginary voltage at <i>bus</i> $i$
$I_{ij\_re}$	Real branch current from <i>bus</i> $i$ to <i>bus</i> $j$
$I_{ij\_im}$	Imaginary branch current from <i>bus</i> $i$ to <i>bus</i> $j$
$g_{ij}$	Conductance between <i>bus</i> $i$ and <i>bus</i> $j$
$b_{ij}$	Susceptance between <i>bus</i> $i$ and <i>bus</i> $j$
$Y_{BUS}$	Bus admittance matrix
$z$	Vector of measurements
$h(x)$	Non-linear function expressing the measurements in terms of the state vector $x$
$H(x)$	Jacobian matrix of $h$
$J(x)$	Minimization function
$g(x)$	Derivative of $J$
$G$	Gain matrix
$R$	Error covariance matrix
$P_i$	Real power injection at <i>bus</i> $i$
$Q_i$	Imaginary power injection at <i>bus</i> $i$

$P_{ij}$	Real power flow from <i>bus i</i> to <i>bus j</i>
$Q_{ij}$	Imaginary power flow from <i>bus i</i> to <i>bus j</i>
$S_{i,from}$	Complex power flow from <i>bus i</i>
$S_{i,to}$	Complex power flow to <i>bus i</i>
$\sigma_i$	Standard deviation of measurement <i>i</i>
$M$	Actual measurements
$B(V)$	Linear function relating $M$ to state vector $V$

University of Cape Town

# 1. Chapter 1: Phasor measurement unit pertinence and placement

## 1.1. Introduction

The electric power system is on the verge of a significant transformation. Modern technology is providing many improved and new options for operation, monitoring and control of the power system. The National Energy Technology Laboratory (NETL) has identified key technology areas (KTAs) that will play a pivotal role in this transformation. The foremost of the KTAs is the need for broadband, secure, low latency channels connecting transmission stations to each other and control centres [1]. Phasor measurement units (PMUs) are to be used for sensing and measurement and to improve interface and decision support by utilising instantaneous PMU data. This data will drive faster simulations and advanced visualisation tools that will help system operators assess dynamic challenges to system stability. In this work, various PMU placement algorithms are reviewed in order to identify and design a method that would enable economic placement of PMUs in the South African grid. The developed placement method is used to locate optimal measurement positions in specific IEEE bus systems so that the effects of incorporating PMUs and the associated effects that PMUs have on the overall accuracy of state estimation can be analysed.

### 1.1.1. South Africa’s plan to utilize PMUs

Under the Integrated Resource Plan (IRP), it has been outlined that South Africa effectively needs to double its’ electrical generation capacity by the year 2030 to maintain a high level of economic growth. It has been suggested that renewable energy forms a more significant, growing percentile of the energy portfolio as a means of generating electricity. There are plans to spread renewable energy generation sources over wide geographic locations to support overall system stability [2]. The increase in total generation capacity and the diversified sources that will be utilised to meet the electricity demands will prompt the improvement of existing transmission and distribution infrastructure, as well as the installation of new infrastructure. PMUs offer Global Positioning System (GPS) time stamped data which will be vital for monitoring, controlling and logging data from new generation sources and geographically dispersed renewable systems.

Table 1: South Africa’s national utility road map for power system development

Goals - Short Term 1-3 years	Goals - Medium term 3-5 years	Goals - Long term > 5 years
Situational awareness - angle/frequency monitoring/damping	Situational awareness - advanced visualization tools	Linear state estimation
Post Event Analysis	Model benchmarking; Parameter estimation	Real-time control
State Estimation (Improve)	Hybrid state estimation	Adaptive protection
Model benchmarking; parameter estimation	Advanced stability monitoring	WA Stabilization (WA-PSS)
Power System Restoration and Island Operations		Planned power system separation - special protections systems
Small signal Stability monitoring applications		

Table 1 gives a road map for future power system development and requirements of the South African national utility. PMUs provide the technology to improve many of these aspects presented in the table. PMUs improve and enable real time monitoring and control; power system State

Estimation (SE); real time congestion management; benchmarking, validation and fine tuning of system models; power system restoration; protection and control applications for distributed generation; overload monitoring and dynamic rating and adaptive protection [3]. Currently the national utility has 4 PMUs in service. The aim is to integrate an additional 15 in the next 5 years. With the oncoming roll out of renewable generation comes an increased need for real time monitoring and control and data capture. These 15 PMUs will have to be optimally placed in order to ensure that the benefits of their placement are maximised. PMUs have become cheaper over the years however the communications requirements associated with PMUs are still very expensive. Due to this high associated cost, it is expected that PMUs will be installed in stages or phases. Therefore the placement of PMUs and the way in which the measurement data is used to improve applications of the power system is of both a global interest and national interest.

In this chapter, the phasor measurement unit is defined. A brief history of phasor measurement units is covered and the importance of PMUs in power systems is highlighted. The current EMS/SCADA system is reviewed and the impact and hierarchy of PMU installation is covered. The chapter concludes with definitions of important concepts related to the optimal placement of phasor measurement units in power systems.

#### 1.1.2. Phasor measurement unit historical overview

The research conducted on computer relaying of transmission lines is the source of development of PMU technology in the 1970s. The research resulted in a new relaying technique which incorporated the use of symmetrical component analysis of line currents and voltages pertaining to the calculation of positive-sequence components. In [4] Phadke et al. identified the role of the positive-sequence voltages of a network in the constitution of the state vector of a power system and the fundamental importance the state vector plays in power system analysis. This paper served as a starting point for the development of PMU devices. In the early 1980s two PMU prototypes were developed at Virginia Tech and were deployed at a few substations. In 1991, Virginia Tech and Macrodyne of the United States of America (USA) collaborated to manufacture and offer PMUs as a commercial product. In 1995 PMU technology prompted the development of a standard to define the use of phasor measurement technology in power system applications. The standard has been revised and is technically referred to by its trademark *IEEE Standard C37.118* [5]. PMU technology has become cheaper over the years. Therefore many modern power system utilities around the world are planning or in the process of installing wide-area measurement systems (WAMS) strengthened by a backbone of PMU devices.

#### 1.1.3. Phasor measurement unit definition

A phasor measurement unit is a device that provides as a minimum synchrophasor and frequency measurements for one or more three phase AC voltage and/or current waveforms [6]. The voltage and current measurements are positive sequence measurements synchronized to within one microsecond [7]. This synchronization has been made possible through the use of a Global Positioning System (GPS) that is able to time stamp the measurements with a very high precision at the source.

The device must provide a real-time data output which conforms to IEEE C37.118 requirements [5]. A pure sinusoidal waveform is given in (1) as:

$$x(t) = X_m \cos(\omega t + \phi) \quad (1)$$

where  $X_m$  is the peak amplitude of the signal;  $\omega$  is the frequency of the signal in radians per second and  $\phi$  is the phase angle in radians.

Equation (1) can be represented as a synchrophasor  $X$  as follows:

$$x(t) = \text{Re}\{X_m e^{j(\omega t + \phi)}\} = \text{Re}\{e^{j(\omega t)}\} X_m e^{j\phi} \quad (2)$$

Equation (2) expressed in phasor representation:

$$\begin{aligned} x(t) &\leftrightarrow X = \frac{X_m}{\sqrt{2}} e^{j\phi} \\ &= \frac{X_m}{\sqrt{2}} (\cos \phi + j \sin \phi) \\ X &= X_r + jX_i \end{aligned} \quad (3)$$

Where  $\frac{X_m}{\sqrt{2}}$  is the rms value of the signal  $x(t)$  and  $\phi$  is its instantaneous phase angle relative to a cosine function at nominal system frequency synchronized to Universal time coordinated (UTC) [5].

A sinusoid and its phasor representation are illustrated in Figure 1 and Figure 2 respectively.

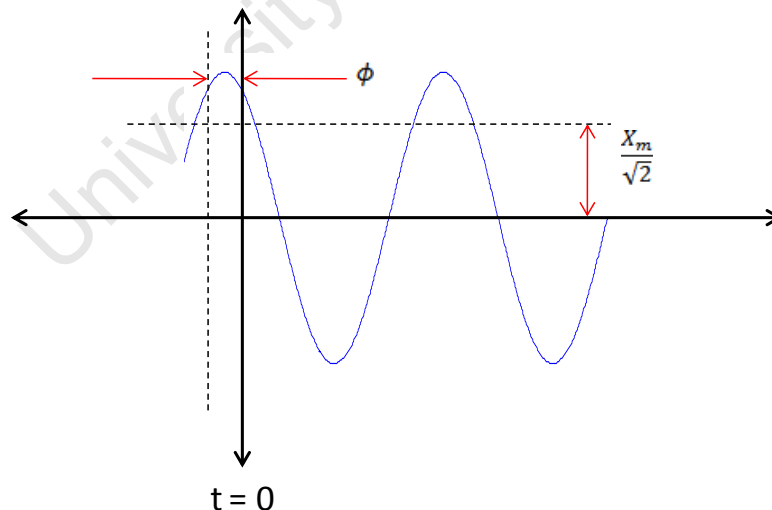


Figure 1: Representation of a sinusoidal signal

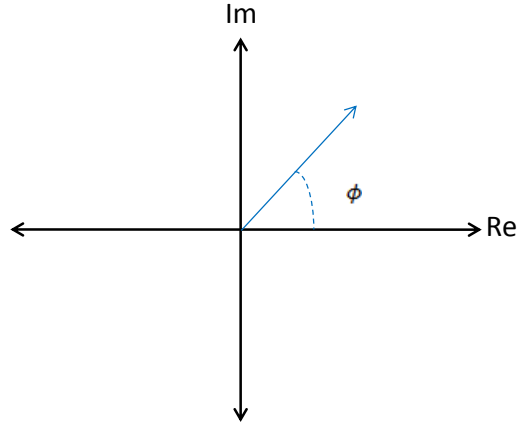


Figure 2: Representation of a sinusoidal phasor component

The phase angle  $\phi$  is determined by the starting time ( $t = 0$ ) of the sinusoid. A time error of 1 microsecond ( $1\mu\text{s}$ ) at 60Hz corresponds to an error of 0.022 degrees and at 50Hz to an error of 0.018 degrees respectively. The total vector error (TVE) for a PMU must not exceed 1 percent: This corresponds to a maximum phase error of 0.01 radians or 0.57 degrees [5]. TVE is calculated using equation (4). A GPS provides the PMU with sufficient time accuracy to keep the TVE within the required limits as well as providing an indication of loss of synchronism.

$$TVE = \sqrt{\frac{(X_r(n) - X_r)^2 + (X_i(n) - X_i)^2}{X_r^2 + X_i^2}} \quad (4)$$

where  $X_{r,i}(n)$  are the real and imaginary measured values of the measurement device and  $X_r, i$  are the theoretical values of the input signal.

The TVE is calculated and used as a compliance test to ensure that the phasor estimates correspond closely to the theoretical estimates. This compliance test is needed due to the fact that all physical measurements have an associated degree of uncertainty.

#### 1.1.4. Importance of PMU technology

The operating conditions of a power system at a specific point in time can be determined if the network model and complex phasor voltages at every system bus are known. Conventionally, substations are equipped with remote terminal units (RTUs) or Intelligent Electronic Devices (IEDs) that are responsible for making various measurements. A supervisory control and data acquisition (SCADA) system facilitates the collection and communication of these measurements transmitting them to the control centre for processing via communication links such as satellite, microwave and fibre optics. A block diagram of the general layout is given in Figure 3. These raw measurements are processed by a state estimator (SE) to filter out gross errors and measurement noise. In essence the state estimator forms a real-time base from which all energy management systems (EMS) applications function. Due to the fact that it is not technically and economically feasible to monitor and telemeter all possible system measurements, an EMS is equipped with an on-line state estimator (SE). The SE is designed to run periodically to provide a consistent and reliable picture of the system state based on the assumed measurement model and the available measurements. The solution is composed of complex bus voltages as well as a best estimate for all the line flows, loads,

transformer taps and generator outputs. However, prior to PMU technology the state of the power system could not be directly measured but only inferred from unsynchronized complex phasor power flow measurements. In a traditional SCADA system data is captured from RTU units in sequence by polling. The process of polling is not instantaneous and therefore the time taken for a complete scan and the changes in generation and load during the scan, alter the accuracy of the observed hypothetical system in comparison to the real system. The approximation was to assume that the system was static in nature. However, although scans have become quicker the introduction of PMUs forces the reconsideration of the static assumption [7].

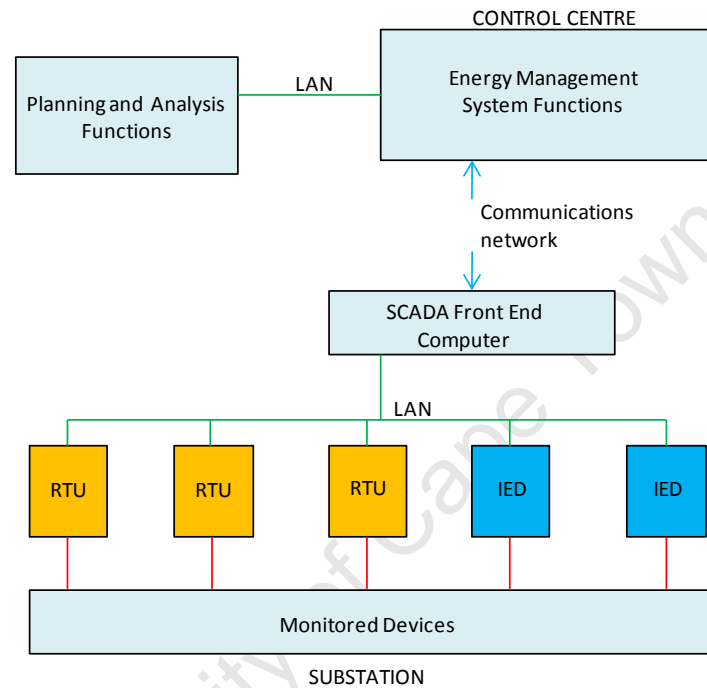


Figure 3: EMS/SCADA system configuration layout block diagram

A PMU that is placed at a bus is able to directly measure the voltage and current phasors at the placement bus, as well as buses that are directly connected to the placement bus. The voltages at the buses incident to the placement bus are estimated using the known transmission line parameters and the measured line currents. PMU technology has the ability to use GPS technology to time-stamp source measurements with a very high precision. All PMU measurements with the same time-stamp are used to ascertain the state of the power system at the moment defined by the time-stamp signature. PMUs may be placed in geographically dispersed locations separated by large distances. Therefore when PMU measurements arrive at a central location, the time-tags provide a time-indexing tool to indicate the state of the power system. Therefore time-tags eliminate data transmission speed as a critical parameter in making use of measurement data. PMU integration benefits applications of the EMS system such as: Post-disturbance analysis; inter-area oscillation monitoring, analysis and control; state estimation and improved observability; power plant monitoring and integration; bad data detection and real-time monitoring and control [3].

#### 1.1.5. PMU equipped system compared to SCADA equipped system

In [8] a joint funding task force was created to assess the benefits of integrating PMU technology into an EMS. It consisted of two phases: Phase I consisted of an off-line preliminary study case and phase

It consisted of on-line state estimation using a hybrid SCADA/PMU data set. Table 2 highlights some differences between PMU/PDC and SCADA measurement sets.

Table 2: Comparisons of PMU and SCADA data sets from [8]

PMU/PDC	SCADA
30 samples per second refresh rate	2 to 5 second refresh rate
Data is time tagged	Data has latency and skew
Compatible with modern communication technology	Relies on older communication technology
Responds to dynamic system behaviour	Responds to static system behaviour
Angle-pair change indicates a transfer change between selected monitored points	Frequency change indicates a generation or load imbalance

Table 2 indicates that the refresh rate per second for PMU/PDC setup is significantly faster than SCADA. As previously mentioned the PMU data is time tagged, eliminating latency and skew effects that are associated with the SCADA system. PMU/PDC use newer communications technology than the SCADA architecture. The resultant of a higher refresh rate and use of more modern communications systems allow PMU/PDC systems to respond to dynamic system behaviour. The angle-pair monitoring indicates a transfer change between selected points: In order to elaborate on this concept, consider the complex power  $S_s$  at the sending end bus given by equation (5) adapted from [9].

$$S_s = E_s I_s^* = \frac{|E_s|^2}{|Z|} \angle \theta - \frac{|E_s||E_R|}{|Z|} \angle \theta + \delta \quad (5)$$

The sending end real power is derived from equation (5) and given as:

$$P_s = \frac{|E_s|^2}{|Z|} \angle \cos \theta - \frac{|E_s||E_R|}{|Z|} \angle \cos (\theta + \delta) \quad (6)$$

where  $|E_s|$  and  $|E_R|$  are the magnitudes of the sending and receiving end voltages respectively.  $|Z|$  and  $\theta$  are the magnitude and angle of the line impedance respectively, between the sending and receiving end buses.  $\delta$  is the difference between the sending and receiving end voltage angles and is referred to as the power angle or load angle.

Equation (6) indicates that if  $\delta > 0$  the sending end power is positive and flows from the sending end to the receiving end. If  $\delta < 0$  the direction of real power reverses. Therefore the direct measurement of these angles by PMUs will help to determine the directions of real power and serves to indicate transfer changes between points rather than relying on frequency changes in a SCADA system to indicate an imbalance in generation or load.

#### 1.1.6. The basics of a generic phasor measurement unit

PMUs are built by various manufacturers. Therefore most manufacturing designs differ from one another in certain aspects and it is difficult to discuss PMU hardware configuration in a way which is universally applicable. Therefore a generic PMU which captures the basics of the principle components, inputs and outputs is outlined in Figure 4 and discussed in this section. Analog inputs to the PMU are voltages and currents obtained from secondary windings of voltage and current

transformers. Positive sequence measurements are captured by utilising three-phase voltages and currents. The voltage and current signals are passed through an anti-aliasing filter with a cut-off frequency of less than or equal half the sampling frequency in order to satisfy the Nyquist criterion. The anti-aliasing filter consists of an analog front end filter and a digital decimation filter in order to ensure that phase angle differences and relative magnitudes of the different signals are unchanged [3]. The PMU sampling clock is phase-locked with the GPS pulse clock. The sampling rate is limited by the analog-to-digital converter. Modern devices are able to sample at 96 or 128 sample per cycle [7]. The microprocessor then calculates the positive sequence voltage and current phasors via discrete Fourier transform applied on a moving data window. The final output of the PMU is the time-stamped measurement which is transferred over a communications link to a higher level in measurement system hierarchy. The time-stamp is created from two signals derived from the GPS receiver and synchronised to UTC.

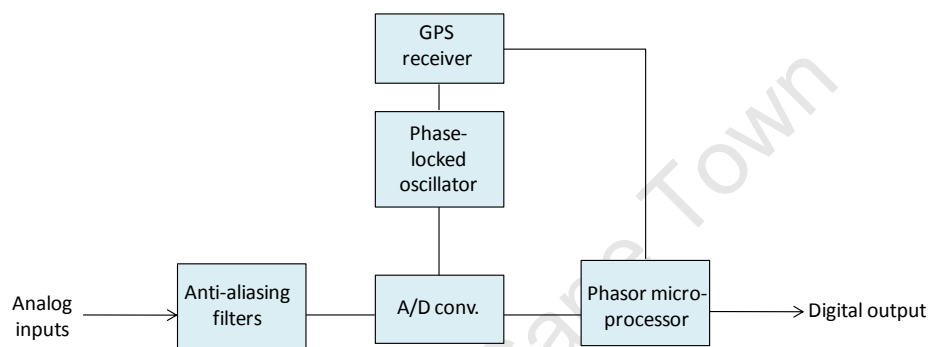


Figure 4: Generic PMU capturing major components

#### 1.1.7. Hierarchy for phasor measurement unit systems

Generally the phasor data generated by PMUs are used in remote locations. The architecture that is used to obtain the full benefit of synchrophasor technology includes PMUs, communication links and phasor data concentrators (PDC). The hierarchy of the system is shown in Figure 5. Similar to RTUs, PMUs are installed in power system substations and provide time-stamped positive sequence voltage and current measurements of all the monitored buses and feeders. PMU data is stored in a limited local manner which can be accessed remotely for diagnostic purposes, or used by local applications. Typically, the phasor data is sent to a PDC. PDC functionality is to gather data from several PMUs reject bad data and align time-stamped data. Local storage is available at the PDC and real-time data can be utilized for local applications. PDCs can be considered to act on a regional basis. On a system-wide scale a super data concentrator is one level higher but has similar functions to regional PDCs, in terms of aligning time-stamps and rejecting bad data, receiving and accumulation measurements from the entire system. The communication links are bidirectional so that downstream components can be configured remotely. Intuitively the upstream channel capacity is far greater than the downstream channel capacity. In the USA and Europe the generation of electricity is deregulated. Therefore each utility is assigned a regional PDC to aggregate and align data from various PMUs in the covered region. The regional PDC will be located at a utilities control centre and will send its data to a demarcated national PDC (super PDC) in order to synchronize the data across utilities [10].

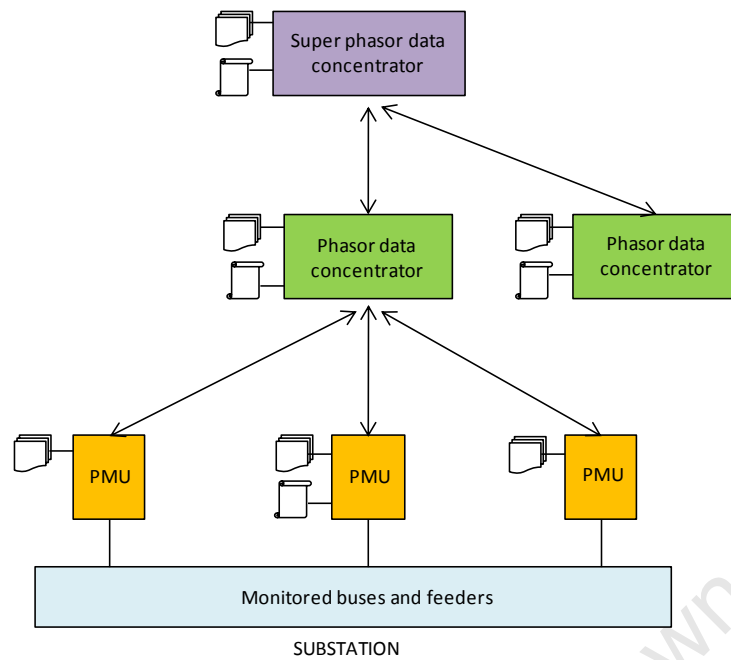


Figure 5: Hierarchy of the phasor measurement unit system

#### 1.1.8. Communication link options for phasor measurement units

There are various options for communication links for PMUs. These communication links are essential in realising remote applications requiring phasor data. Reference [7] identified two aspects of data transfer that are significant in any communication task, namely channel capacity and latency. Channel capacity is the measure of the data rate that can be reliably sustained over the available data link measured in bits per second. Latency is the measure of time-delay in a system. In this context latency is assumed to be the time difference between data creation and data availability for the desired application. Recently the U.S. Department of Energy, American Electric Power and Ameripon demonstrated the viability of broadband over power line (BPL) for application on transmission lines. An 8 kilometre, 69-kV transmission line is operating at megabit-per-second data rates with a latency of less than 10ms. Research is underway to extend BPL to 138-kV transmission lines [1]. There is a modest volume of created PMU data [7]. Therefore channel capacity is not a limiting factor. Applications to realise real-time monitoring and control of power systems require a relatively small latency. The medium of choice for PMU data transfer is fibre-optic links due to the high channel capacity, high data transfer rates and immunity to electromagnetic interference. Microwaves have been previously used as well. Fibre-optics are most popularly deployed in the ground wires of transmission lines, but may be placed on separate towers or buried beneath the ground. Many different installation methods as well as types of fibres exist. Many communication protocols exist for PMU devices including common protocols such as transmission control protocol (TCP) and user datagram protocol (UDP). The general requirements for communications with PMUs are addressed in Annex I of the *IEEE Std C37.118-2005* [5]. Reference [7] identified the fact that in recent years IEC Standard 61850 has been introduced to facilitate electricity substation automation. However, in its present version, this standard has not been identified as being useable for PMUs.

## 1.2. Phasor measurement unit placement in a power system networks

In this section concepts of observability, zero-injection, redundancy and phasing will be explained. Figure 4 and derivatives will be used to illustrate the practical concepts relative to PMU placement in a power system network. This test bus system is a standard IEEE 14 bus system [12] and is as a common benchmarking tool for PMU placement optimisation.

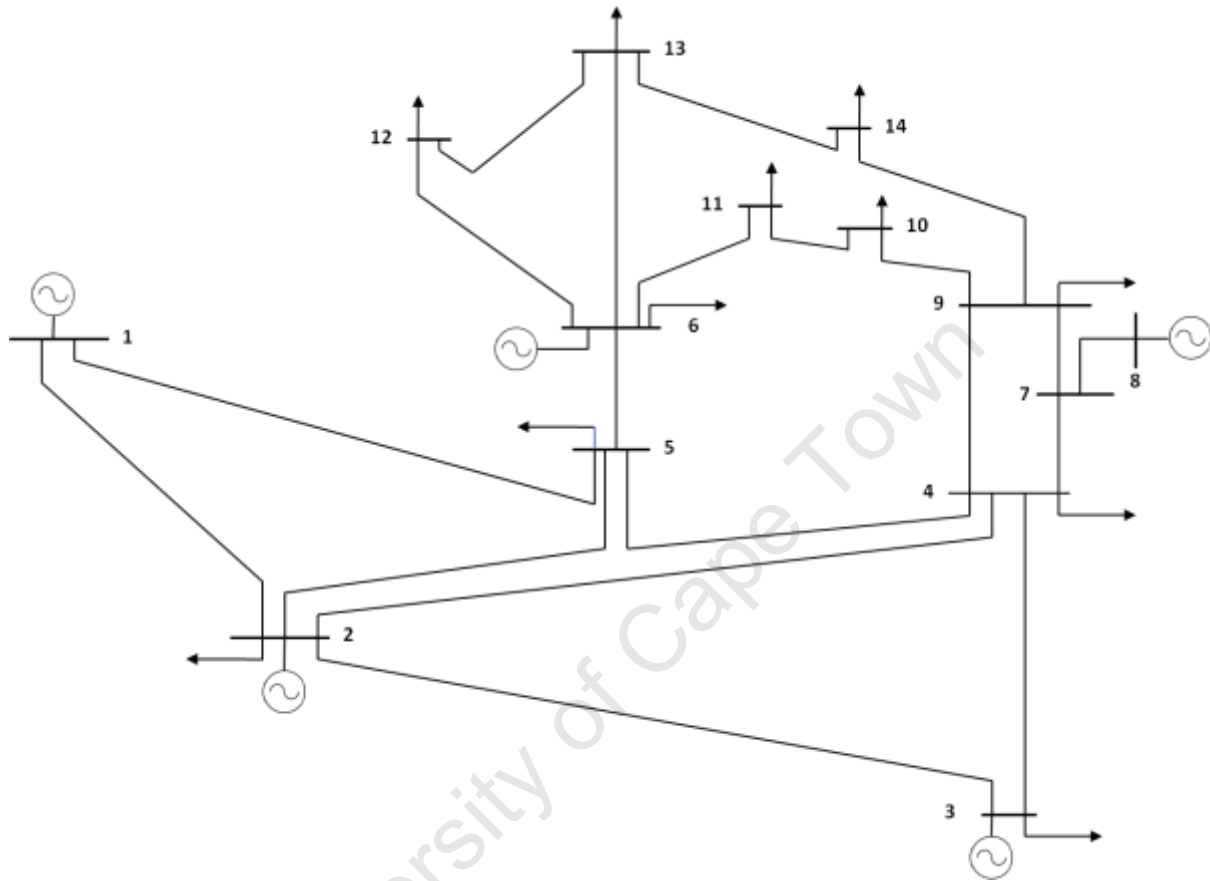


Figure 6: IEEE 14 bus system diagram

A PMU placed at a bus is able to measure the voltage phasor at the placement bus, as well as current phasors in the lines connected to the placement bus. The measured line currents are used in conjunction with the transmission line parameters to provide a voltage phasor estimate of all buses directly connected to the placement bus. The estimation of voltage is based on the fundamental Ohm's Law. For example consider Figure 7. If it is assumed that a PMU is placed at bus 2 (indicated by a red dot), the PMU measures the voltage phasor  $\vec{V}_2$  and current phasors  $\vec{I}_{2-1}$ ,  $\vec{I}_{2-3}$ ,  $\vec{I}_{2-4}$  and  $\vec{I}_{2-5}$  (indicated by green arrows). Therefore the use of line current phasors and transmission line parameters provides voltage phasor estimates at buses 1,3,4 and 5. Therefore, a PMU placed at bus 2 enables the observation of measurements at buses 1,2,3,4 and 5 (indicated by green circles).

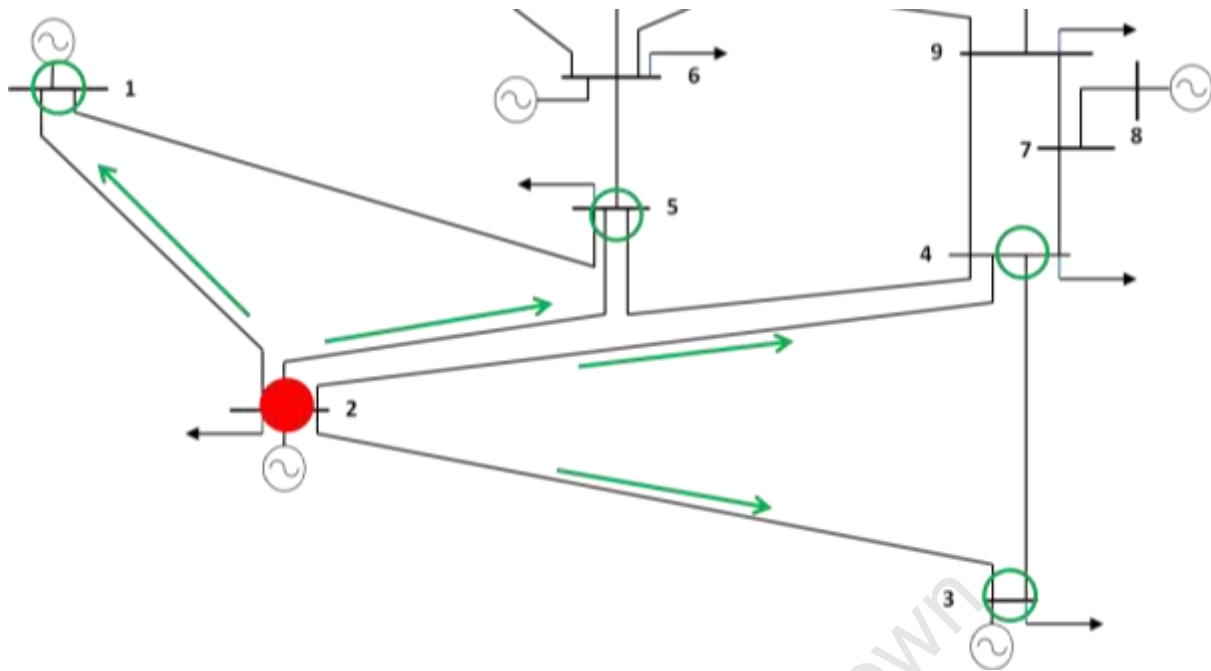


Figure 7: Partitioned IEEE 14 bus system indicating PMU placed at bus 2

### 1.2.1. Observability

It can be concluded that the placement of a PMU at bus 2 enables '*full observability*' of buses 1, 2, 3, 4 and 5. However, with a PMU placed only at bus 2 in this system, the system as a whole is said to be partially observable. Full system observability will occur when all the buses in the system are observed by at least one PMU.

### 1.2.2. Minimum PMU placement

The main objective of optimal PMU placement in power networks is to minimise the number of PMUs needed to enable full system observability. This is fairly intuitive due to the fact that the state of the power system can only be estimated if there is available measurement data provided by the PMU. Many theoretical implementations of minimum PMU placement focus only on minimising the number of PMUs of a given network without considering contingencies. However, many factors must be considered for optimising minimal PMU placement. A PMU placement scheme should provide functional security when presented with contingencies such as the outage of a PMU or communication line and a limited number of PMU measurement channels such that full observability is always maintained during operation of the power system.

### 1.2.3. Redundancy

In the context of PMU placement, redundancy is used as an index to quantify the number of individual PMUs observing a specified bus. For example, in Figure 7, a PMU at bus 2 observes buses 1 to 5 with a redundancy of 1 indicating that one PMU observes each bus. Figure 8 shows PMUs deployed in a power system network to enable full observability with a minimum number of PMUs placed at buses 2, 6, 7 and 9. Each bus in the system is observed by at least one PMU. Therefore the system is said to have a redundancy level of at least 1. Buses 4, 5, 7 and 9 have redundancies of 2 as they are observed at least twice by two individual PMUs.

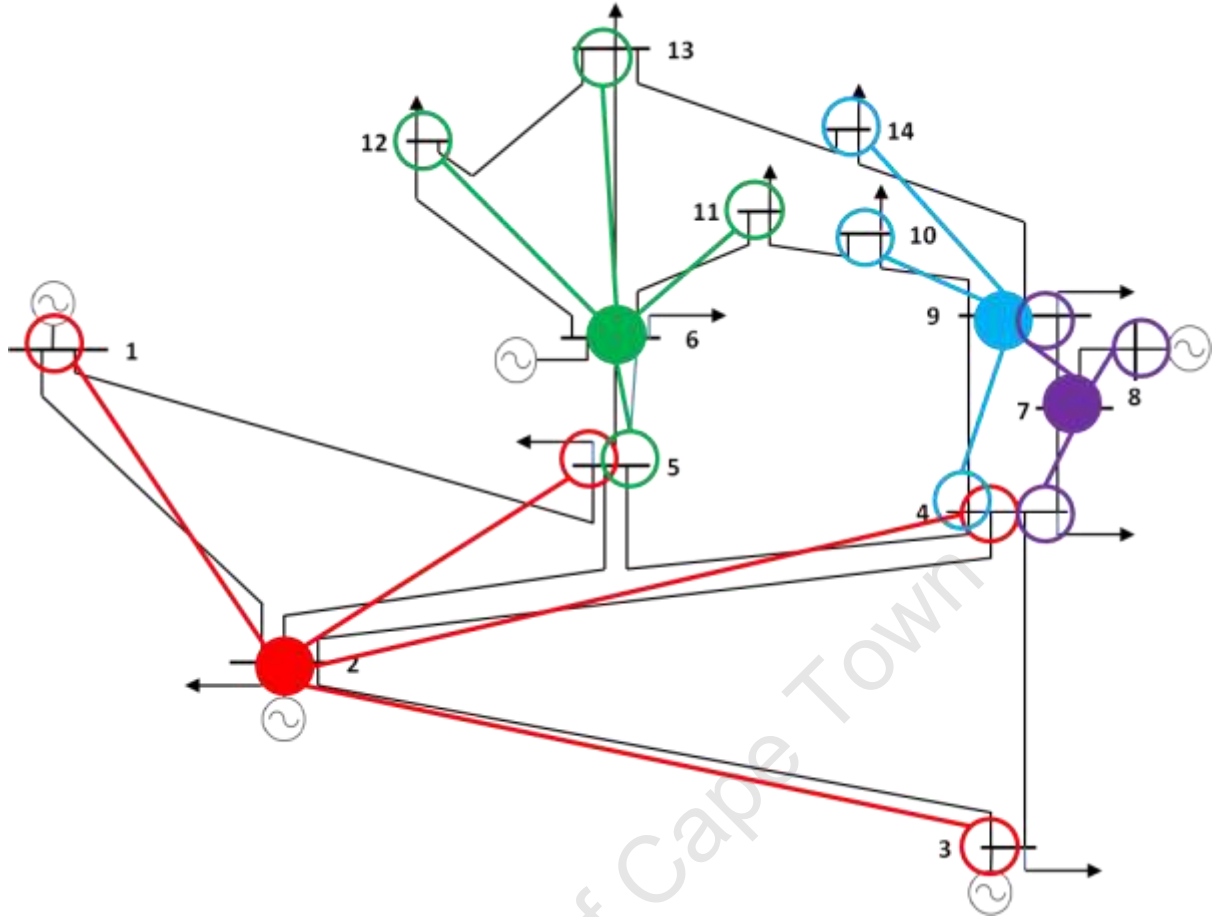


Figure 8: PMU placement for full observability and redundancy level of at least 1

#### 1.2.4. Zero-injection buses

A zero-injection bus has no generation or load directly connected to the bus. Therefore the line currents flowing into and out of the bus should sum to zero. Therefore if all buses directly connected to a zero-injection bus are observable except one, that unobserved bus can be made observable by applying Kirchoff's Current Law (KCL) at the zero-injection bus. Therefore a PMU placement at a zero-injection bus is not necessary to observe the voltage at that bus. A detailed derivation and analysis of KCL can be found in reference [9].

For example in Figure 8, bus 7 is known to be a zero injection bus. This can be verified by checking the network data for the IEEE 14 bus system in Appendix A. If no PMU is placed at the zero-injection bus, all buses connected to bus 7 are observable, except for bus 8. Bus 9 is made observable by a PMU placement at bus 9 and bus 4 is made observable by a PMU placement at bus 2. Bus 8 is the unobserved bus. Therefore the line currents in two out of three lines are directly measured by PMUs. The known line currents are from bus 9 to bus 7 ( $\vec{I}_{9-7}$ ) and from bus 4 to bus 7 ( $\vec{I}_{4-7}$ ). Due to the fact that there is no generation or load connected to bus 7, the line current from bus 7 to bus 8 ( $\vec{I}_{8-7}$ ) can be estimated based on equation (7).

$$\vec{I}_{9-7} + \vec{I}_{4-7} + \vec{I}_{8-7} = 0 \quad (7)$$

Therefore bus 8 can be made observable by calculating the bus voltage phasor using the resultant line current and transmission line parameters. Therefore a PMU placed at a zero-injection bus is not necessary and may be removed to give a lower optimum number of PMUs for this bus system. This methodology can be applied to all bus systems and is used extensively in the literature to lessen the required number of PMU for full observability.

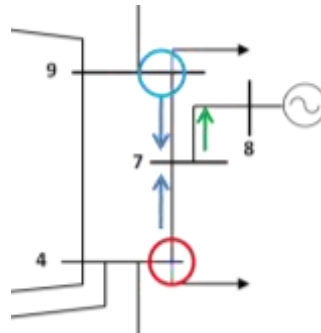


Figure 9: Partitioned diagram of bus 7 as a zero-injection bus

#### 1.2.5. Phasing

PMU phasing is the process of installing a certain number of PMUs in stages over a specified time frame. The goal of phasing is to maximise the impact of PMU placement. For example, three PMUs are needed to realise full observability of the bus system shown in Figure 8 at buses 2, 6 and 9. However there is a constraint that a utility is only able to install one PMU per month. Therefore an effective phasing scheme should be devised to identify the most important sites to locate the 1<sup>st</sup> PMU, then the 2<sup>nd</sup> PMU and then the 3<sup>rd</sup> PMU. Phasing becomes very important as the size of the system increases and the cost of PMU procurements and installations versus cost benefits increase.

#### 1.2.6. Outage of a PMU and/or communication line

The minimum PMU placement problem should take the outage of a PMU and/or communication line into consideration. For example if PMUs are placed in a system with a redundancy level of 1, if one PMU were to fail, the system would become partially observable and the ability to monitor the entire system would be lost. Many options are available for mitigating these effects such as ensuring an overall redundancy level equal or higher than 2 or placing PMUs at critical buses in a system.

#### 1.2.7. Depth of unobservability

Reference [11] introduced the concept of depth of unobservability. The depth of unobservability is an indication of the depth of all the unobserved buses in a system. When a subset of buses is unobservable by PMUs, that subset of system bus voltages cannot be directly calculated from the known PMU measurements. Consider Figure 10 as an example of depth of unobservability.

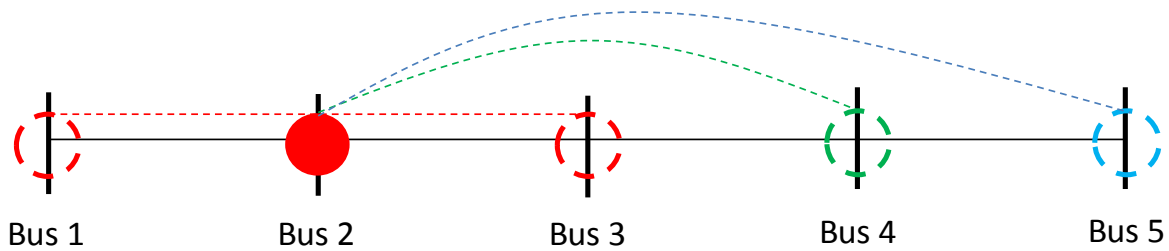


Figure 10: Concepts of depth of unobservability

Buses 1, 2 and 3 are directly observed by the PMU placed at bus 2. However, assuming there is no other PMU present in this system, buses 4 and 5 are both unobserved. Bus 4 is said to have a depth-of-one unobservability, while bus 5 has a depth-of-two unobservability. Therefore a certain depth of unobservability can be used to drive PMU placement to ensure that PMUs are well distributed throughout a power system. In addition, the known bus voltages can be used to estimate the unknown voltages using an interpolation method.

#### 1.2.8. Test bus systems

All algorithms and methods are tested on the standardised IEEE test bus systems [12]. Images and tables detailing the bus and line parameters of these test systems have been included in Appendix A. The bus systems commonly referred to in this work as follows:

- IEEE 14 bus
- IEEE 30 bus
- IEEE 57 bus

The major objectives of this thesis are to:

- a) Investigate and develop a method for placement of a minimum number of PMUs into a system to ensure full observability.
- b) Investigate and develop a state estimation technique to use the PMU measurement data to perform state estimation and study the effects that differing PMU placement positions have on the accuracy of state estimation.

The investigated topics in detail are as follows:

- 1.) A PMU placement literature review is undertaken to investigate various methods to incorporate a minimum number of PMUs for specific test bus systems. The objective is to identify and record the best performing methods that require the smallest number of PMU as well as the methods that provide adaptability to deal with contingencies of PMU placement.
- 2.) A placement method to minimise the number of PMUs for full system observability is developed using the most suitable algorithm identified in chapter 2. The method is applied on three test bus systems and the results are compared to previous results identified in chapter 2 in order to assess the adequacy of the developed placement method in this work.
- 3.) A broad review of utilisation of PMU data for state estimation utilisation is undertaken to identify and develop state estimators to incorporate PMU data as state variables. The

structure of the developed state estimators are explained and applied to a small hypothetical 4 test bus system.

- 4.) The developed state estimators are tested on the conventional IEEE 14, 30 and 57 bus test systems with the aim to assess the impact that the addition of PMUs have on the complex power flow and voltage errors of the systems. In addition the effects that differing PMU phasing schemes have on the accuracy of state estimation are investigated in order to identify the most suitable phasing scheme for PMUs.

This thesis is composed of five main chapters including this introduction. The chapters are presented chronologically so that each of the four main objectives presented above is contained in one chapter. Chapter 6 summarises all the findings of this work and recommends direction for future research.

University of Cape Town

## 2. Chapter 2: PMU Placement literature review

The optimal placement problem (OPP) is a multifaceted problem due to the fact that PMU placement is dependent on multiple factors such as observability, redundancy, phasing and contingencies. In addition a specific OPP is subject to utility discretion in terms of required security of operation, network parameters and topology and PMU procurement, installation, requirements and monitoring needs. One of the key issues for PMU applications is the selection of placement sites. Therefore strategies for the optimal PMU placement problem have been concentrated as a research interest.

In this review ‘algorithm’ refers to the underlying mathematical structure such as linear programming or genetic algorithm and ‘method’ refers to an implementation of a method in a referenced paper. Many methods have been developed as a tool to provide a utility with a guideline for optimally placing PMUs. The content of this chapter covers a broad spectrum of methods that utilise differing algorithms to reach an optimal bus placement solution. The goal is to acquire information and knowledge to build a method that provides an optimal number of PMUs for both a theoretical test system and a practical test system.

From a variety of methods incorporating mathematical algorithms, a broad spectrum of the best performing methods has been compiled. The methods can be categorized into two groups, namely meta-heuristic optimization methods and conventional deterministic techniques.

### 2.1. Meta-Heuristic Methods

Meta-heuristic methods involve intelligent search processes that can deal with discrete variables and non-continuous cost functions. These methods cover genetic algorithms, particle swarm optimization, topology and tree search.

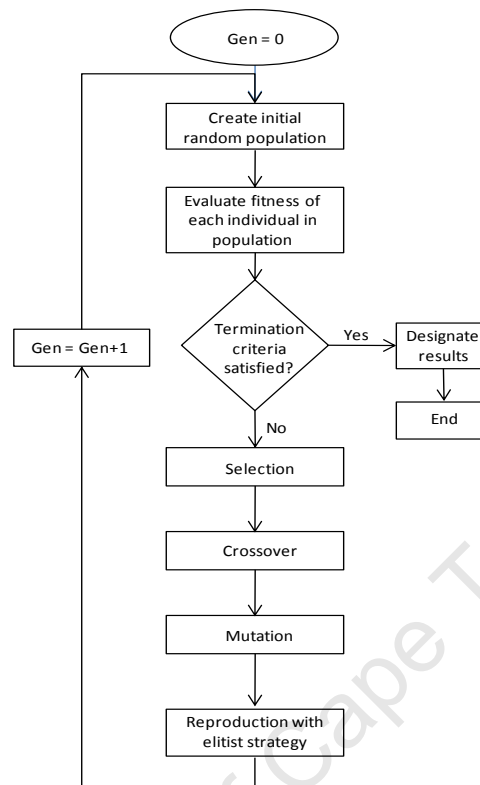
#### 2.1.1. Genetic Algorithm

Marin et al. [13] proposed the use of a genetic algorithm (GA). GA is based on the process of genetic breeding whereby two operators, crossover and mutation ensure the optimisation of a particular individual, resulting in new genetic information from generation to generation. The GA encoding scheme is as follows: Binary genes form the chromosome of an individual. Each bus of a network has a binary gene that indicates the existence of a PMU at that bus typically referred to as a bus gene. In addition every bus has a gene for each line that is used to indicate if the corresponding phasor current measurement is available for a specific branch. The fitness of each individual is calculated using an observability analysis. The observability analysis is based on the PMU observability properties covered in section 1.2. A bus is made observable by placing a PMU at that bus. A PMU placement bus provides observability to all buses directly connected to the placement bus. In addition, if a bus has all its branches observable, except one, a pseudo-measurement can be assigned to this branch. This observability analysis is recursively applied to find the number of unobserved buses  $N_H$  and the number of PMUs in the network  $N_{PMU}$  using an optimised graph search procedure. The fitness function is calculated according to equation (8).

$$f = aN_{PMU} + bN_H + cN_{PMU}N_H \quad (8)$$

where the constants set to  $a = 1$ ,  $b = 2$  and  $c = 1$  gave the best results.

The placement problem is resolved through the steps in Flowchart 1.



Flowchart 1: Genetic algorithm progression

After the fitness function has been evaluated, individuals with the lowest fitness function (best performance) are selected for reproduction. A lower numerical value of the fitness function indicates better performance and a lower minimum number of PMUs and unobserved buses in the solution. The selection of individuals for reproduction is done by probabilistically selecting individuals based on their fitness performance such that the best performing individuals produce a higher number of offspring. Half the genetic information of an individual (Parent 1) is then crossed with another half of another individual (Parent 2) to produce an offspring sharing both parents genetic material through the process of crossover shown in Figure 11. The initial parent genes consist of randomly assigned ones and zeroes that represent network variables. A '1' indicates that a PMU is placed at the bus corresponding to the position of the '1' in the parent gene and a zero indicates that no PMU should be placed at the bus.

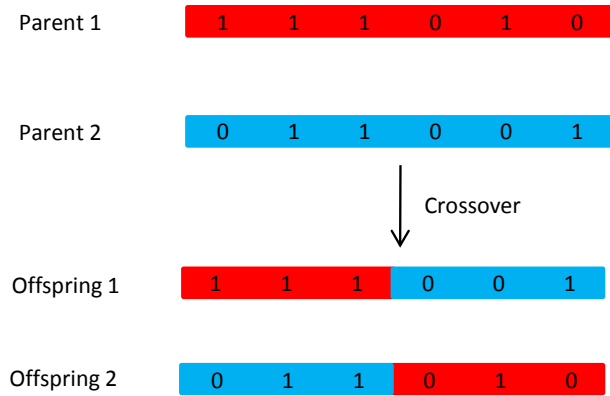


Figure 11: Chromosome crossover

Mutation is then applied over randomly selected gene positions to create new genetic material as shown in Figure 12. This mutation results in changes in gene binary variables.

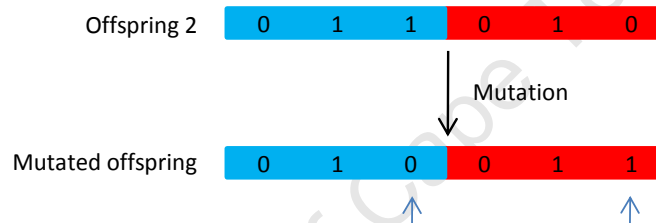


Figure 12: Chromosome mutation

The best performing genes are deterministically maintained to increase the fitness of the population through an elitist strategy. The new generation is then tested for fitness and the algorithm performs  $G$  iterations.

The results of this method are shown in Table 3

Table 3: Optimal PMU locations obtained by [13]

Power System	Number of PMUs	Placement sites	No. concurrent measurements
IEEE 14-bus	3	2,6,9	4
IEEE 30-bus	7	1,5,10,12,15,20,27	3
IEEE 57-bus	12	*not provided	3
IEEE 118-bus	29	*not provided	5

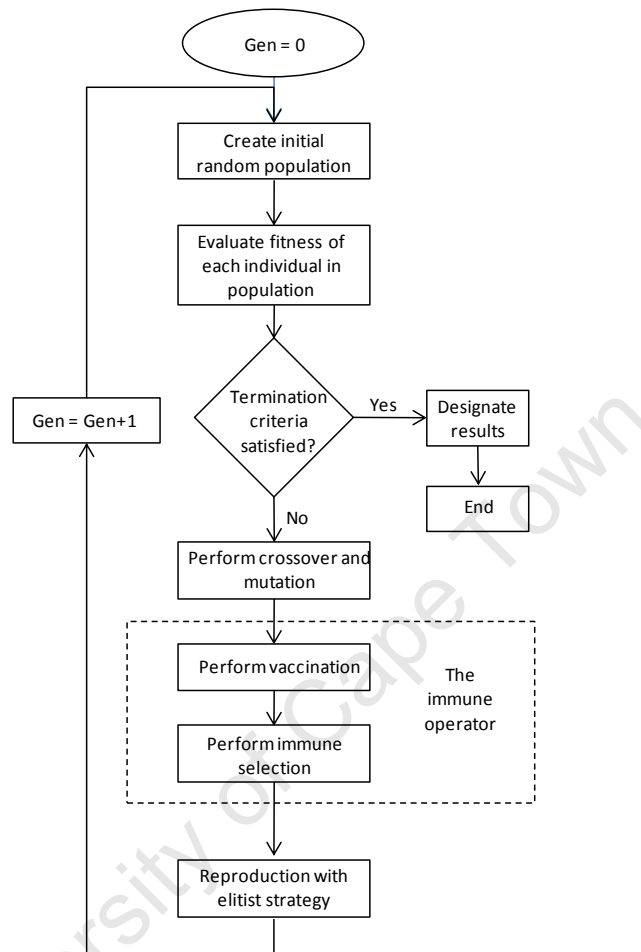
\*The authors do not give the specific sites for PMU placement

Placement sites are provided for IEEE 14-bus and 30-bus systems. The number of current measurements to be made by each individual PMU is detailed in Table 3 above. This measure has a significant impact if the number of concurrent measurements that a PMU can make is limited.

Aminifar et al. [14] identified that the two operators of crossover and mutation in [13] caused a degeneracy effect. These authors proposed a revised method by introducing operators of

vaccination and immunity to abstract effective vaccines based on topological observability rules to prevent the degeneracy effect. This method is referred to as the immunity genetic algorithm (IGA).

The placement problem is resolved through the steps in Flowchart 2.



Flowchart 2: IGA flow diagram courtesy of [14]

Vaccines are abstracted from local information or prior knowledge of the problem. A critical vaccine is a vaccine that improves the efficiency of the algorithm greatly. For IGA there are three critical vaccines that are implemented to gain a higher fitness. These vaccines are as follows:

Vaccine 1: The buses with only one incident line should have no PMU installed.

Vaccine 2: A PMU should be assigned to a bus connected to a non-zero injection buses with one incident line.

Vaccine 3: Zero-injection buses may not need to have a PMU installed at that bus.

The results for minimum PMU placement in the IEEE bus networks are given in Table 4.

Table 4: Optimal PMU locations obtained by [14]

Power System	Number of PMUs	Placement sites	Execution time (seconds)
IEEE 14-bus	3	2,6,9	2
IEEE 30-bus	7	1,5,10,12,18,24,30	4
IEEE 57-bus	11	1,6,13,19,25,29,32,38,51,54,56	11
IEEE 118-bus	28	3,8,11,12,17,21,25,28,34,35,40,45,49,53,56,62,72,75,77,80,85,86,90,94,102,105,110,114	72

IGA gives different PMU placement positions to [13] as well as finding a smaller minimum number of PMUs for both an IEEE-57 bus and IEEE-118 bus system. No execution times were provided by the method in [13] however for IGA execution times associated with the test bus systems are indicated in Table 4. IGA was used to place PMUs in a network containing 2746 buses and 3514 lines. It converged to a solution in 44 hours. Neither [13] nor [14] considered modelling contingencies in their network models.

Milosevic et al. [15] used graph theory and a non-dominating sorting genetic algorithm to search for the best trade-off between competing objectives of maximising observability and redundancy. The objectives are conflicting due to the fact that the improvement of one leads to the degradation of the other. Concepts of pareto-optimal solutions were utilized, the detail of which will not be divulged in this work. The method was tested on IEEE-39 and IEEE-118 bus systems. It was indicated that 8 PMUs were needed for full observability of the IEEE-39 bus system however the number of PMUs needed for the full observability of the IEEE-118 bus system was not provided.

#### 2.1.2. Tree search and topology

Nuqui et al. [16] made use of spanning trees of the power system graph to find the optimal placement locations of PMUs based on the desired depth of observability. Tree topology maps the network branches of a power system as sequential trees. The trees have direction and indicate the direction for the next PMU candidate placement.

For example consider Figure 13 which is a spanning tree of 14 nodes and 13 branches. If the search for the optimal placement with a depth of observability of zero is begun at the root node, node 1, the algorithm moves to from the root node to node 2. The algorithm places a PMU at node 2 (PMU-A) as it observes the root node. Then, a series of forwards moves is taken along the path **2** → **5** → **6** querying every position as a possible location for PMU placement. Node 5 is neglected as a placement node as it is observed however node 6 is the next logical step for PMU placement (PMU-B) as it is currently unobserved. The algorithm then proceeds along the path **6** → **5** → **4** → **9** once again querying every position. All positions are observed except node 9. Once again this is the logical place of placement for a PMU (PMU-C). Provided the algorithm has knowledge of observability of zero-injection buses, any direction the algorithm now moves and any node observability query it makes will be satisfied as every bus is observed. This search will be re-run from a different root node to ensure the number of PMUs is minimised for a defined level of depth of observability. Also, the search can be expanded on a subset of spanning trees of the power system graph.

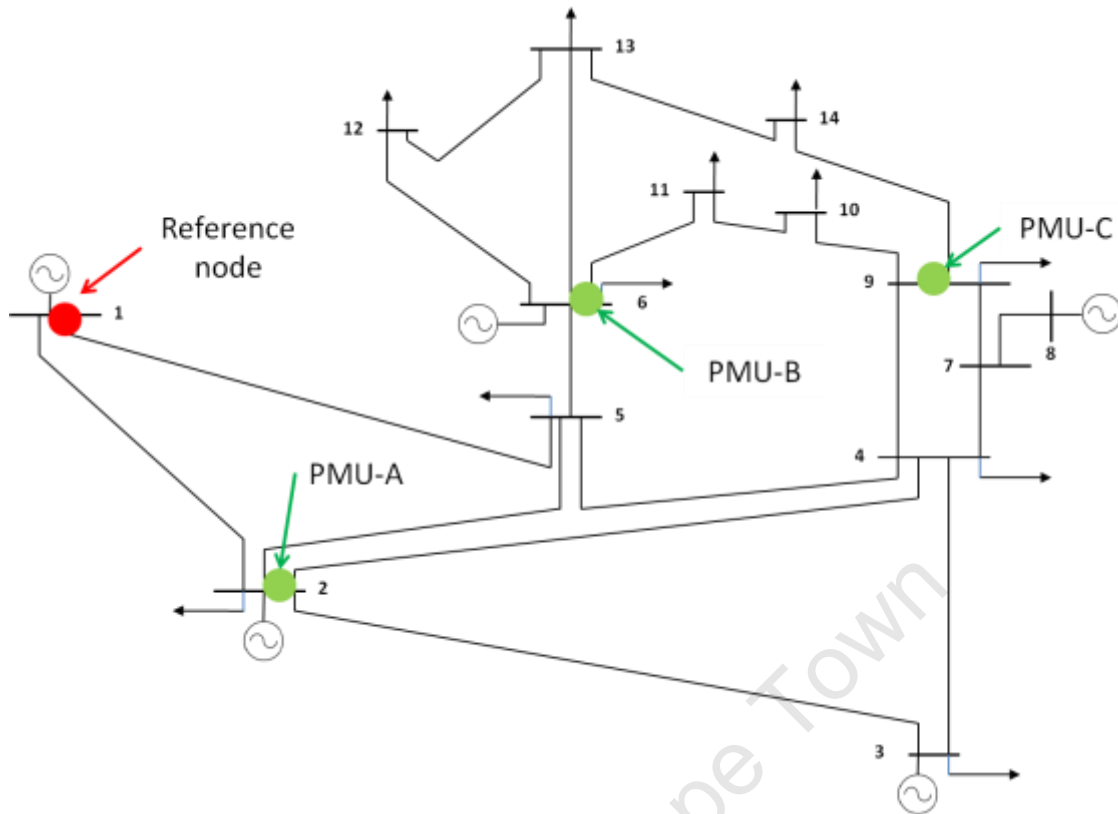


Figure 13: Tree search PMU placement technique

The depth of unobservability used in this work ranged from 1 to 3. The placement results are presented in Table 5.

Table 5: Required number of PMU placements for incomplete observability [16]

Power System	Number of PMUs for complete observability	Incomplete observability		
		Depth of 1	Depth of 2	Depth of 3
IEEE 14-bus	3	2	2	1
IEEE 30-bus	7	4	3	2
IEEE 57-bus	11	9	8	7

This work stated that complete PMU placement at each substation in large networks is rarely conceivable due to cost or non-existence of communication facilities in some substations. It considered communication constrained PMU placement using simulated annealing (SA) to constrain the placement of a PMU on a bus with no existing communications infrastructure. It also considered phased installation of phasor measurement units. At every stage of phasing the resulting depth of observability was lowered. It finally considered indentifying locations of new communications facilities to move towards complete observability.

Baldwin et al. [17] used a dual bisecting search algorithm and simulated annealing method based on topological observability to choose optimal minimum PMU and placement locations. This method suffered from excessive calculation burden when applied to a large power system.

Table 6: Number of PMUs needed for full system observability [17]

Power System	Number of PMUs needed for full observability
IEEE 14-bus	3
IEEE 39-bus	8
IEEE 118-bus	29

Peng et al. [18] introduced a topological method based on the augment matrix and Tabu Search (TS). The results of the method are given in Table 7.

Table 7: Optimal number of PMUS needed for full system observability [18]

Power System	Number of PMUs needed for full observability
IEEE 14-bus	3
IEEE 39-bus	10
IEEE 57-bus	13

Rakpenthai et al. [19] used a PMU placement method based on the minimum condition number of the normalized measurement matrix. It used binary integer programming to optimise redundant measurements then used a heuristic algorithm to rearrange the measurements to minimize the number of PMU placement sites. It considered single branch outages and measurement loss contingencies.

### 2.1.3. Particle Swarm Optimization

Particle Swarm Optimisation (PSO) was first developed by Kennedy and Eberhart in 1995 and it was inspired by the behaviour of bird flocks and fish schools [20]. PSO is a population-based search in which individuals, referred to as particles, fly around in a multidimensional search space, changing their positions as time progresses. Their positions are recorded in a position array. The position array is a possible solution to the problem. In addition, each particle has a velocity array. The velocity array is used to adjust the position of the particle at each iteration. During flight each particle adjusts its position according to its best experience and its neighbour's best experience.  $pbest$  and  $gbest$  are defined as the particles best solution and the neighbour's best solution respectively. Equations (9) and (10) show the iterative mechanism of conventional PSO.

$$v_i^{k+1} = w_i v_i^k + c_1 * rand * (pbest - x_i^k) + c_2 * rand * (gbest - x_i^k) \quad (9)$$

$$x_i^{k+1} = x_i^k + v_i^{k+1} \quad (10)$$

where  $v_i^k$  is the current velocity particle  $i$  at iteration  $k$ ;  $v_i^{k+1}$  is the modified velocity of particle  $i$ ;  $x_i^k$  is the current position of particle  $i$  at iteration  $k$ ;  $w_i$  weight function for velocity of particle  $i$ ; weight function for velocity of particle  $i$  and  $c_i$  is the acceleration coefficient of each term.

The first term of the velocity equation,  $w_i v_i^k$  represents the inertia of the previous velocity, the second term known as the *cognition term*,  $c_1 * rand * (pbest - x_i^k)$ , represents the individual particles and the third term known as the *social term*,  $c_2 * rand * (gbest - x_i^k)$ , represents the

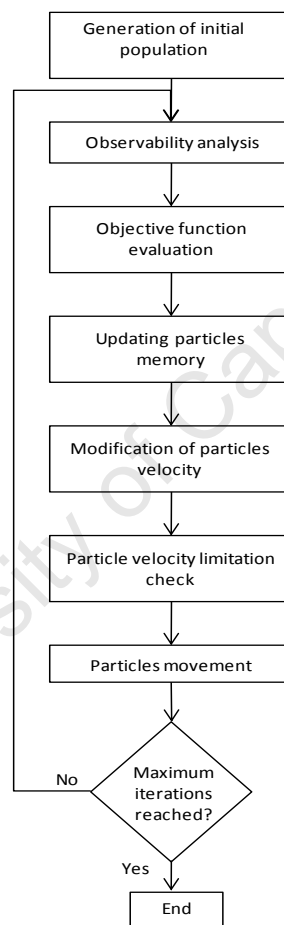
cooperation among neighbouring particles. The ‘rand’ terms are stochastic numbers arranged between 0 and 1. The best positions are derived according to this calculation in an iterative manner. Every time a better position is found, that position becomes the best solution.

The evaluation function evaluates the fitness of each individual in the population and is defined as:

$$f = c_1 * N_{PMU} + c_2 * N_H \quad (11)$$

where  $N_{PMU}$  and  $N_H$  are the number of installed PMUs and number of unobservable buses, respectively. The coefficients  $c_1$  and  $c_2$  are determined by trial and error.

The flowchart for the process of particle swarm optimisation is shown below in Flowchart 3.



Flowchart 3: Application of PSO for PMU placement algorithm.

The generation of the initial population is done using the graph theory search procedure and an initial PMU placement is made for complete system observability. Therefore this placement is assigned to a particle, with all the other particles generated randomly. An observability analysis is carried out to determine the number of existing PMUs and the number of unobserved buses corresponding to each particle. The fitness of each particle in the population is then checked using the evaluation function defined by equation (11). The algorithm uses the following logic: If the evaluation of each particle is better than the previous, set the current value to *pbest*. If *pbest* is better than *gbest* replace *gbest* with *pbest*. The next steps simply modify the particle’s velocity and

position and check whether they are not violating operational constraints. The algorithm finishes when the maximum iteration limit is reached.

For PMU placement Binary Particle Swarm Optimisation (BPSO) performs a better solution than conventional PSO as its search space is discrete and the variables can only take on values of 0 and 1 [21]. The position array of a particle in BPSO gives the information of PMU installation location. A binary '1' indicates the installation of a PMU at a bus and a binary '0' represents no installation of a PMU at a bus.

Hajain et al. [21] uses a BPSO to minimise the number of PMUs for full system observability. The results are summarised in Table 8.

Table 8: Minimum number of PMUs required for complete observability

Power System	Number of PMUs	Placement sites
IEEE 14-bus	3	2,6,9
IEEE 30-bus	7	2,3,10,12,18,24,27
IEEE 57-bus	11	1,5,13,19,25,29,32,38,41,51,54
IEEE 118-bus	28	2,8,11,12,17,21,25,28,33,34,40,45,49,52,56,62,72,75,77,80,85,86,90,94,101,105,110,114

Su et al. [22] used BPSO to optimise PMU placement relative to a cost function based on the number of adjacent branches joining a bus with an installed PMU. Peng et al. [23] used a BPSO combined with an immunity algorithm to place PMUs in a power system whilst taking into account N-1 observability redundancy. Gao et al. [24] utilized BPSO combined with a genetic algorithm to increase the speed of convergence. All three introduced some novel ideas however in retrospect none improved on the minimum number of PMUs required for full system observability.

#### 2.1.4. Binary search

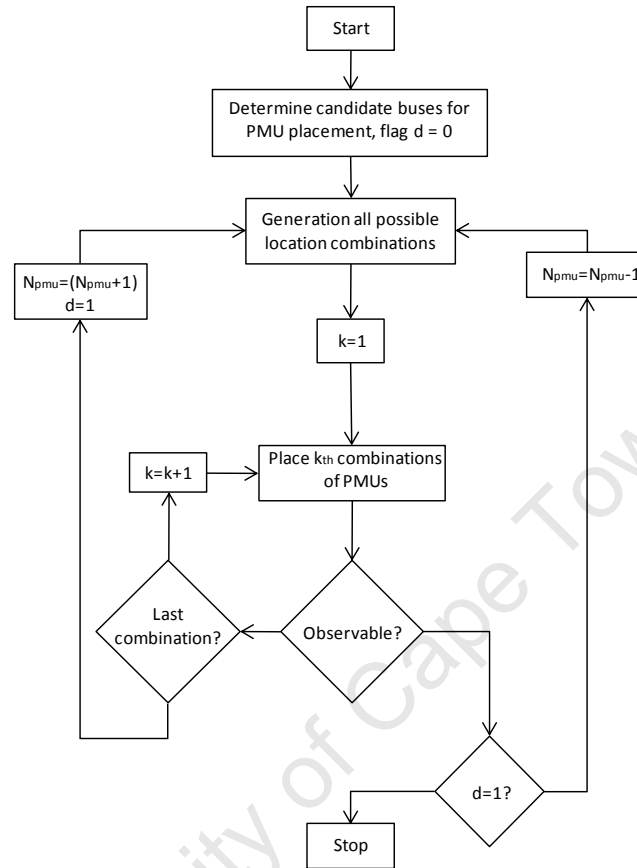
Binary search is an exhaustive algorithm that examines all possible combinations of locations before arriving at a minimum number of PMUs needed to make the system observable. The search process for the minimum PMU number is outlined in Flowchart 4. Baldwin et al. [17] identified an upper theoretical bound on the minimum number of PMUs that are needed for full observability given by equation (12).

$$N_{PMU}^{ub} = \left\lceil \frac{N + \frac{s}{2}}{3} \right\rceil \quad (12)$$

where  $N$  is the total number of candidate buses in the system and  $s$  is the number of unknown power injections.  $N_{PMU}^{ub}$  is the rounded up value of the quantity in the brackets. The initial number of PMUs is taken as equal to the upper bound of the minimum number of PMUs in given by equation (12) and a flag  $d = 0$  is set. The algorithm then generates an exhaustive set of combinations of  $N_{PMU}^{ub}$  out of  $P$  candidate buses using equation (13).

$$N_{solution} = \frac{P!}{N_{PMU}! (P - N_{PMU})!} \quad (13)$$

The algorithm considers one combination at a time. If the system is found to be unobservable for every combination of PMU location then the minimum number is increased by one. Intuitively, if the system is found to be observable for any combination of PMU locations the minimum number of PMUs is decreased by one. The search is repeated until the minimum number of PMUs is found.



Flowchart 4: Binary search algorithm to determine minimum number of PMUs required for full system observability

Chakrabarti et al. [25] used binary search to propose a method that provided the most preferred pattern of measurement redundancy. In addition the method focused on placing PMUs so that observability was maintained in the event of a single branch outage. The results are tabulated in Table 9 and Table 10.

Table 9: Minimum number of PMUs to make the system observable under normal operating conditions

Power System	Number of PMUs	Placement sites
IEEE 14-bus	3	2,6,9
IEEE 30-bus	7	1,2,10,12,15,20,27
IEEE 39-bus	8	3,8,12,16,20,23,25,29

Table 10: Minimum number of PMUs to make the system observable under single line outages

Power System	Number of PMUs	Placement sites
IEEE 14-bus	7	2,4,5,6,9,10,13
IEEE 30-bus	10	2,3,5,10,12,15,17,19,24,27
IEEE 39-bus	11	2,3,6,10,16,20,21,23,25,26,29

## 2.2. Deterministic techniques

Deterministic techniques make extensive use of integer programming and numerical based methods. Integer programming requires all unknown variables to take on integer values. Unknown variables are inserted into a linear equation that can be solved with an optimization technique such as TOMLAB Optimization Toolbox Mixed Integer Linear Programming (MILP) [26].

### 2.2.1. Integer linear programming

Linear programming (LP) is a mathematical method for determining the best outcome for a list of requirements represented as linear relationships. More specifically linear programming is a technique for the optimisation of a linear objective function subject to linear equality and inequality constraints. A linear programming problem can be expressed in standard form as:

$$\begin{aligned}
 & \text{maximise } c^T x \\
 & \text{subject to } Ax \leq b \\
 & \text{and } x \geq 0
 \end{aligned} \tag{14}$$

where  $x$  represents the vector of variables to be determined,  $c$  and  $b$  are vectors of known coefficients and  $A$  is a matrix of known coefficients.  $c^T x$  is called the objective function and the equations  $Ax \leq b$  and  $x \geq 0$  are the constraints to be satisfied. Integer linear programming (ILP) has all the variables restricted to integer values. ILP is commonly referred to as mixed integer programming.

Work utilizing ILP for the optimal placement problem (OPP) has been pioneered by Abur et al. [27], [28] to place PMUs to satisfy full observability criteria and to take the presence of conventional measurements into account. For an  $n$ -bus system the PMU placement problem is based on the manipulation of equation (14) and can be formulated as follows:

$$\begin{aligned}
 & \min \sum_i^n W_i \cdot x_i \\
 & \text{subject to } f(X) \geq \hat{1}
 \end{aligned} \tag{15}$$

where  $W_i$  is the cost of the PMU installed at bus  $i$ ;  $f(X)$  is a vector function whose entries are non-zero if the corresponding bus voltage is solvable using the provided measurement set and zero otherwise;  $X$  is a binary decision variable vector whose entry is equal to 1 if a PMU is installed at bus  $i$  and 0 otherwise;  $\hat{1}$  is a vector whose entries are all ones. The minimization function ensures that the number and cost of PMUs are minimized subject to the vector function solution being greater than or equal to 1 which ensures full observability.

Consider Figure 14 as a test bus system for the application of ILP to solve OPP.

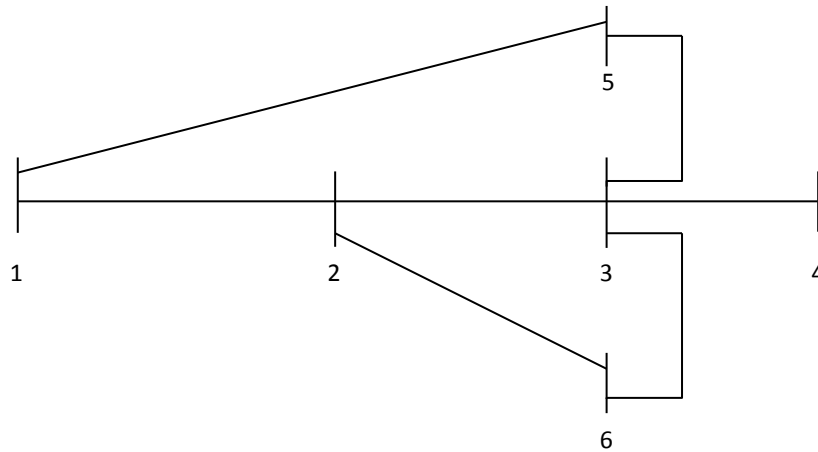


Figure 14: 6-Bus test system for ILP application

The connectivity matrix  $A$  can be directly obtained by inspection of Figure 14 and is given as:

$$A = \begin{bmatrix} 1 & 1 & 0 & 0 & 1 & 0 \\ 1 & 1 & 1 & 0 & 0 & 1 \\ 0 & 1 & 1 & 1 & 1 & 1 \\ 0 & 0 & 1 & 1 & 0 & 0 \\ 1 & 0 & 1 & 0 & 1 & 0 \\ 0 & 1 & 1 & 0 & 0 & 1 \end{bmatrix} \quad (16)$$

The connectivity matrix can be used to form constraints given by  $f(X) = Ax \geq 1$

$$f(X) = \begin{cases} f_1 = & x_1 + x_2 + x_5 & \geq 1 \\ f_2 = & x_1 + x_2 + x_3 + x_6 & \geq 1 \\ f_3 = & x_2 + x_3 + x_4 + x_5 + x_6 & \geq 1 \\ f_4 = & x_3 + x_4 & \geq 1 \\ f_5 = & x_1 + x_3 + x_5 & \geq 1 \\ f_6 = & x_2 + x_3 + x_6 & \geq 1 \end{cases} \quad (17)$$

The '+' operator serves as the logical 'OR'. Therefore the presence of a 1 in the right hand side of the inequality ensures that at least one of the variables present in the sum will have a non-zero value. For example, consider the constraint associated with bus 1 given as:

$$f_1 = x_1 + x_2 + x_5 \geq 1 \quad (18)$$

This constraint implies that at least one PMU must be placed at either bus 1, bus 2 or bus 5 in order to make bus one observable. The results from [27] are tabulated in Table 11 below.

Table 11: Minimum PMU placement for [27]

Power System	Number of PMUs	Execution time (seconds)
IEEE 14-bus	3	2
IEEE 57-bus	12	4
IEEE 118-bus	29	44

This method used network analysis and cost of PMU installation with mixed measurement sets, which included conventional power flow and injection measurements as constraints for optimal PMU placement.

Gou [29] used an integer programming technique accounting for power networks with and without conventional power flow and injection measurements. This concept was extended in [30] to consider zero-injection buses, incomplete observability and depth of observability. The results are presented in Table 12 to Table 13 below.

Table 12: Number of PMU placement for observability without zero-injections

Power System	Complete observability	Depth-of-1 unobservability	Depth-of-2 unobservability
IEEE 14-bus	4	2	2
IEEE 30-bus	10	4	3
IEEE 57-bus	17	11	8

Table 13: Number of PMU placement for observability including zero-injections

Power System	Complete observability	Depth-of-1 unobservability	Depth-of-2 unobservability
IEEE 14-bus	3	2	2
IEEE 30-bus	7	4	3
IEEE 57-bus	11	9	8

Results bearing the impact of zero-injection bus consideration were included here to demonstrate the fact that the modelling of zero-injection buses effectively decreases the minimum number of PMUs needed for full observability. Depth of observability results give exactly the same number of PMUs as was proposed by Nuqui in [16] using a tree search placement method.

Dua et al. [31] used an ILP approach for phasing of PMU placement over a given time horizon. PMU placement for each stage maximized observability. This paper proposed using two indices bus observability index (BOI) and system observability redundancy index (SORI) to rank multiple solutions for PMUs observing a given bus. BOI indicates the number of PMUs that observe a given bus. SORI is the sum of all the BOIs for a given system. Therefore it used SORI to qualitatively compare PMU placement solutions with the aim to maximise overall system redundancy. This method considered phasing, zero-injection buses and PMU outages. The results for the minimum PMU placement are given in Table 14.

Table 14: Minimum number of PMUs for complete observability

Power System	Complete observability	Single PMU outage
IEEE 14-bus	3	7
IEEE 57-bus	14	29
IEEE 118-bus	29	64

Aminifar et al. [32] developed a basic ILP model for network observability. This method considered the effect of zero-injection buses, line outages and loss of measurement. The results for minimum PMU placement number are given in Table 15 and Table 16.

Table 15: PMU placement for IEEE standard test systems in different states

Power System	Complete observability	Line outage	Loss of measurement	Line outage or loss of measurement
IEEE 14-bus	3	7	7	8
IEEE 30-bus	7	13	15	17
IEEE 39-bus	8	15	18	22
IEEE 57-bus	11	19	26	26
IEEE 118-bus	28	53	63	65

Table 16: PMU placement for IEEE standard test systems for the base case

Power System	Base case	Placement buses
IEEE 14-bus	3	2,6,9
IEEE 30-bus	7	3,5,10,12,18,24,27
IEEE 39-bus	8	3,8,11,16,20,23,25,29
IEEE 57-bus	11	1,4,13,20,25,29,32,38,51,54,56
IEEE 118-bus	28	3,9,11,12,17,21,25,28,34,37,40,45,49,53,56,62,72,75,77,80,85,86,90,94,102,105,110,114

### 2.3. Summary of literature review

From the literature review, it is apparent that many methods exist for solving the optimum number of PMUs required for full system observability. The methods that have been reviewed are summarised in Table 17 for comparison.

Table 17: Minimum PMU placement comparison for reviewed methods

Method	Test systems				
	IEEE 14-Bus	IEEE 30-Bus	IEEE 39-Bus	IEEE 57-Bus	IEEE 118-Bus
Particle Swarm Optimisation [21]	3	7	-	11	28
Dual Search and SA [17]	3	-	-	-	29
Integer Programming [27]	3	-	-	12	29
Search Tree and SA [16]	3	7	-	11	-
Genetic algorithm [13]	3	7	-	12	29
Tabu Search [18]	3	-	10	13	-
Immunity Genetic Algorithm [14]	3	7	8	11	28
Nondominated sorting genetic algorithm [15]	-	-	8	-	29
Optimal Multi-stage [31]	3	-	-	14	29
Contingency-constrained [32]	3	7	8	11	28
Binary Search [25]	3	7	8	-	-
Generalized integer linear programming [30]	3	7	-	11	-

Nearly all of the reviewed algorithms converge to the same minimum number of PMUs for each standardized IEEE test bus system. The lowest number of PMUs required for full system observability for each test system has been derived from the review of the aforementioned algorithms and is given in Table 18.

Table 18: Optimal minimum number of PMUs for full system observability

Test System	Optimal minimum number of PMUs
IEEE 14-Bus	3
IEEE 30-Bus	7
IEEE 39-Bus	8
IEEE 57-Bus	11
IEEE 118-Bus	28

On this basis, the best performing algorithms can be singled out. [14], [21] and [32] converge to the lowest optimal number of PMUs based on integer programming, immunity genetic algorithm and binary particle swarm optimisation respectively. However, the classification and choice of algorithm does not only depend on reaching the optimal minimum number. An algorithm should be adaptable in terms of the ability for a user to model zero-injection buses, contingencies, redundancy, depth of observability and phasing. In addition it is preferred that an algorithm converge quickly for large power systems so that different modeling scenarios can be compared. For this reason, a chart has been created that indicates the documented adaptability of each algorithm in this regard.

	PSO	Binary Search	GA	IP	Tree Search	Topology based
Optimal PMU number	•	•	•	•	•	•
Zero-injection	•	•	•	•	•	•
Phasing				•	•	
Redundancy	•			•	•	•
Depth of observability				•	•	
Line outage		•		•	•	•
PMU outage				•	•	•
Limited communications				•	•	
Critical buses	•	•	•	•	•	•
Fast execution time for large systems				•		

Figure 15: Algorithm adaptability assessment

From Figure 15 it is clear that integer programming is the most adaptable algorithm. Therefore a method incorporating integer linear programming will be designed and implemented for optimal PMU placement in this work.

### 3. Chapter 3: Integer linear programming method

This chapter explains the concepts and equations behind designing an optimal placement method to utilise ILP (integer linear programming). ILP has been chosen due to its adaptability and relatively quick execution time. It should be mentioned that many methods that were reviewed mentioned the execution time for the method to converge to a solution. The author of this work is of the opinion that the execution time is not of vital importance as the process of PMU placement is an offline process. However, a short execution time is helpful due to the fact that many placement strategies can be studied without running into significant time constraints.

#### 3.1. Integer programming method development

ILP has been previously utilised in [27], [28], [29], [30], [31] and [32]. In these instances, CPLEX solver was used in either a Matlab or GAMS environment to solve the mixed integer programming problem. In this work TOMLAB CPLEX MILP solver will be used in the Matlab environment. The guide to using TOMLAB CPLEX can be found at [26].

Although the basics behind ILP were outlined in chapter 2, the basic equations will be reviewed here once again to provide greater context and flow to the work.

Work utilizing ILP for OPP has been pioneered by Abur et al. [27].

For an  $N$  (number of buses) system the PMU placement problem is modelled as follows:

$$\begin{aligned} \min_x f(x) &= c^T x \\ \text{such that } x_L &\leq x \leq x_U \\ \text{and } b_L &\leq Ax \leq b_U \end{aligned} \quad (19)$$

where  $x$  represents each bus;  $c$  is a transpose of vector of  $N$  rows and one column representing the number of state variables and  $A$  is the connectivity matrix.

$x_L$  and  $x_U$  are given as:

$$x_L = [0 \quad 0 \quad 0 \quad \cdots \quad 0] \quad (\text{All columns set to zero})$$

$$x_U = [1 \quad 1 \quad 1 \quad \cdots \quad 1] \quad (\text{All columns set to one})$$

$x_L$  and  $x_U$  sets the binary limitation that the specific entity is either present or not. Both  $x_L$  and  $x_U$  have a  $N$  number of columns and one row.

The values of the  $b_L$  vector determine the desired redundancy level of each bus with all of its constituents bigger or equal to one.

If  $b_L$  was made up of just ones then it would mean that all of the buses need to be observed by one PMU. This is the basic criterion for full observability. If some or all of the columns of  $b_L$  are greater than one, for example, 3, it means that at least 3 PMUs are required for that specific optimization.

The basic form of  $b_L$  is therefore:

$b_L = [1 \ 1 \ 1 \ \dots \ 1]$  (All columns set to one)

$b_U$  is the maximum number of times a PMU observes a specific bus in the system and should not be limited since for the optimal placement problem, the  $b_L$  vector is the main constraint that is used.

So  $b_U$  is set to:

$b_U = [inf \ inf \ inf \ \dots \ inf]$  (All columns set to infinity)

Both  $b_L$  and  $b_U$  have a  $N$  number of columns and one row.

Consider Figure 16 as a test bus system for the application of ILP to solve OPP. There are no conventional measurements. Bus 2 is a zero-injection bus. Although this test bus is not used to benchmark this method, it serves as a small system to demonstrate the concepts effectively.

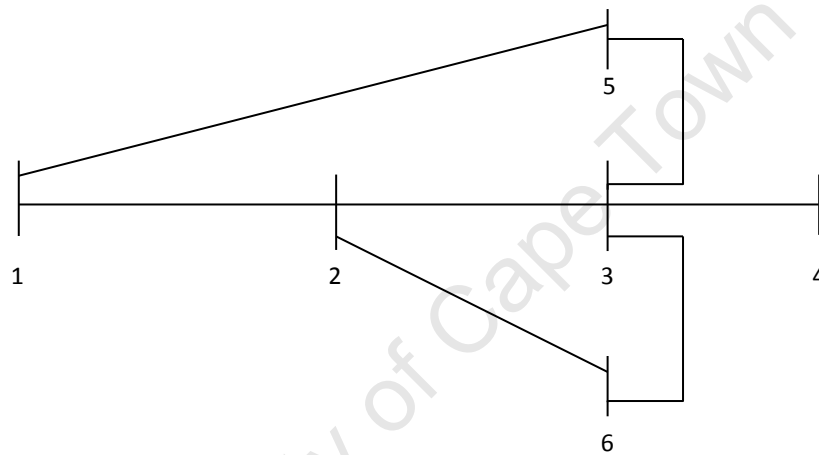


Figure 16: 6-Bus test system for ILP application

The connectivity matrix can be directly obtained by inspection of the figure above and is given as:

$$A = \begin{bmatrix} 1 & 1 & 0 & 0 & 1 & 0 \\ 1 & 1 & 1 & 0 & 0 & 1 \\ 0 & 1 & 1 & 1 & 1 & 1 \\ 0 & 0 & 1 & 1 & 0 & 0 \\ 1 & 0 & 1 & 0 & 1 & 0 \\ 0 & 1 & 1 & 0 & 0 & 1 \end{bmatrix} \quad (20)$$

The constraints can be formed as:

$$f(X) = \begin{cases} f_1 = & x_1 + x_2 + x_5 & \geq 1 \\ f_2 = & x_1 + x_2 + x_3 + x_6 & \geq 1 \\ f_3 = & x_2 + x_3 + x_4 + x_5 + x_6 & \geq 1 \\ f_4 = & x_3 + x_4 & \geq 1 \\ f_5 = & x_1 + x_3 + x_5 & \geq 1 \\ f_6 = & x_2 + x_3 + x_6 & \geq 1 \end{cases} \quad (21)$$

CPLEX is set up to run so that all buses have a redundancy of one (fully observable). This is done by setting  $b_L = [1 \ 1 \ 1 \ 1 \ 1 \ 1]$ . The resulting placement is calculated to be  $x_{optimal} = [1 \ 0 \ 1 \ 0 \ 0 \ 0]$ . This result states that PMU placement at buses 1 and 3 provide full observability for this 6 bus system. As the system is small, this can be verified by placing PMUs at these buses to ensure that all the system buses are indeed observed.

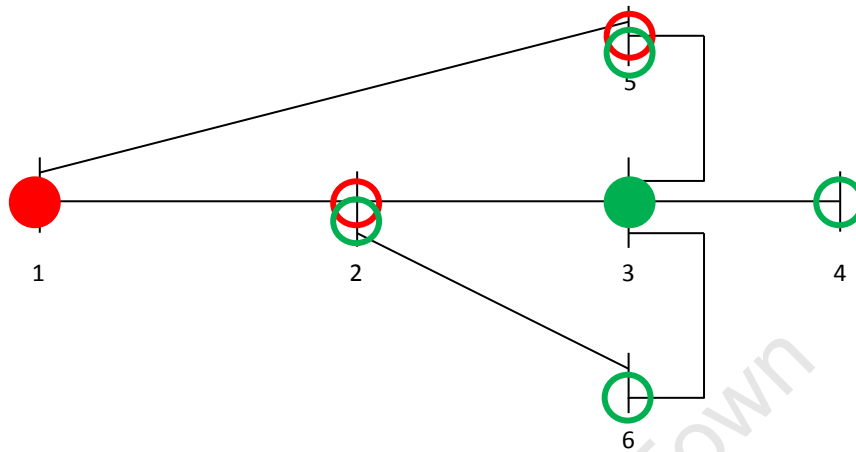


Figure 17: Minimum PMU placement number for full observability for the base case

The figure above indicates that a PMU placed at bus 1 observes buses 2 and 5, while a PMU placed at bus 3 observes buses 2, 4, 5 and 6. Therefore, this PMU placement strategy renders the system completely observable.

### 3.1.1. Dealing with zero-injection buses

If it is assumed that bus 2 is a zero-injection bus then the PMU placement strategy can be altered by applying the following zero-injection bus properties:

- 1.) When buses incident to an observable zero-injection bus are all observable, except for one, the unobservable bus will be made observable by applying KCL at the zero-injection bus.
- 2.) When buses incident to an unobservable zero-injection bus are all observable, the zero-injection bus will be made observable by applying KCL at the zero-injection bus.

This is modeled by ensuring that all buses minus one,  $n - 1$ , incident to a zero-injection bus are observable. Therefore in the 6 bus example, buses 1, 3 and 6 are incident to the zero-injection bus. Two of these buses must be made observable at all times. Bus 3 is identified as being the most critical bus due to the fact that it has many incident lines. As a practical example, the term 'critical bus' could be used to indicate that bus 3 has a high capacity generation source that is imperative to power system operation that must be monitored at all times. Therefore bus 3 should be directly monitored by a PMU and not be estimated through the use of the zero-injection bus. Therefore either bus 1 or 6 should be considered as a PMU placement position.

Therefore if bus 6 is to be made observable through the zero-injection bus rules, bus 6 is eliminated from equation (22) by setting the row equal to zero.

The constraints can be formed as:

$$f(X) = \begin{cases} f_1 = & x_1 + x_2 + x_5 & \geq 1 \\ f_2 = & x_1 + x_2 + x_3 + x_6 & \geq 1 \\ f_3 = & x_2 + x_3 + x_4 + x_5 + x_6 & \geq 1 \\ f_4 = & x_3 + x_4 & \geq 1 \\ f_5 = & x_1 + x_3 + x_5 & \geq 1 \\ f_6 = & x_2 + x_3 + x_6 & \geq 0 \end{cases} \quad (22)$$

Solving equation (22) results in the PMU placement result of  $x_{optimal} = [1 \ 0 \ 1 \ 0 \ 0 \ 0]$ .

The other option is to assume that bus 1 is made observable through the zero-injection bus.

The constraints can be formed as:

$$f(X) = \begin{cases} f_1 = & x_1 + x_2 + x_5 & \geq 0 \\ f_2 = & x_1 + x_2 + x_3 + x_6 & \geq 1 \\ f_3 = & x_2 + x_3 + x_4 + x_5 + x_6 & \geq 1 \\ f_4 = & x_3 + x_4 & \geq 1 \\ f_5 = & x_1 + x_3 + x_5 & \geq 1 \\ f_6 = & x_2 + x_3 + x_6 & \geq 1 \end{cases} \quad (23)$$

Solving this equation results in the PMU placement result of  $x_{optimal} = [0 \ 0 \ 1 \ 0 \ 0 \ 0]$ . This placement strategy requires one less PMU. It can be verified by placing a PMU at bus 3 to ensure that all system buses are made fully observable.

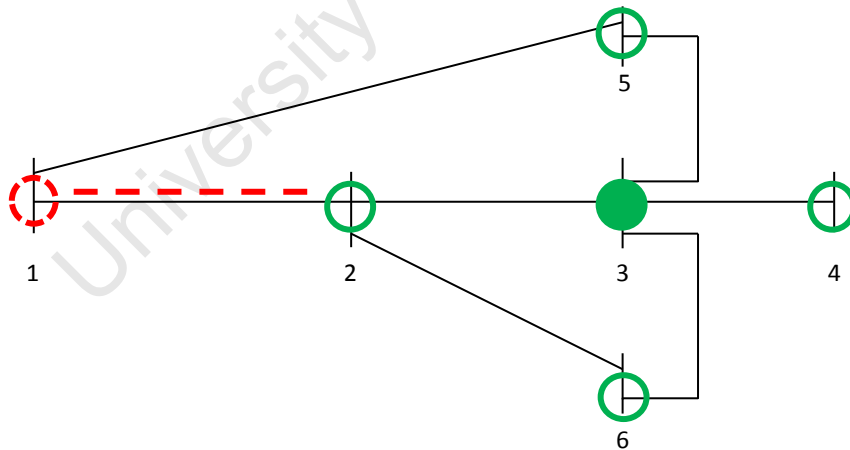


Figure 18: Minimum PMU placement number for full observability considering zero-injections

It is seen that the placement of a PMU at bus 3 enables bus 1 to be made observable through the properties of the zero-injection bus at bus 2.

### 3.1.2. Loss of measurement

In the event of a PMU or line failure the system should remain fully observable. This can be achieved by having every bus in the system observed by at least two individual PMUs. In a practical situation however, the number of PMUs may be limited due to a factor such as cost constraints. Under these

conditions, where not every bus is observed by at least two PMUs, the system observability redundancy index (SORI) can be used to qualitatively compare PMU placement solutions with the aim to maximise overall system redundancy.

The constraints can be formed as:

$$f(X) = \begin{cases} f_1 = & x_1 + x_2 + x_5 & \geq 2 \\ f_2 = & x_1 + x_2 + x_3 + x_6 & \geq 2 \\ f_3 = & x_2 + x_3 + x_4 + x_5 + x_6 & \geq 2 \\ f_4 = & x_3 + x_4 & \geq 2 \\ f_5 = & x_1 + x_3 + x_5 & \geq 2 \\ f_6 = & x_2 + x_3 + x_6 & \geq 2 \end{cases} \quad (24)$$

Every bus in the system must be observed by at least two times. Once again bus 2 is considered as a zero-injection bus. The role of the zero-injection bus becomes significant due to the fact the each bus connected to the zero-injection bus can be made observable provided the entire system has a redundancy of at least one.

Solving this equation results in the PMU placement result of  $x_{optimal} = [1 \ 0 \ 1 \ 1 \ 0 \ 0]$ . Therefore 3 PMUs placed at buses 1, 3 and 4 are required for the system to remain fully observable should any one PMU fail. It should be noted that the PMU placed at bus 1 provides a redundancy of 2 for bus 6 through the zero-injection bus at bus 2. The same principle applies to bus 3 providing a redundancy of 2 for bus 1.

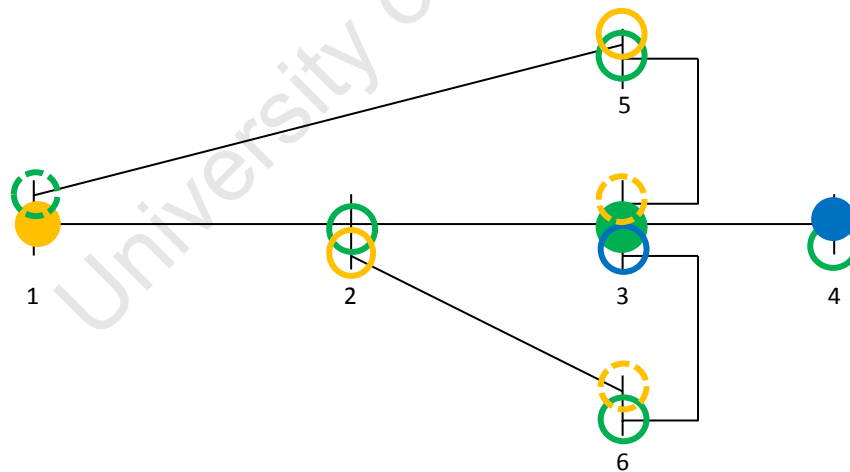


Figure 19: Minimum PMU number required for system redundancy of two

Figure 19 shows the redundancy at each bus. In all cases the redundancy is greater than 2. For example, consider Figure 20 where the PMU placed at bus 3 fails.

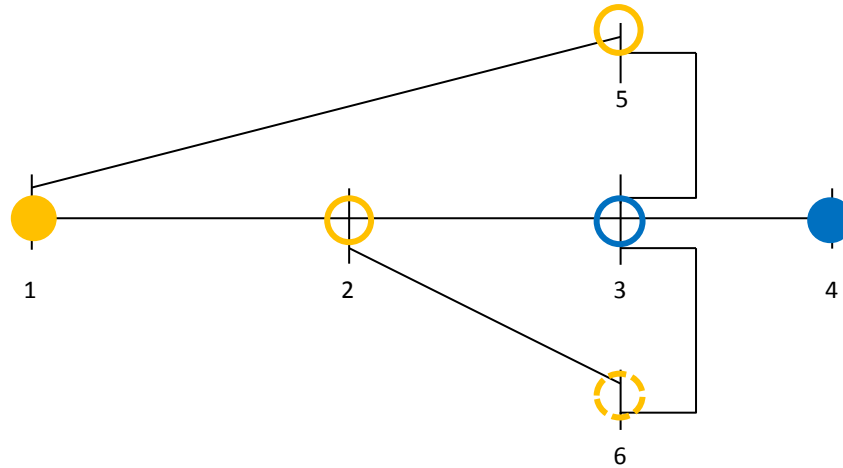


Figure 20: PMU device failure at bus 3

If the PMU at critical bus 3 failed, the bus would remain observable through PMU placed at bus 4. Bus 6 would remain observable through the PMU placed at bus 1 via the zero-injection bus at bus 2.

### 3.1.3.Placement results for test bus positions

The ILP algorithm was developed tested on the IEEE 14, 30 and 57 bus systems. It considered minimal placement of PMUs under three objectives: (1) Place a minimum number of PMUs in a system for full observability without considering zero-injection buses. (2) Place a minimum number of PMUs in a system for full observability considering the effects of zero-injection buses. (3) Place a minimum number of PMUs in the system so that in the case of a line outage or loss of measurement the entire system remains fully observable. Table 19 gives the results of the ILP algorithm.

Table 19: Results of optimal placement positions for ILP algorithm

Bus Type	No. of PMU	Positions	Zero-injection included	Positions	Line outage or loss of measurement	Positions
14	4	2,6,7,9	3	2,6,9	9	1,2,4,6,7,8,9,10,13
30	10	1,2,6,9,10,12,15,18,25,27	7	1,5,10,12,15,18,27	21	1,2,3,5,6,8,9,10,11,12,13,15,16,18,19,21,23,25,26,27,29
57	17	1,6,9,15,19,22,24,28,30,32,36,38,41,47,51,53,57	11	1,4,13,20,25,29,32,38,51,54,56	33	1,2,4,6,9,12,15,19,20,22,24,25,26,28,29,31,32,33,35,36,38,39,41,43,44,46,47,50,51,53,54,56,57

The minimum number of PMUs needed for full system observability is four and three for the 14 bus system with the later number including the effects of zero-injection buses. Nine PMUs are needed to maintain full system observability in the case of line outage or loss of measurement..

The minimum number of PMUs needed for full system observability is ten and seven for the 30 bus system with the later number including the effects of zero-injection buses. Twenty one PMUs are needed to maintain full system observability in the case of line outage or loss of measurement.

The minimum number of PMUs needed for full system observability is seventeen and eleven for the 57 bus system with the later number including the effects of zero-injection buses. Thirty three PMUs are needed to maintain full system observability in the case of line outage or loss of measurement.

For objectives (1) and (2) the numbers match exactly to the minimum number of PMUs obtained in the literature summarised in Table 18. The modelling of zero-injection buses effectively decreases the needed number of PMUs for a given system. However, for objective (3) for line outage or loss of measurement the number of PMUs obtained is not optimal due to the fact that this minimum number does not include the effects of zero-injection buses.

It is easily proved that the number of PMUs needed for objective (3) for the 14 bus system can be decreased by one by removing the PMU located at bus 7. With this PMU placement scheme, all buses still have a redundancy of at least two, due to the fact that they are observed through use of the zero-injection bus properties. However, this scenario was not effectively modeled for all bus types and therefore the results have not been included in the above table. Reference [32] has an eloquent ILP that deals effectively with zero-injection buses for all contingencies.

The purpose of designing a placement algorithm is to use the minimum PMU number and placement positions to model the effects of including phasor measurement data in a hybrid and linear state estimator. Therefore the results of this ILP method will be used in subsequent chapters as a base for incorporating PMU phasor measurement data in state estimators.

## 4. Chapter 4: Utilising PMU measurement data to improve state estimation:

### 4.1. Process of State Estimation

Due to the fact that it is neither economically nor technically feasible to monitor a power system state at all buses and transmit all these measurements to a control centre, it becomes necessary to estimate the state of a power system. Fred Schweppe first proposed the idea of State Estimation (SE) in power systems [33],[34], [35]. SE refers to the procedure of obtaining the voltage phasors at all of the system buses at a specific point in time. SE collects redundant measurements in a power system and computes a state vector of the voltage at each bus. In the case of conventional state estimation (CSE), the measurements are non-linear functions of the system state. These measurements are collected and iterative calculations are performed to determine the most probable system state from the known information. In this chapter the methods for incorporating PMU measurements into a state estimator; the effects that the PMUs have on state estimation and the effect that the PMU placement location has on the state estimation accuracy are reviewed and modeled.

The operating conditions of a power system at a specific point in time can be determined if the network model and complex phasor voltages at every system bus are known. Since the set of complex phasor voltages fully specifies the system, it is referred to as the static state of the system [36]. A power system may move into one of three possible states, namely normal, emergency and restorative, as the operating conditions change [38]. A power system is said to be operating in a secure normal state if the occurrence of each contingency from a list of critical contingencies does not alter the system state from its normal state of operation. The goal of a Total System Operator (TSO) is to maintain a normal operating state by monitoring the system conditions, identifying the operating state and determining necessary preventive actions in case the system state is found to be insecure. The monitoring of the system state requires an acquisition and processing of measurements from all parts of the system. Conventionally, substations are equipped with RTUs that are responsible for making measurements. Measurements made by RTUs pertinent to state estimator include line power flows, power injections from generators and bus voltage and line current magnitudes. These raw measurements are processed by a state estimator to filter out gross errors and measurement noise. In essence the state estimator forms of real-time base from which all energy management systems (EMS) applications function. EMS applications include automatic generation and control, contingency analysis, load forecasting, optimal power flow, etc. Due to the fact that it is not technically and economically feasible to monitor and telemeter all possible system measurements, an EMS is equipped with an on-line state estimator. The state estimator is designed to run periodically to provide a consistent and reliable state of the system state based on the assumed measurement model and the available measurements. The solution is composed of complex bus voltages as well as a best estimate for all the line flows, loads, transformer taps and generator outputs.

A conventional state estimator utilizes measurements of bus voltage magnitudes, power flows and injections to predict the state variables of a power system. The magnitude and phase angle of bus voltages are considered as the state variables. The measurements model of state estimation is a nonlinear problem with the most common solution obtained through an iterative weighted least squares (WLS) technique which converts nonlinear equations into approximations by using a first-

order Taylor series. Conventional state estimators do not directly measure voltage and current phasor angle. Therefore the solution of the state estimator provides the best estimate of phasor angles based on conventional measurements. However, this is set to change with the introduction of the phasor measurement unit (PMU). The introduction of PMU technology is expected to significantly improve existing SE algorithms regarding accuracy, observability, bad data detection and topology estimation properties [39]. A state estimator is one of the more important utility network management applications that could benefit from the addition of synchronized phasor measurements. The inclusion of PMU measurements is expected to produce a more accurate state estimation due to the relatively small measurement variance.

In this work, state estimators are classified into three classes namely, a conventional state estimator, a hybrid state estimator and a linear state estimator. A conventional state estimator (CSE) uses power flows, power injections and voltage and current magnitude measurements to obtain a state vector solution. A hybrid state estimator (HSE) incorporates power flows, power injections, voltage and current magnitude measurements and voltage and current phasors from a defined number of PMUs to obtain a state vector solution. A linear state estimator uses only voltage and current phasor PMU measurements to obtain a state vector solution. The methods for incorporation of PMU measurements into a state estimator and accuracy effects of placement of PMUs into power systems are investigated in this work. The incorporation of PMUs into power systems is directly linked to the placement of PMUs covered in chapter 2.

Optimal placement solutions from chapter 3 are then used as placement positions for PMUs in the test bus systems and the effect of these PMU measurements on the accuracy of the state estimated are assessed.

## 4.2. Component modelling and assumptions

The state of a power system is a function of known and unknown system parameters. Known system parameters include network topology, resistance, reactance and shunt impedance of transmission lines. Unknown parameters include conventional measurements such as real and reactive power flows, real and reactive power injections and bus voltages. The unknown parameters are to be measured or estimated via state estimation.

It is assumed that the power system is operating under steady state conditions. This implies that all three phases of the network are balanced and that a single phase positive sequence equivalent circuit model can be used to represent the entire power system. In this work all network data are expressed in the per unit system on a 100 MVA base. IEEE test bus systems are utilised namely the 14, 30 and 57 test bus systems [8]. The optimal state solution for these systems is obtained by using a Matlab Power System Simulation Package known as Matpower 4.0 [40]. The following component models will thus be used in representing the entire network.

### 4.2.1. Transmission lines

Transmission lines are represented by a two-port  $\pi$ -model whose parameters correspond to the positive sequence equivalent circuit of transmission lines. This model is generally used for medium length transmission lines of lengths from 80km up to 240km [41]. Longer transmission lines are represented by a different model, however power flow calculations and most state estimation techniques use only four parameters to characterise the transmission line. The four parameters are: real copper losses in the conductor modeled by resistance; magnetic field surrounding the conductor

modeled by inductance; line charging modeled by shunt impedance and voltage at the node. Figure 21 shows the modeled components.

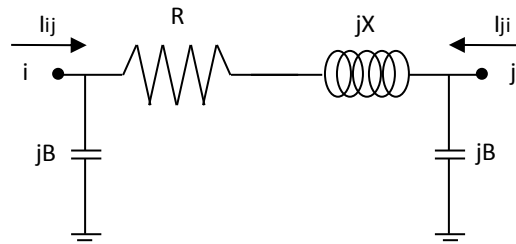


Figure 21: Equivalent circuit for a transmission line

$$\begin{bmatrix} I_{ij} \\ I_{ji} \end{bmatrix} = \begin{bmatrix} y_{ij} + y_{i0} & -y_{ij} \\ -y_{ij} & y_{ij} + y_{j0} \end{bmatrix} \begin{bmatrix} V_i \\ V_j \end{bmatrix} \quad (25)$$

$$\text{where } y_{ij} = \frac{1}{R+jX} \text{ and } y_{i0} = j\frac{B}{2}$$

The relationship between branch current, admittance and voltage is given by equation (25).

#### 4.2.2. Transformers

The equivalent circuit for an ideal off-nominal tap transformer is shown in Figure 22. The series impedance models the real losses in the copper coils and the inductance is a result of the conductors arranged in a coil. The expression 'a:1' represents the transformer turns ratio.

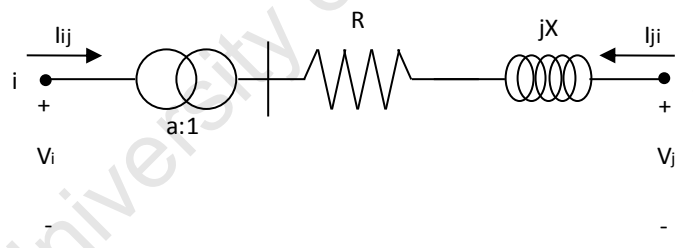


Figure 22: Equivalent circuit for an off-nominal tap transformer

The circuit can be represented as an equivalent circuit of an in-phase tap transformer depicted in Figure 23.

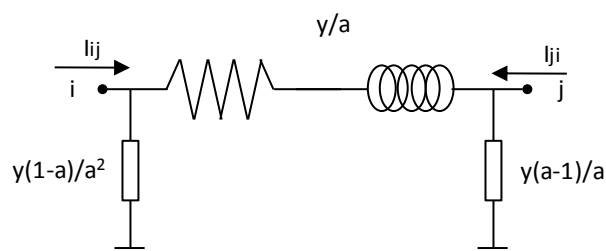


Figure 23: Equivalent circuit of an in-phase tap transformer

The relationship between the sending and receiving end current, voltage and admittance is given by equation (26).

$$\begin{bmatrix} I_{ij} \\ I_{ji} \end{bmatrix} = \begin{bmatrix} \frac{y_{ij}}{a} & \frac{-y_{ij}}{a} \\ \frac{-y_{ij}}{a} & y_{ij} \end{bmatrix} \begin{bmatrix} V_i \\ V_j \end{bmatrix} \quad (26)$$

#### 4.2.3. Shunt capacitors or reactors

Shunt capacitors and reactors are devices which are installed in the network to function as reactive power support and voltage control [36]. The sign of the susceptance value will determine the type of shunt element. Therefore it will be positive or negative corresponding to a shunt capacitor or shunt reactor respectively.

#### 4.2.4. Generators and loads

Generators and loads are modeled as equivalent complex power injections and therefore have no effect on the network model.

#### 4.2.5. Expression of current in rectangular co-ordinates

In this work it is necessary to express the relationship between conductance  $g$ , susceptance  $b$ , real and reactive current and real and reactive voltage for sending and receiving end buses as these properties are utilised in the Jacobian matrix of the state estimator. Figure 24 expands on the two-port  $\pi$ -model by including conductance, susceptance and real and reactive current and voltage.

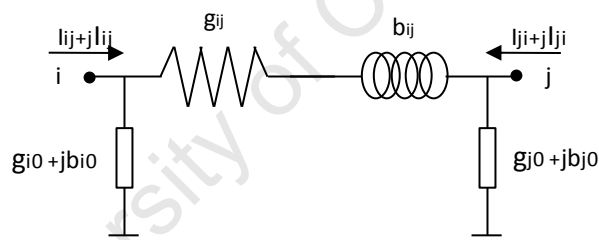


Figure 24: Two-port  $\pi$ -model of a network branch

This relationship can be expressed in matrix form as:

$$\begin{bmatrix} I_{ij\_re} \\ I_{ij\_im} \\ I_{ji\_re} \\ I_{ji\_im} \end{bmatrix} = \begin{bmatrix} g_{ij} + g_{i0} & -g_{ij} & -(b_{ij} + b_{i0}) & b_{ij} \\ b_{ij} + b_{i0} & -b_{ij} & g_{ij} + g_{i0} & -g_{ij} \\ -g_{ij} & g_{ij} + g_{j0} & b_{ij} & -(b_{ij} + b_{j0}) \\ -b_{ij} & b_{ij} + b_{j0} & -g_{ij} & g_{ij} + g_{j0} \end{bmatrix} \begin{bmatrix} V_{i\_re} \\ V_{j\_re} \\ V_{i\_im} \\ V_{j\_im} \end{bmatrix} \quad (27)$$

where the admittance is expressed the sum of conductance and susceptance as:

$$y = g_{ij} + jb_{ij} \quad (28)$$

Note that equation (28) is usually expressed in uppercase letters. However in this work, there is a sign difference between the upper and lower case representations. This difference is dealt with in section 4.3.1.

#### 4.2.6. The bus-admittance matrix

In order to assess the topology of the network the components and their connections are modeled using the bus-admittance matrix or the  $Y_{bus}$ . The  $Y_{bus}$  of a power system is of the following form:

$$I = \begin{bmatrix} I_1 \\ I_2 \\ \vdots \\ I_N \end{bmatrix} = \begin{bmatrix} Y_{11} & Y_{12} & \cdots & Y_{1N} \\ Y_{21} & Y_{22} & \cdots & Y_{2N} \\ \vdots & \vdots & \ddots & \vdots \\ Y_{N1} & Y_{N2} & \cdots & Y_{NN} \end{bmatrix} \begin{bmatrix} V_1 \\ V_2 \\ \vdots \\ V_N \end{bmatrix} = [Y_{bus}][V] \quad (29)$$

where  $N$  is equal to the number of buses in the system. The matrix is populated by deriving two rules from Kirchoff's Law of current injection at a node.

The two basic rules are as follows:

1. The  $Y_{ii-th}$  element of the admittance matrix is the sum of all the branch admittances connected to bus  $i$ .
2. The  $Y_{ij-th}$  element of the admittance matrix is the negative value of the branch admittance connecting bus  $i$  to bus  $j$ .

A simple four bus power system example shown in Figure 25 will be used to demonstrate the Y-bus construction.

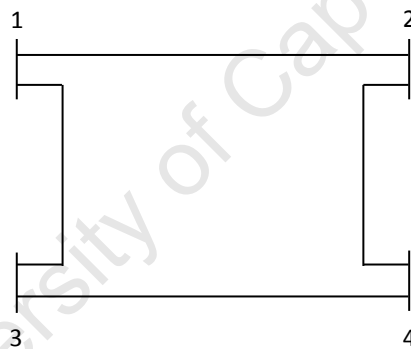


Figure 25: Four bus example topology

The network data of the four bus example are given in Table 20.

Table 20: Four bus network data

From bus	To bus	R (p.u.)	X (p.u.)	B (p.u.)
1	2	0.01008	0.0504	0.1025
1	3	0.00744	0.0372	0.0775
2	4	0.00744	0.0372	0.0775
3	4	0.01272	0.0636	0.1275

The  $Y_{bus}$  is expressed as follows:

$$Y_{bus} = \begin{bmatrix} 8.9852 - j44.8360 & -3.8156 + j19.0781 & -5.1696 + j25.8478 & 0 \\ -3.8156 + j19.0781 & 8.9852 - j44.8360 & 0 & -5.1696 + j25.8478 \\ -5.1696 + j25.8478 & 0 & 8.1933 - j40.8638 & -3.0237 + j15.1185 \\ 0 & -5.1696 + j25.8478 & -3.0237 + j15.1185 & 8.1933 - j40.8638 \end{bmatrix}$$

The nominal pie model is used in modelling the  $Y_{bus}$  so that effectively each susceptance value is halved and added to each end of branch  $ij$ .

### 4.3. The mathematical modeling of state estimation

CSE (conventional state estimation) provides a state solution through an iterative process, necessary because of the non-linear equations between measurements and variables. The nonlinear equations are linearized and an iterative Weighted Least Square (WLS) estimator is applied to the measurement set. Real-time complex power and voltage magnitude measurements are obtained throughout the system by scanning, and the new measurements are used to update the state estimate with the previous estimate as the starting point [37].

The decision variables are the state variables, and the objective function to be minimized is a measure of the deviation of the measurement function from the actual measurement. The state estimator maps the states of  $x$  to the measurements of  $z$  with measurement errors  $e$  as shown in equation (30).

$$z_i = H_i(x) + e \quad (30)$$

where  $H_i(x)$  is known as the measurement function and relates the system state vector  $x$ , to the measured quantities of voltage magnitudes  $V_i$ , bus power injections  $P_i, Q_i$  and branch power flows,  $P_{ij}, Q_{ij}$ . The measurement errors are assumed stochastic with a Gaussian probability distribution, zero mathematical expectation values and mutual independences [42].

The maximum likelihood function is the mathematical theory which drives state estimation. The Gaussian (normal) probability density function for a random variable  $z$  is defined as:

$$f(z) = \frac{1}{\sqrt{2\pi}\sigma} e^{-\frac{1}{2}\left(\frac{z-\mu}{\sigma}\right)^2} \quad (31)$$

where  $z$  is a random variable,  $\mu$  is the mean of  $z$  and  $\sigma$  the standard deviation of  $z$ . Therefore the probability density function gives the probability of measuring the random variable  $z$ . In state estimation  $z$  represents measurements made in the power system such as power flows, power injections, voltages etc. If it is assumed that there are  $m$  independent measurements of  $z$ , each with the same Gaussian probability density function, then the joint probability of measuring these measurements is defined by the product of the associated probability density functions termed the likelihood function. Mathematically this is defined as:

$$f_m(z) = \prod_{i=1}^m f(z_i), \quad i = 1, \dots, m. \quad (32)$$

The Maximum likelihood estimation aims to maximize this function to determine the unknown parameters of the probability density function of each of the measurements. The likelihood function is maximised by varying the parameters  $\mu$  and  $\sigma$  of the probability density function. This is achieved by maximizing the logarithm of the likelihood function,  $f_m(z)$ , or minimizing the weighted sum of squares of the residuals [36]. It can be expressed as:

$$\text{minimize } \sum_{i=1}^m W_{ii} r_i^2 \quad (33)$$

$$\text{subject to } z_i = h_i(x) + r_i, \quad i = 1, \dots, m.$$

where  $W_{ii} = \sigma_i^{-2}$  and  $h_i(x)$  is a nonlinear measurement function relating the state vector  $x$  to the  $i^{\text{th}}$  measurement. The solution to equation (33) is known as the weighted least squares (WLS) estimate for  $x$ .

The solution to the state estimation problem can be formulated as the minimization of the following objective scalar function:

$$J(x) = \sum_{i=1}^m \frac{(z_i - h_i(x))^2}{R_{ii}} \quad (34)$$

The errors in the measurements are assumed to be Gaussian normal with zero-mean, uncorrelated as modeled by the diagonal covariance matrix  $R$ . Therefore the covariance error matrix can be defined according to equation (35).

$$\text{Cov}(e) = E(e \cdot e^T) = R = \text{diag}(\sigma_1^2, \sigma_2^2, \dots, \sigma_n^2) \quad (35)$$

Equation (34) represents the summation of the square of the measurement residuals weighted by the respective measurement covariance matrix. It can be expressed in matrix form as:

$$J(x) = [z - h(x)]^T R^{-1} [z - h(x)] \quad (36)$$

The solution to the minimization function  $J(x)$  is obtained when the derivative of the function is set to zero. Let the derivate of this function be known as  $g(x)$ . Therefore,

$$g(x) = \frac{dJ(x)}{dx} = - \left[ \frac{dh(x)}{dx} \right]^T R^{-1} [z - h(x)] = 0 \quad (37)$$

Let

$$H(x) = \frac{dh(x)}{dx} \quad (38)$$

where  $H(x)$  is known as the measurement Jacobian and represents the derivate of the measurement function  $h(x)$ . If  $g(x)$  is expanded by the use of Taylor series and the higher terms are neglected, the iterative solution of the state vector at iteration  $k$  is given as:

$$x^{k+1} = x^k + \{ [H(x^k)]^T R^{-1} H(x^k) \}^{-1} [H(x^k)]^T R^{-1} [z - h(x^k)] \quad (39)$$

The solution to equation (39) is known as the Gauss-Newton method.

The gain matrix  $G(x)$  is expressed as:

$$G(x) = H(x^k)^T R^{-1} H(x^k) \quad (40)$$

Typically the gain matrix is not inverted as in equation (39) but solved by forwards/backwards factorisation of  $G$ . The measurement function and measurement Jacobian can be constructed using the known system model including branch parameters, network topology, and measurement type and locations. The error covariance matrix should be populated prior to the iterative procedure with the accuracy information of the meters installed in the system. Equation (40) will converge slowly or diverge if the numerical stability is bad. The numerical stability is denoted by the equation condition number given in equation (41).

$$\text{Cond}(G) = \|G\| \times \|G^{-1}\| \quad (41)$$

The larger the condition number, the larger the numerical instability. The condition number is correlative with the measurements placement, type, weight, amount and size of the power system [50].

#### 4.3.1. Measurement functions $\mathbf{h}(\mathbf{x})$ and $\mathbf{H}(\mathbf{x})$

There are many different kinds of measurements in a power system. The ones that are commonly used in the measurement function are line power flows, power injections, bus voltage magnitudes and line voltage magnitudes. These measurements can be expressed in terms of the state variables using either polar or vector co-ordinates. Equations relating the state vector to each measurement will be based on Figure 24.

The real and reactive power injections at bus  $i$  are given as:

$$P_i = V_i \sum_{j \in N_i} V_j (G_{ij} \cos \theta_{ij} + B_{ij} \sin \theta_{ij}) \quad (42)$$

$$Q_i = V_i \sum_{j \in N_i} V_j (G_{ij} \sin \theta_{ij} - B_{ij} \cos \theta_{ij}) \quad (43)$$

The real and reactive power flows from bus  $i$  to bus  $j$  are given as:

$$P_{ij} = V_i^2 (g_{si} + g_{ij}) - V_i V_j (g_{ij} \cos \theta_{ij} + b_{ij} \sin \theta_{ij}) \quad (44)$$

$$Q_{ij} = -V_i^2 (b_{si} + b_{ij}) - V_i V_j (g_{ij} \sin \theta_{ij} - b_{ij} \cos \theta_{ij}) \quad (45)$$

Line current flow magnitude from bus  $i$  to bus  $j$ :

$$I_{ij} = \frac{\sqrt{P_{ij}^2 + Q_{ij}^2}}{V_i} \quad (46)$$

where  $V_i$  and  $\theta_i$  are the voltage magnitude and phase angle at bus  $i$  respectively.  $\theta_{ij}$  is the angle between two buses, therefore  $\theta_{ij} = \theta_i - \theta_j$ .  $N_i$  represents the set of bus numbers directly connected to bus  $i$ . Importantly it must be noted that  $G_{ij}$  and  $B_{ij}$  are not the same as  $g_{ij}$  and  $b_{ij}$ . Although both represent the admittance of the series branch connecting bus  $i$  to bus  $j$ ,  $g_{ij} + jb_{ij} = -(G_{ij} + jB_{ij})$ . By conventional  $g_{ij} + jb_{ij}$  are obtained from the  $Y_{bus}$  off-diagonals (which are negative by convention).  $g_{si}$  and  $b_{si}$  represent the admittance of the shunt branch connected to bus  $i$ .

The measurement Jacobian is structured as follows:

$$H = \begin{bmatrix} \frac{\partial P_{inj}}{\partial \theta} & \frac{\partial P_{inj}}{\partial V} \\ \frac{\partial P_{flow}}{\partial \theta} & \frac{\partial P_{flow}}{\partial V} \\ \frac{\partial Q_{inj}}{\partial \theta} & \frac{\partial Q_{inj}}{\partial V} \\ \frac{\partial Q_{flow}}{\partial \theta} & \frac{\partial Q_{flow}}{\partial V} \\ \frac{\partial I_{mag}}{\partial \theta} & \frac{\partial I_{mag}}{\partial V} \\ 0 & \frac{\partial V_{mag}}{\partial V} \end{bmatrix} \quad (47)$$

The expressions for each segment are given below in equations (48)-(68).

Elements corresponding to real power injections:

$$\frac{\partial P_i}{\partial \theta_i} = \sum_{j=1}^N V_i V_j (-G_{ij} \sin \theta_{ij} + B_{ij} \cos \theta_{ij}) - V_i^2 B_{ii} \quad (48)$$

$$\frac{\partial P_i}{\partial \theta_j} = V_i V_j (G_{ij} \sin \theta_{ij} - B_{ij} \cos \theta_{ij}) \quad (49)$$

$$\frac{\partial P_i}{\partial V_i} = \sum_{j=1}^N V_j (G_{ij} \cos \theta_{ij} + B_{ij} \sin \theta_{ij}) - V_i^2 G_{ii} \quad (50)$$

$$\frac{\partial P_i}{\partial V_j} = V_j (G_{ij} \cos \theta_{ij} + B_{ij} \sin \theta_{ij}) \quad (51)$$

Elements corresponding to reactive power injections:

$$\frac{\partial Q_i}{\partial \theta_i} = \sum_{j=1}^N V_i V_j (G_{ij} \cos \theta_{ij} + B_{ij} \sin \theta_{ij}) - V_i^2 G_{ii} \quad (52)$$

$$\frac{\partial Q_i}{\partial \theta_j} = V_i V_j (-G_{ij} \cos \theta_{ij} - B_{ij} \sin \theta_{ij}) \quad (53)$$

$$\frac{\partial Q_i}{\partial V_i} = \sum_{j=1}^N V_j (G_{ij} \sin \theta_{ij} - B_{ij} \cos \theta_{ij}) - V_i^2 B_{ii} \quad (54)$$

$$\frac{\partial Q_i}{\partial V_j} = V_j (G_{ij} \sin \theta_{ij} - B_{ij} \cos \theta_{ij}) \quad (55)$$

Elements corresponding to real power flow measurements:

$$\frac{\partial P_{ij}}{\partial \theta_i} = V_i V_j (g_{ij} \sin \theta_{ij} - b_{ij} \cos \theta_{ij}) \quad (56)$$

$$\frac{\partial P_{ij}}{\partial \theta_j} = -V_i V_j (g_{ij} \sin \theta_{ij} - b_{ij} \cos \theta_{ij}) \quad (57)$$

$$\frac{\partial P_{ij}}{\partial V_i} = -V_j (g_{ij} \cos \theta_{ij} + b_{ij} \sin \theta_{ij}) + 2(g_{ij} + g_{si}) V_i \quad (58)$$

$$\frac{\partial P_{ij}}{\partial V_j} = -V_i (g_{ij} \cos \theta_{ij} + b_{ij} \sin \theta_{ij}) \quad (59)$$

Elements corresponding to reactive power flow measurements:

$$\frac{\partial Q_{ij}}{\partial \theta_i} = -V_i V_j (g_{ij} \cos \theta_{ij} + b_{ij} \sin \theta_{ij}) \quad (60)$$

$$\frac{\partial Q_{ij}}{\partial \theta_j} = V_i V_j (g_{ij} \cos \theta_{ij} + b_{ij} \sin \theta_{ij}) \quad (61)$$

$$\frac{\partial Q_{ij}}{\partial V_i} = -V_j (g_{ij} \sin \theta_{ij} - b_{ij} \cos \theta_{ij}) - 2(b_{ij} + b_{si}) V_i \quad (62)$$

$$\frac{\partial Q_{ij}}{\partial V_j} = -V_i (g_{ij} \sin \theta_{ij} - b_{ij} \cos \theta_{ij}) \quad (63)$$

Elements corresponding to voltage magnitude measurements:

$$\frac{\partial V_i}{\partial V_i} = 1, \frac{\partial V_i}{\partial V_j} = 0, \frac{\partial V_i}{\partial \theta_i} = 0, \frac{\partial V_i}{\partial \theta_j} = 0 \quad (64)$$

Elements corresponding to current magnitude measurements (ignoring the branch shunt impedance):

$$\frac{\partial I_{ij}}{\partial \theta_i} = \frac{g_{ij}^2 + b_{ij}^2}{I_{ij}} V_i V_j \sin \theta_{ij} \quad (65)$$

$$\frac{\partial I_{ij}}{\partial \theta_j} = -\frac{g_{ij}^2 + b_{ij}^2}{I_{ij}} V_i V_j \sin \theta_{ij} \quad (66)$$

$$\frac{\partial I_{ij}}{\partial V_i} = \frac{g_{ij}^2 + b_{ij}^2}{I_{ij}} (V_i - V_j \cos \theta_{ij}) \quad (67)$$

$$\frac{\partial I_{ij}}{\partial V_j} = \frac{g_{ij}^2 + b_{ij}^2}{I_{ij}} (V_j - V_i \cos \theta_{ij}) \quad (68)$$

#### 4.4. Controlled test metrics

In this work, the accuracy of the state estimator will be assessed by comparing 'true' system conditions, determined from a solved power flow, against the 'estimated' measurements, derived

from the state estimator solution. Various ways of measuring accuracy have been documented in the literature. The applicability of each method to this work is briefly reviewed and discussed.

#### 4.4.1. Accuracy metrics

One of the most common methods for assessing accuracy is choose a power flow solution metric of interest and define a norm-like calculation that evaluates the difference between the ‘true’ measurement and the ‘estimated’ measurement. For example, consider  $|V|_i^{true}$  and  $|V|_i^{est}$  to be the true voltage magnitude and the estimated voltage magnitude respectively at bus  $i$ . The difference between these defined variables can be assessed in more than one way, with each form of the metric having a different implication. Consider equations (69)-(71) below.

$$\sum_{i=1}^L (|V|_i^{true} - |V|_i^{est}) \quad (69)$$

$$\sum_{i=1}^L (|V|_i^{true} - |V|_i^{est})^2 \quad (70)$$

$$\max_{i=1, \dots, L} (|V|_i^{true} - |V|_i^{est}) \quad (71)$$

Reference [44] notes that both (69) and (70) can return very different scores for very similar network models. Equation (71) gives an indication of the worst error however an outlier in the measurement solution may erroneously indicate a poor measurement solution. These metrics are useful for analysing different results between algorithms based on identical networks but should be treated with caution when comparing two different network models.

Two additional metrics are proposed in [44]. Equation (72) gives the accuracy of the complex power flow and equation (73) gives the accuracy of the norm of the complex voltage.

$$Macc_{s\ flow} = \left\{ \sum_i \frac{|\tilde{S}_{i,from}^{true} - \tilde{S}_{i,from}^{est}|^2 + |\tilde{S}_{i,to}^{true} - \tilde{S}_{i,to}^{est}|^2}{MVA_i^2} \right\}^{\frac{1}{2}} \quad (72)$$

$$Macc_v = \left\| \vec{V}^{error} \right\| = \left( \sum_i |\vec{V}_i^{true} - \vec{V}_i^{est}|^2 \right)^{\frac{1}{2}} \quad (73)$$

In equation (72)  $i$  is the summation index ranging over all network branches.  $a$  uses the complex flows from all branches in the network. Every flow error of branch  $i$  is weighted by the MVA in order to ensure that the scale of the error is relative. For example the same error on a 100MVA base carries a larger significance than on a 50MVA base.

In equation (73) it is important to use the same reference bus for the true and estimated complex voltage.

A metric in reference [39] is used to measure the accuracy of power flow measurements known as the performance index (PIP) equation (74). However according to [44] this metric does not have the

ability to include the estimation accuracy for unmetered lines and should therefore not be used in cases when lines are unmetered.

$$PIP = \frac{\sum_{i=1}^{m_{pf}} (Pf_i^{true} - Pf_i^{est})^2}{\sum_{i=1}^{m_{pf}} (Pf_i^{true} - Pf_{ei}^{meas})^2} \quad (74)$$

where  $Pf$  denotes the power flow on  $m_{pf}$  branches and  $m$  is the total number of network branches.

Reference [16] used the mean standard deviation of line power flow errors and voltage angles as a performance metric for benchmarking a estimator incorporating PMU measurements against a CSE given by equation (75).

$$\sigma_i = \sqrt{\frac{1}{M} \sum_{j=1}^M (P_{i,j}^{est} - P_{i,j}^{true})^2} \quad (75)$$

$$\therefore \bar{\sigma} = \frac{\sum_{i=1}^N \sigma_i}{N}$$

The authors of that paper used a Monte Carlo simulation with  $M = 100$  to generate a sufficient amount of statistics to determine the standard deviation ( $\sigma_i$ ) of line flows and angles. The mean standard deviation was then obtained over all  $N$  flows or angles of the network.

#### 4.4.2. Convergence criteria

A conventional state estimator uses an iterative process to obtain a solution. Therefore it will run until it meets specific precision criteria. The precision of an estimator can be judged by its ability to converge [44]. The following metrics in equations (76)-(78) are used commonly in control centres to test for convergence.

$$Mconv_{obj} = \left| 1 - \frac{J^k}{J^{k-1}} \right| \quad (76)$$

$$Mconv_v = \max_{i \in B_{int}} \left| 1 - \frac{V_i^k}{V_i^{k-1}} \right| \quad (77)$$

$$Mconv_{\theta} = \max_{i \in B_{int}} |\theta_i^k - \theta_i^{k-1}| \quad (78)$$

The state estimation will continue to run until convergence criteria are satisfied. In the equations above  $k$  is the terminal term.  $J$  is the solution to equation (36) which represents the objective function. Equations (77) and (78) use the maximum error to check for convergence of bus voltage and angle respectively. Midwest ISO published acceptable criteria for  $Mconv_v$  and  $Mconv_{\theta}$  stating the values should be less than or equal to 0.002 [44]. In this work, the metrics for complex power flow error and complex voltage error will be used to assess the accuracy of the state estimator solution. In this work the voltage magnitude and voltage phase angle absolute change between iterations are used as the convergence criteria. If the changes of both the voltage magnitude and voltage phase angle on consecutive runs are less than  $1 \times 10^{-4}$  the convergence criteria are

satisfied. A review of state estimator incorporation of PMU measurements must first be undertaken and is provided in the next section.

#### 4.5. Literature review of incorporating PMU measurements into state estimators

Zivanovi et al. [39] state that it is possible to mix phasor measurements with conventional active and reactive power flow and injection measurements in order to improve CSE accuracy. The PMU voltage magnitude measurements can be used as a straight forward replacement of the classical measurements in the WLS algorithm [45]. The angle phasor measurements are incorporated through the direct use of absolute voltage phasor angle measurements or the use of angle difference between voltage phasor measurements resulting in a modification to the Jacobian matrix. The appendage of phasor measurements to the traditional state estimator results in the direct manipulation of the Jacobian matrix. The findings of the paper indicate that voltage measurements must be accurate (standard deviation less than or equal to  $0.1^\circ$ ) in order to have any real impact on the improvement of the accuracy of state estimation. The work concludes with the suggestion of utilising separate nonlinear and linear state estimators. The linear state estimator would start by covering a small area and grow over time as PMU penetration increased. Eventually the nonlinear estimator would be eclipsed by the linear estimator and the LSE would become the predominant method for obtaining a state solution. This essentially constitutes the use of a distributed state estimation technique.

Jiang et al. [46] addressed the combination of nonlinear and linear measurements using a distributed state estimation technique to utilize phasor measurements by reviewing a vast number of previous attempts and proposing a unique model for distributed state estimation. Basically, distributed estimation techniques break down large complex systems into smaller, more manageable areas. This decentralizes the computation by distributing computation across the system, rather than to centralize computation at the control centre. This work may be useful as the implementation of a hybrid or linear state estimator becomes practically realisable, due to the fact that areas observed by PMUs may be isolated and treated separately by utilising the properties of boundary buses.

Cheng et al. [47] used a linear state transformation by the iterative transformation of power phasors to current phasors enabling conventional measurements to be mixed with PMU measurements. It states that there is a discrepancy between distributed state estimators and integrated state estimators. The suggested process could be applied without splitting the whole system into subsystems to avoid the discrepancy between boundary buses eliminating inconsistencies in distributed state estimation.

Qin et al. [48] proposed a method that transforms the voltage phasor measurements into indirect branch current measurements which are integrated into the state estimator along with conventional measurements which are used to calculate the corrections of state variables. The results indicate that the method improves the convergence speed, the estimation precision and the performance index of the state estimator.

Yang et al. [49] proposed a two-level PMU based linear state estimator where topology processing and bad data detection-identification was done at the substation level instead of at the control centre. This work is mentioned due to the fact that it may have application to PMU instalment in South Africa, but the content falls outside the scope of this research.

Zhao et al. [50] proposed a double state estimation model whereby the nonlinear SE was done on the condition of taking the state variable measured or calculated by PMU as the state variable of the nodes. The linear SE was then done with both nonlinear SE results and PMU measurements. This work noted that LSE can use either polar or Cartesian co-ordinates to relate the nonlinear output solution to the linear inputs. The methods were tested on IEEE 14 and 57 bus systems. The results indicate that the Cartesian co-ordinate system provided the lowest variance on the output state vector solution. In addition the condition number decreased with an increasing number of PMUs. This method added to the calculation time, but improved the SE equations and convergence speed.

Zhou et al.[51] proposed that a mathematically equivalent yet more attractive option for including phasor measurements in state estimation was to use them in a post processing step. Thus the results of the traditional state estimator and the PMU measurements are considered to be a set of measurements that are linear functions of the state vector. This leads to a non-iterative estimation step that requires no modification of the traditional EMS software. This work used the angle error and magnitude error to show that an increasing number of PMUs progressively increased the quality of the estimated state.

Nuqui et al. [16] used a non-invasive two-pass approach where the first pass executed a traditional state estimation problem without phasor measurements. The second pass appended the state vector solution with the vector of phasor measurements and solved a linear state estimation problem using rectangular coordinates. The numerical experiments assumed dense metering conditions, with the criterion of PMU placement being to improve the accuracy of the state estimate. The best PMU placement strategy was taken from a Monte Carlo experiment of random PMU placement sets resulting in the greatest SE accuracy. However it was noted that more elaborate methods for evaluating PMU placement locations exist, such as the evaluation of the reduction in diagonal entries of the state error covariance matrix of the conventional state estimator. With the optimal PMU placement set, the phased incorporation of PMUs was investigated on both a fully and partially metered New England 39 test bus system. The results indicated that for a fully metered system, greater PMU metering accuracy was needed to improve the state solution and flow estimate. This work showed that a partially metered system benefitted significantly from the addition of a few PMUs as the standard deviation of the real power flows and voltage angle errors decreased with an increasing number of PMU. The benchmarking was done using equation (75).

#### 4.5.1. Summary of state estimator literature review

The inclusion of PMUs in a hybrid state estimator decreases the state estimator variance which indicates an improved state estimate solution in terms of improving accuracy and power flows. From the preceding literature review the techniques for including PMU measurements into a state estimator can be divided into two broad methods: Methods 1 rely on devising a relationship between the conventional measurements and PMU measurements, often resulting in the PMU measurements being transformed and incorporated directly into the Jacobian matrix. The measurements are combined with the conventional SCADA measurements and used as direct inputs to the conventional nonlinear state estimator. Figure 26 indicates the process of methods 1.

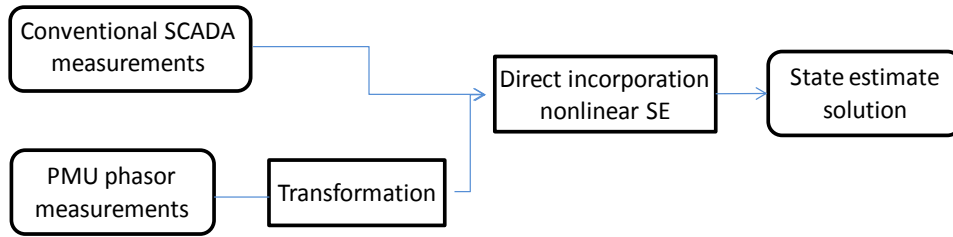


Figure 26: Traditional nonlinear hybrid state estimator

Methods 2 utilise a mathematically equivalent two-pass approach that incorporates separate nonlinear and linear state estimation steps as shown in Figure 27. These methods have the benefit of maintaining the original composition of the Jacobian matrix. This would serve to benefit utilities as the new linear step incorporating PMU measurements could be appended as a post-processing step. However, this does bring about the choice of whether to use polar or Cartesian co-ordinates. In this work a hybrid state estimator will be designed using concepts of methods 2. In addition, this post-processing step serves as a good starting platform for implementing pure linear state estimation. The structure and composition of the method for hybrid and linear state estimators are covered in detail in the next section.

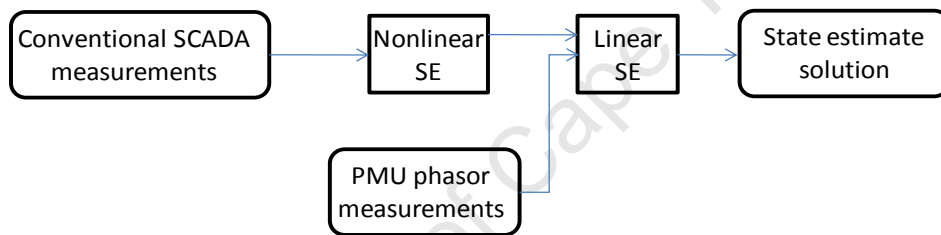


Figure 27: Two pass approach incorporating linear and nonlinear state estimation

#### 4.6. Hybrid and linear state estimation models

A linear state estimator is proposed under the condition that all bus voltage phasors and all branch currents can be measured by PMUs placed in the network. PMUs and communications are costly to install and most networks, especially in a South African context, are not fully equipped with PMUs. Therefore a hybrid estimator: one utilizing both traditional measurements and PMU measurements; becomes practically necessary.

##### 4.6.1. Standard State Estimator combined with PMUs (Hybrid state estimator)

The conventional state estimator is appended with a linear state estimation method incorporating PMU measurements to give a non-iterative estimate of the state vector. The measurements are incorporated using the same reference as the conventional state estimation algorithm to eliminate phase angle inaccuracies as a result of choice of reference bus. The method is based on [16]. The linear solution to equation 79 gives the state vector estimate.

$$M = B(V) + \epsilon \tag{79}$$

$$\therefore M = \begin{bmatrix} V_r(SE) \\ V_i(SE) \\ V_r(PMU) \\ V_i(PMU) \\ I_r(PMU) \\ I_i(PMU) \end{bmatrix} = \begin{bmatrix} B_{11} & B_{12} \\ B_{21} & B_{22} \\ B_{31} & B_{32} \\ B_{41} & B_{42} \\ \frac{\delta I_r}{\delta V_r} & \frac{\delta I_r}{\delta V_i} \\ \frac{\delta I_i}{\delta V_r} & \frac{\delta I_i}{\delta V_i} \end{bmatrix} \begin{bmatrix} V_r \\ V_i \end{bmatrix} + \begin{bmatrix} \epsilon_{V_r(SE)} \\ \epsilon_{V_i(SE)} \\ \epsilon_{V_r(PMU)} \\ \epsilon_{V_i(PMU)} \\ \epsilon_{I_r(PMU)} \\ \epsilon_{I_i(PMU)} \end{bmatrix}$$

where  $B_{11}, B_{22}$  are matrices with ones along the diagonal.  $B_{12}, B_{21}, B_{32}, B_{41}$  are null matrices (composed only of zeroes.)  $B_{31}, B_{42}$  represent PMU voltage measurement at a bus. For example if there are four buses in a system, and two PMUs placed at buses 1 and 4 the elements of the Jacobian matrix are represented as follows:

$$B_{11} = \begin{bmatrix} 1 & 0 & 0 & 0 \\ 0 & 1 & 0 & 0 \\ 0 & 0 & 1 & 0 \\ 0 & 0 & 0 & 1 \end{bmatrix} \begin{bmatrix} V_{r1se} \\ V_{r2se} \\ V_{r3se} \\ V_{r4se} \end{bmatrix} \quad B_{22} = \begin{bmatrix} 1 & 0 & 0 & 0 \\ 0 & 1 & 0 & 0 \\ 0 & 0 & 1 & 0 \\ 0 & 0 & 0 & 1 \end{bmatrix} \begin{bmatrix} V_{i1se} \\ V_{i2se} \\ V_{i3se} \\ V_{i4se} \end{bmatrix}$$

$$B_{31} = \begin{bmatrix} 1 & 0 & 0 & 0 \\ 0 & 0 & 0 & 1 \end{bmatrix} \begin{bmatrix} V_{r1pmu} \\ V_{r4pmu} \end{bmatrix} \quad B_{42} = \begin{bmatrix} 1 & 0 & 0 & 0 \\ 0 & 0 & 0 & 1 \end{bmatrix} \begin{bmatrix} V_{i1pmu} \\ V_{i4pmu} \end{bmatrix}$$

where  $B(V)$  is the linear function relating actual measurements  $M$  to the state vector  $V$ .  $V_{r1se}$  and  $V_{i1se}$  represent the indices of real and imaginary voltage obtained from the solution of the conventional state estimator for bus 1.  $V_{r1pmu}$  and  $V_{i1pmu}$  represent the real and imaginary voltage measured from a PMU placed at a bus 1. Note the column positions of the ones in the  $B_{31}$  and  $B_{42}$  correspond to the bus placement positions of the PMUs at buses 1 and 4.

The nominal pie model is used to represent the transmission lines in the test models. The current derivatives  $\frac{\delta I_r}{\delta V_r}, \frac{\delta I_r}{\delta V_i}, \frac{\delta I_i}{\delta V_r}$  and  $\frac{\delta I_i}{\delta V_i}$  are computed using equation (27) and are as follows:

$$\begin{aligned} \frac{\delta I_{pq,r}}{\delta V_{p,r}} &= g_{ij} + g_{si} & \frac{\delta I_{pq,r}}{\delta V_{q,r}} &= -g_{ij} \\ \frac{\delta I_{pq,r}}{\delta V_{q,r}} &= -b_{ij} - b_{si} & \frac{\delta I_{pq,r}}{\delta V_{q,i}} &= b_{ij} \end{aligned} \quad (80)$$

$$\begin{aligned} \frac{\delta I_{pq,i}}{\delta V_{p,r}} &= b_{ij} + b_{si} & \frac{\delta I_{pq,i}}{\delta V_{q,r}} &= -b_{ij} \\ \frac{\delta I_{pq,i}}{\delta V_{p,i}} &= g_{ij} + g_{si} & \frac{\delta I_{pq,i}}{\delta V_{q,i}} &= -g_{ij} \end{aligned} \quad (81)$$

#### 4.6.2. Polar to Cartesian co-ordinate transformation

The output of the traditional state estimator is in polar form. The linear state estimator used in this paper requires a conversion from polar to Cartesian co-ordinates. This requirement is due to the fact

that the state vector is composed of real and imaginary parts. A voltage with magnitude  $V$  and angle  $\theta$  is transformed to real and imaginary Cartesian co-ordinates using the equation (82) which represents a rotation matrix.

$$R_{Rot} = \begin{bmatrix} \cos\theta & -\sin\theta \\ \sin\theta & \cos\theta \end{bmatrix} \quad (82)$$

Reference [16] proposed equations (83)-(86) for transforming the variance from the state estimation process and PMU measurements from polar co-ordinates to Cartesian co-ordinates based on the rotation matrix in (82).

$$\sigma_{|vr|}^2 \approx \cos^2\theta\sigma_{|v|}^2 + |V|^2\sin^2\theta\sigma_{|\theta|}^2 \quad (83)$$

$$\sigma_{|vi|}^2 \approx \sin^2\theta\sigma_{|v|}^2 + |V|^2\cos^2\theta\sigma_{|\theta|}^2 \quad (84)$$

$$\sigma_{|vri|}^2 \approx \cos^2\Phi\sigma_{|v|}^2 + |I|^2\sin^2\Phi\sigma_{|\theta|}^2 \quad (85)$$

$$\sigma_{|vii|}^2 \approx \sin^2\Phi\sigma_{|v|}^2 + |I|^2\cos^2\Phi\sigma_{|\theta|}^2 \quad (86)$$

where  $\theta$  and  $\Phi$  are the phase angle of the complex voltage and current respectively. The covariance matrix  $R$  is populated along the diagonal through the use of equations 83-86.

#### 4.6.3. Linear state estimation model

Due to the fact that phasor measurement units (PMUs) provide precise, real-time, synchronized GPS phasor measurements of voltage and current, enables state estimation equations utilizing PMU measurements to be modelled in an inherently linear manner.

The linear state estimation post-processing step is based on the non-iterative solution to equation (87).

$$M = B(V) + \epsilon \quad (87)$$

Equation (87) is manipulated into equation (88) below:

$$V = [B^T R^{-1} B]^{-1} B^T R^{-1} M \quad (88)$$

where  $R$  is the diagonal covariance matrix consisting of actual measurement variances. The solution to equation (88) gives the state vector of the power system.

#### 4.6.4. Measurement errors

All measurements in a system contain noise due to measurement inaccuracies. Therefore it is important to quantify and include noise in the modeled system. Many references have used specific noise standard deviation values for power flows, power injections, voltage measurements, current measurements and PMU angle measurements. The values are summarized in Table 21 to Table 24 below.

Table 21: Current phasor standard deviation

Reference	Magnitude error (p.u.)	Angle error (degrees)
[16]	0.00600	0.52000
[16]	0.00300	0.26000
[42]	0.00600	1.04000

Table 22: Voltage phasor standard deviation

Reference	Magnitude error (p.u.)	Angle error (degrees)
[16]	0.00600	1.04000
[16]	0.00300	0.52000
[42]	0.01200	1.04000

Table 23: PMU voltage and current phasor standard deviations

Reference	Magnitude error (p.u.)	Angle error (degrees)
[42]	0.01200	1.04000
[47]	0.00001	0.00001
[50]	0.00500	0.11500
[51]	0.03 (3%)	0.02000
[52]	0.00100	0.02000
[53]	0.00001	0.00001
[54]	0.00010	0.00010
[55]	0.00030	0.01000

Table 24: Conventional measurements standard deviations

Reference	Power injection error (p.u.)	Power flow error (p.u.)	Voltage magnitude error (p.u.)
[47]	0.01000	0.00800	0.00400
[53]	0.01000	0.08000	0.04000
[54]	-	0.05000	0.01660
[55]	0.02000	0.02000	0.00200
[56]	0.03500	0.03500	0.00200
[57]	0.01000	0.00800	0.00400

The tables indicate that there is a great deal of variation in the choice of values for theoretical modeling of measurement errors. However, the choice of the error value greatly influences the output of the state estimator, hybrid state estimator and linear state estimator due to the noise values being the weighting components of the covariance matrix.

A few observations can be made with regards to the choice of measurement error values for this work. Reference [44] states that most measurement schemes are purely fictional as there is a difficulty in ascertaining measurement errors for actual field devices – this could explain the vast variation in measurement error choice. It further states that the weights used in commercial

estimators are often chosen and modified to achieve a consistent algorithmic convergence. However, in the tables above, a few references assumed that the standard deviation of PMU magnitude measurements and PMU angle measurements are the same. This is an incorrect assumption. PMUs use conventional voltage and current transformers to measure magnitude. Therefore the PMU magnitude standard deviation value should be the same to those of conventional voltage and current measurements in the system. Reference [44] discusses inaccurate, accurate and very accurate PMU classes with associated angle errors of  $1^\circ$ ,  $0.1^\circ$  and  $0.001^\circ$  respectively. For this work, the choice of measurement errors is given in Table 25 below.

Table 25: Quantified standard deviations for conventional measurements and PMU measurements

Power injection (p.u.)	Power flow (p.u.)	Voltage/Current magnitude (p.u.)	Angle error (degrees)
0.02000	0.02000	0.00500	0.10000

These choices are justified by the fact that they are similar in orders of magnitude to documented values used in both theoretical and practical cases. It is important to note that the voltage and current magnitude error of both conventional measurements and PMUs are considered to be identical. It is further assumed that accurate PMUs are utilized that have an associated 0.1 degree phase error.

#### 4.7. Model applied to a 4 bus test scenario

The broad procedure to calculate the state estimate for a given system is adapted from [44] and outlined as follows:

1. For a specific network model with known topology and system conditions modeled in Matpower 4.0, solve the power flow and extract voltage magnitudes, voltage angles, real and reactive branch power flows and injections.
2. Create input measurement data for the state estimator by adding randomly distributed Gaussian noise uncorrelated with zero mean to the true power flow solution.
3. Solve the process through an iterative process in the case of CSE and HSE, or non-iterative in the case of LSE.
4. Produce a state estimator solution from the derived quantities at the converged state.
5. Assess the solution of the state estimator through the use of equations (72)-(73).
6. Plot graphs of power flow and voltage error comparisons between CSE, HSE and LSE.

##### 4.7.1. Conventional state estimator

The 4 bus ( $n = 4$ ) example shown in Figure 25 is once again considered for the application of a CSE, HSE and LSE. The algorithm was implemented in MATLAB. Power flows, power injections and bus voltage phasors were generated from power flow software Matpower4.0. The 4-bus system properties that will be used to reach a CSE solution and a HSE solution are given in Table 26.

Table 26: 4-bus system properties

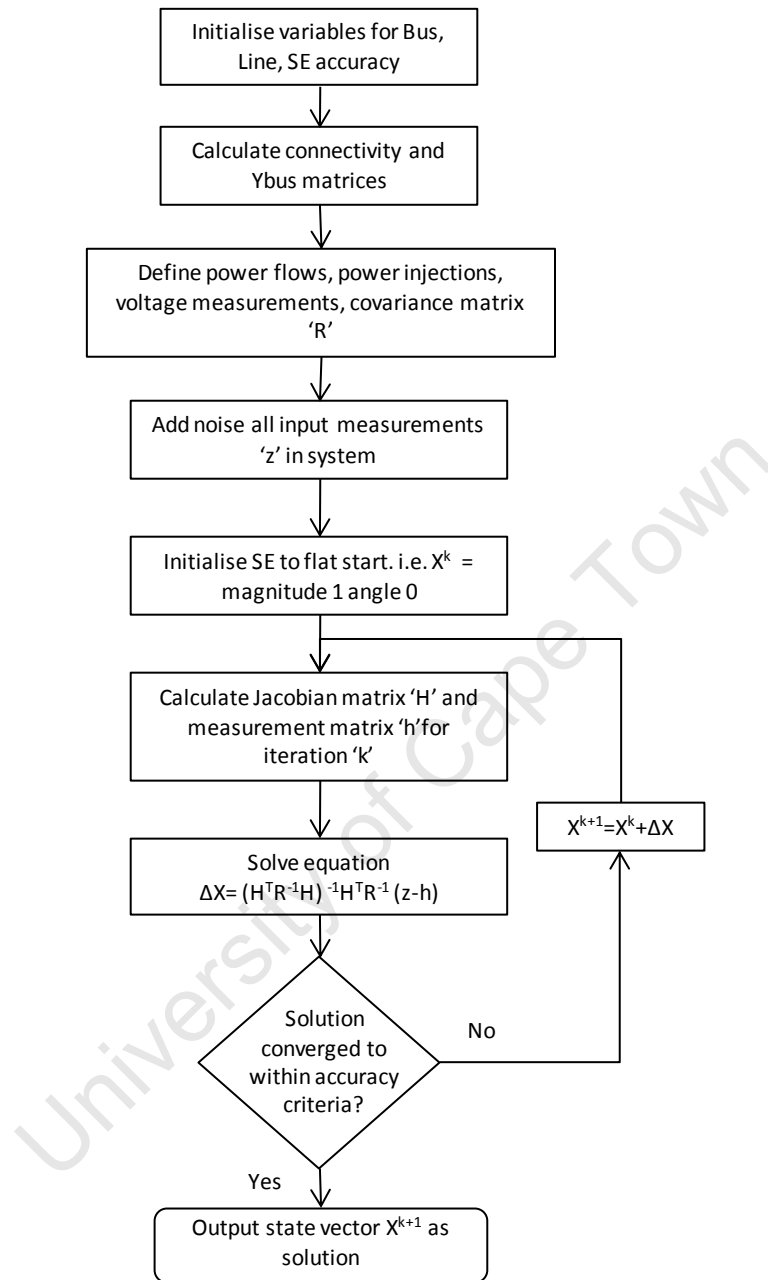
4 Bus test system (4 lines)		
Measurement	Number	Buses
PMU	2	1,4
Power flow	2	1-2, 3-4
Power injection	2	1,4
Voltage measurements	2	1,2
Zero-injections	0	0

The voltage magnitudes and angles given in Table 27 below are the bus voltages of the static 4-bus system.

Table 27: Bus voltages of 4 bus system

Bus number	Voltage magnitude (p.u.)	Voltage angle (radians)
1	1.000	0.000
2	0.982	-0.017
3	0.969	-0.033
4	1.020	0.027

The process presented in Flowchart 5 is followed to obtain a solution for CSE:



Flowchart 5: Process to obtain state solution for CSE

The type and value for the covariance of system measurements are presented in Table 28.

Table 28: Measurement type and associated covariance for 4-bus system

Measurement type	Value (p.u.)	Covariance (p.u.)
$p_{1-2}$	0.387	0.01
$p_{3-4}$	-1.029	0.01
$p_1$	1.368	0.01
$p_4$	2.380	0.01
$q_{1-2}$	0.223	0.01
$q_{3-4}$	-0.604	0.01
$q_1$	0.835	0.01
$q_4$	1.318	0.01
$V_1$	1.000	0.005
$V_2$	0.982	0.005

where  $p_{i-j}$  and  $q_{i-j}$  represent the real and reactive power flows between buses  $i$  and  $j$ .  $p_i$  and  $q_i$  represent the real and reactive power injections at bus  $i$  and  $V_i$  represents the voltage magnitude at bus  $i$ .

The covariance error matrix  $R$  is composed of the associated measurement error values along the diagonal.

$$R = \begin{bmatrix} 0.01 & 0 & 0 & 0 & 0 & 0 & 0 & 0 & 0 & 0 \\ 0 & 0.01 & 0 & 0 & 0 & 0 & 0 & 0 & 0 & 0 \\ 0 & 0 & 0.01 & 0 & 0 & 0 & 0 & 0 & 0 & 0 \\ 0 & 0 & 0 & 0.01 & 0 & 0 & 0 & 0 & 0 & 0 \\ 0 & 0 & 0 & 0 & 0.01 & 0 & 0 & 0 & 0 & 0 \\ 0 & 0 & 0 & 0 & 0 & 0.01 & 0 & 0 & 0 & 0 \\ 0 & 0 & 0 & 0 & 0 & 0 & 0.01 & 0 & 0 & 0 \\ 0 & 0 & 0 & 0 & 0 & 0 & 0 & 0.01 & 0 & 0 \\ 0 & 0 & 0 & 0 & 0 & 0 & 0 & 0 & 0.005 & 0 \\ 0 & 0 & 0 & 0 & 0 & 0 & 0 & 0 & 0 & 0.005 \end{bmatrix}$$

Random Gaussian noise with a zero mean, uncorrelated and with associated covariance is added to the measurements presented in Table 28. The state vector has  $2n - 1 = 7$  states which represent voltage angle,  $\theta$  at buses 2-4 and voltage magnitude,  $V$  at buses 1-4. The reason that the voltage angle at bus 1 is excluded from the state vector is due to the fact that it is set as the reference bus and will always remain at a zero value. The state vector estimate is initialised as a flat start with all system buses set to  $1\angle 0$  radians.

$$x^{k=0} = \begin{bmatrix} 0 \\ 0 \\ 0 \\ 1 \\ 1 \\ 1 \\ 1 \end{bmatrix} \begin{matrix} \theta_2 \\ \theta_3 \\ \theta_4 \\ \theta_1 \\ \theta_2 \\ \theta_3 \\ \theta_4 \end{matrix}$$

Noise is added to the 10 input measurements  $z$  to give:

$$z = \begin{bmatrix} 0.3786 \\ -1.0382 \\ 1.3593 \\ 2.3745 \\ 0.2249 \\ -0.6197 \\ 0.8277 \\ 1.3376 \\ 1.0009 \\ 0.9795 \end{bmatrix} \begin{matrix} p_{1-2} \\ p_{3-4} \\ p_1 \\ p_4 \\ q_{1-2} \\ q_{3-4} \\ q_1 \\ q_4 \\ V_1 \\ V_2 \end{matrix}$$

The representation of the measurement is given on the right hand side for both  $x$  and  $z$  vectors.

The process of the first iteration is shown below beginning with the initial measurement Jacobian  $H$  calculated based upon equation (47).

$$H = \begin{bmatrix} -19.0781 & 0 & 0 & 3.815629 & -3.81563 & 0 & 0 \\ 0 & 15.11853 & -15.1185 & 0 & 0 & 3.023706 & -3.02371 \\ -19.0781 & -25.8478 & 0 & 9.07519 & -3.81563 & -5.16956 & 0 \\ -25.8478 & -15.1185 & 40.96634 & 0 & -5.16956 & -3.02371 & 8.295767 \\ 3.815629 & 0 & 0 & 18.97564 & -19.0781 & 0 & 0 \\ 0 & -3.02371 & 3.023706 & 0 & 0 & 14.99103 & -15.1185 \\ 3.815629 & 5.169562 & 0 & 44.74595 & -19.0781 & -25.8478 & 0 \\ 5.169562 & 3.023706 & -8.19327 & 0 & -25.8478 & -15.1185 & 40.76134 \\ 0 & 0 & 0 & 1 & 0 & 0 & 0 \\ 0 & 0 & 0 & 0 & 1 & 0 & 0 \end{bmatrix}$$

The associated matrices are used to find the solution to the equation  $\Delta x^{0 \rightarrow 1} = \{[H(x^k)^T R^{-1} H(x^k)]^{-1} [H(x^k)^T R^{-1} [z - h(x^k)]]\}$  which represents the change between the initial flat start estimate at  $k = 0$  and the state vector solution at  $k = 1$ . The  $\Delta x$  is checked to see whether the maximum value is less than the required convergence value of  $10^{-4}$ . For this example, the convergence criterion is not met after one iteration. Therefore the starting value for state vector at the next iteration is:  $x^1 = x^0 + \Delta x^{0 \rightarrow 1}$ .

$$x^{k=1} = \begin{bmatrix} 0.0000 \\ -0.0173 \\ -0.0321 \\ 0.0277 \\ -0.0021 \\ -0.0212 \\ -0.0314 \\ 0.0191 \end{bmatrix}$$

The minimization function  $J(x)$  value is calculated using equation (36) and found to be  $J = 1.2888 \times 10^5$ .

This process continues until the convergence criterion is met. The final CSE state vector solution is obtained after four iterations and is calculated as:

$$x^{k=4} = \begin{bmatrix} 0.0000 \\ -0.0165 \\ -0.0328 \\ 0.0266 \\ 0.9999 \\ 0.9826 \\ 0.9689 \\ 1.0206 \end{bmatrix}$$

The minimization function  $J(x)$  value after four iterations is found to be  $J = 0.7261$ .

#### 4.7.2. Hybrid state estimator

The optimal PMU placement scheme for full observability is obtained from the solution to the ILP algorithm in chapter 2. Therefore PMUs are placed at buses 1 and 4 and phased into the system in the order of 1→4. A PMU can directly measure the voltage phasor at the placement bus and line currents in the lines directly connected to the placement bus. Therefore in this example PMUs at buses 1 and 4 measure buses 1 and 4 voltage phasors as well as the line currents in all system branches. In a practical scenario a PMU would directly measure the current, however in this situation the true voltage phasors and known network admittance parameters are used in equation (29) to calculate the branch currents. The currents in branches 1-2, 1-3, 2-4 and 3-4 are calculated as:

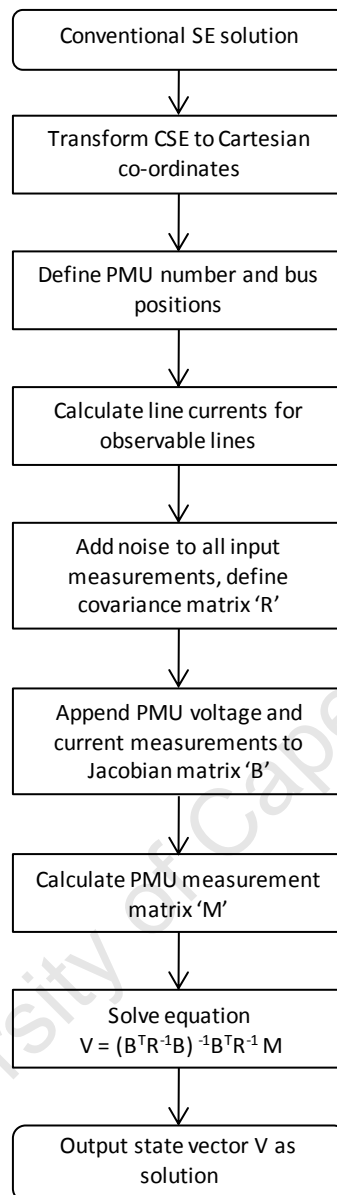
$$I_{1-2} = 0.3869 - j0.2230$$

$$I_{1-3} = 0.9812 - j0.6121$$

$$I_{4-2} = 1.3254 - j0.6995$$

$$I_{4-3} = 1.0411 - j0.5306$$

The method for implementing hybrid state estimation is shown in Flowchart 6.



Flowchart 6: Hybrid linear state estimation procedure

The state vector solution from the classical state estimator, the PMU voltage phasors and the current phasors are transformed from polar to Cartesian co-ordinates using the transformation in equation (82). The Jacobian measurement matrix is calculated based on equation (47).

$$H_{pmu} = \begin{bmatrix} 1 & 0 & 0 & 0 & 0 & 0 & 0 & 0 \\ 0 & 1 & 0 & 0 & 0 & 0 & 0 & 0 \\ 0 & 0 & 1 & 0 & 0 & 0 & 0 & 0 \\ 0 & 0 & 0 & 1 & 0 & 0 & 0 & 0 \\ 0 & 0 & 0 & 0 & 1 & 0 & 0 & 0 \\ 0 & 0 & 0 & 0 & 0 & 1 & 0 & 0 \\ 0 & 0 & 0 & 0 & 0 & 0 & 1 & 0 \\ 0 & 0 & 0 & 0 & 0 & 0 & 0 & 1 \\ 1 & 0 & 0 & 0 & 0 & 0 & 0 & 0 \\ 0 & 0 & 0 & 1 & 0 & 0 & 0 & 0 \\ 0 & 0 & 0 & 0 & 1 & 0 & 0 & 0 \\ 0 & 0 & 0 & 0 & 0 & 0 & 0 & 1 \\ 3.8156 & -3.8156 & 0 & 0 & 19.0269 & -19.0781 & 0 & 0 \\ 5.1696 & 0 & -5.1696 & 0 & 25.8091 & 0 & -25.8478 & 0 \\ 0 & -5.1696 & 0 & 5.1696 & 0 & -25.8478 & 0 & 25.8091 \\ 0 & 0 & -3.0237 & 3.0237 & 0 & 0 & -15.1185 & 15.0548 \\ -19.0269 & 19.0781 & 0 & 0 & 3.8156 & -3.8156 & 0 & 0 \\ -25.8091 & 0 & 25.8478 & 0 & 5.1696 & 0 & -5.1696 & 0 \\ 0 & 25.8478 & 0 & -25.8091 & 0 & -5.1696 & 0 & 5.1696 \\ 0 & 0 & 15.1185 & -15.0548 & 0 & 0 & -3.0237 & 3.0237 \end{bmatrix}$$

The voltage phasors from CSE are expressed in Cartesian co-ordinates. The PMUs voltage measurements and current measurements are expressed in Cartesian co-ordinates and appended to the measurement vector  $M$  with Gaussian noise.

$R$  in this case is a large matrix and is not shown here due to space considerations. However it is populated along the diagonal with the errors that are transformed from polar to Cartesian co-ordinates using equations (83)-(86).

Therefore the results of the initial CSE as well as the PMU measurements are considered to have a linear relationship with the state vector solution and therefore the state vector can be calculated in a non-iterative manner using equation (88).

$$M = \begin{bmatrix} 1.0077 & V_{r1se} \\ 0.9894 & V_{r2se} \\ 0.9763 & V_{r3se} \\ 1.0265 & V_{r4se} \\ 0 & V_{i1se} \\ -0.0180 & V_{i2se} \\ -0.0295 & V_{i3se} \\ 0.0269 & V_{i4se} \\ 0.9978 & V_{r1pmu} \\ 1.0068 & V_{r4pmu} \\ 0.0010 & V_{i1pmu} \\ 0.0261 & V_{i4pmu} \\ 0.3853 & I_{r1-2pmu} \\ 0.9755 & I_{r1-3pmu} \\ 1.3310 & I_{r4-2pmu} \\ 1.0382 & I_{r4-3pmu} \\ -0.2221 & I_{i1-2pmu} \\ -0.6070 & I_{i1-3pmu} \\ -0.7041 & I_{i4-2pmu} \\ -0.5270 & I_{i4-3pmu} \end{bmatrix}$$

The measurement vector  $M$  is shown above with the measurement representation appearing to the right.

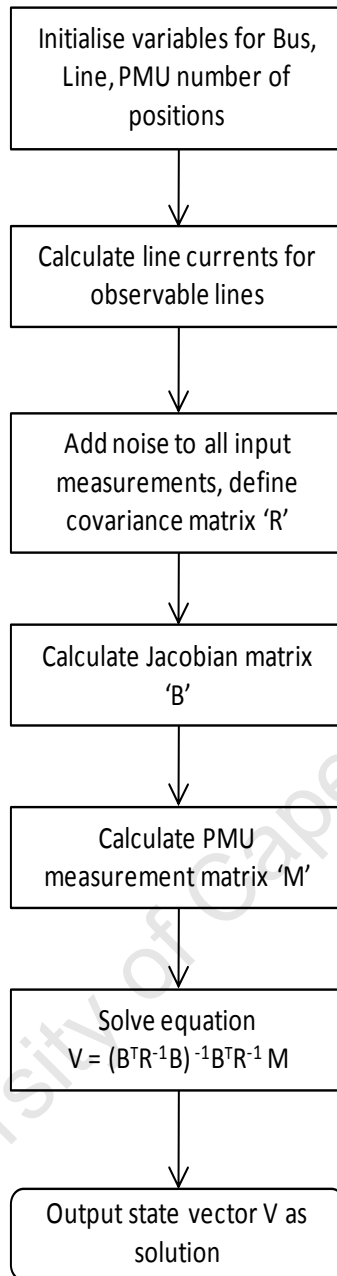
The HSE solution to equation (88) gives a state vector calculated as:

$$x_{k=4} = \begin{bmatrix} 0.0000 \\ -0.0171 \\ -0.0325 \\ 0.0263 \\ 1.0039 \\ 0.9861 \\ 0.9730 \\ 1.0237 \end{bmatrix}$$

#### 4.7.3. Linear state estimator

If there are a sufficient number of PMU to ensure full system observability, the system can be modeled by using only voltage and current phasors measured by the PMUs. In this example, the PMUs at buses 1 and 4 provide full system observability, therefore the LSE becomes feasible.

The method for implementing linear state estimation is shown in Flowchart 7.



Flowchart 7: Linear state estimation procedure

The method is essentially the same as the hybrid state estimator. The only difference is that the linear state estimator does not include the solution of the CSE in the Jacobian matrix. Therefore the only measurements that are found in the Jacobian matrix are voltage and current phasor measurements made by the PMUs. Due to the fact that the LSE is a stand-alone algorithm, it is necessary to compute the topology of the system in the form of a  $Y_{bus}$ .

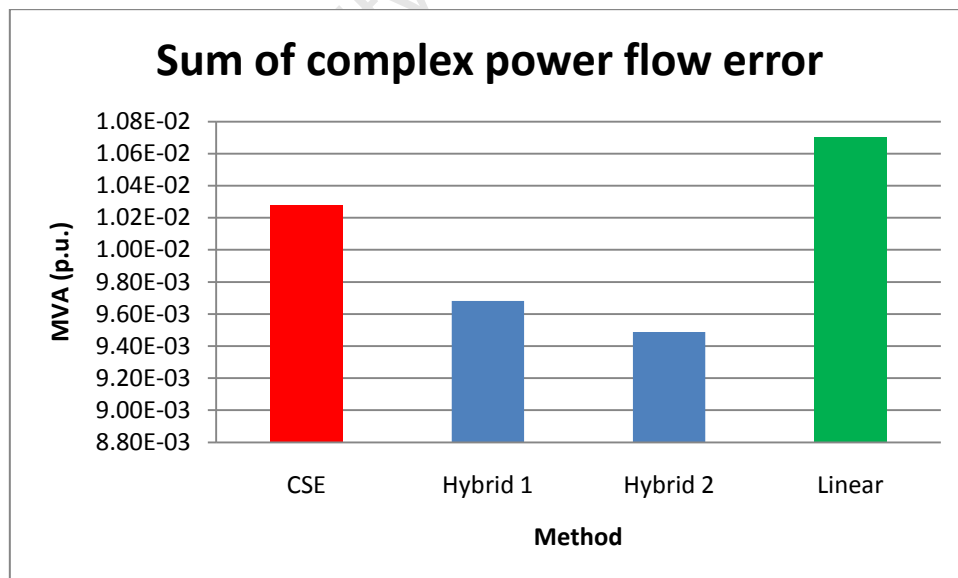
The LSE state vector solution obtained via equation (88) and calculated as:

$$x_{LSE} = \begin{bmatrix} 1.0000 \\ 0.9823 \\ 0.9685 \\ 1.0197 \\ 0.0000 \\ -0.0167 \\ -0.0316 \\ 0.0271 \end{bmatrix}$$

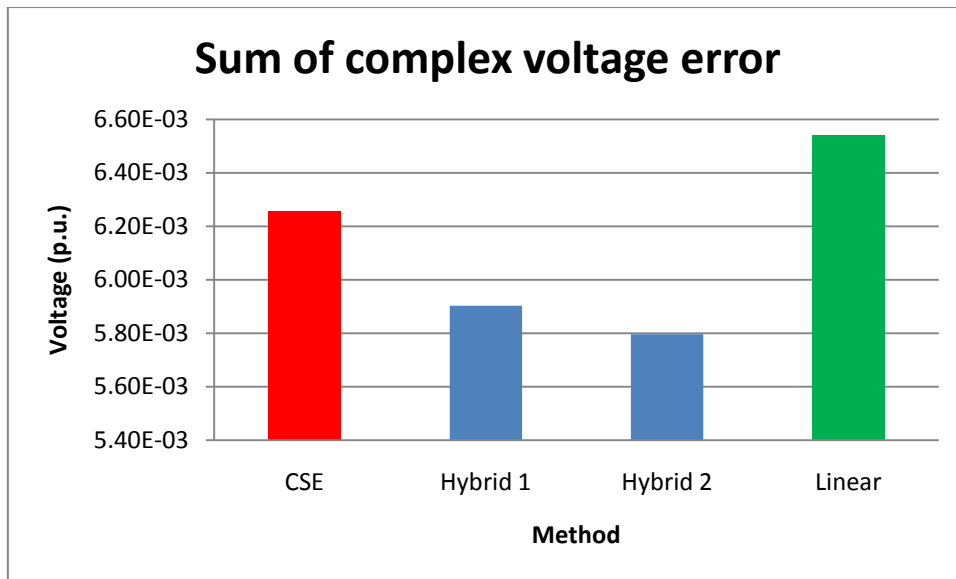
All algorithms are executed and run 1000 times to ensure a diverse data set. In all scenarios it is assumed that the PMUs are placed according to the solution provided by the ILP algorithm detailed in chapter 3. For the 4 bus example, the placement positions are buses 1 and 4, phased in the order of 1→4.

The red bars represent the results of only the CSE that uses power flows, power injections and voltage magnitudes to provide an estimate of the state of the system. The blue bars labelled 'hybrid  $x$ ' represent the HSE that uses the solution of the CSE and an appended linear post-processing step to obtain a solution. *Hybrid 'x'* indicates that there are  $x$  number of PMUs placed in the system. The green bars labelled '*linear*' represent the LSE that uses only voltage and current PMU phasor measurements to obtain a state solution. The dark grey bars, present in Graph 3 and Graph 4 on page 68, labelled *PMU bus x* indicate an HSE solution with only one PMU installed at bus  $x$ . The same colour schemes are used throughout the results. The results are assessed by computing the complex power flow error and complex voltage error discussed in section 4.4 and given by equations (72) and (73) respectively.

Graph 1 and Graph 2 show the complex power flow error (PFE) and complex voltage error (VE) respectively for the example 4 bus system.



Graph 1: Sum of complex power flow error for 4 bus system



Graph 2: Sum of complex voltage error for 4 bus system

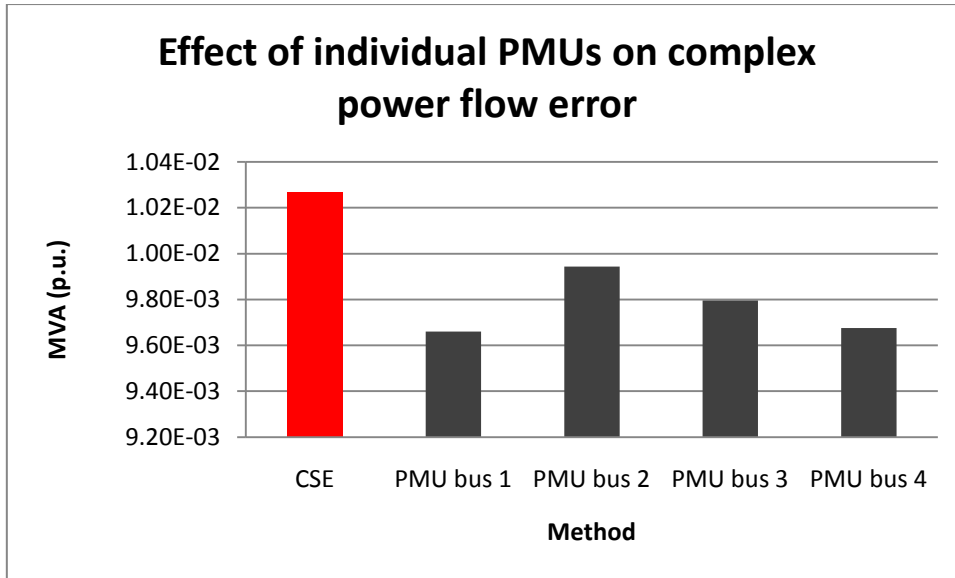
The above graphs indicate that the introduction of PMUs into the system using an HSE result in the lowest PFE and VE errors. The LSE produces a result that is not as accurate as the HSE or CSE. The time taken to reach the solution and the average amount of iterations for CSE and HSE are given in Table 29 below.

Table 29: Iteration number and time taken for convergence for 4-bus system

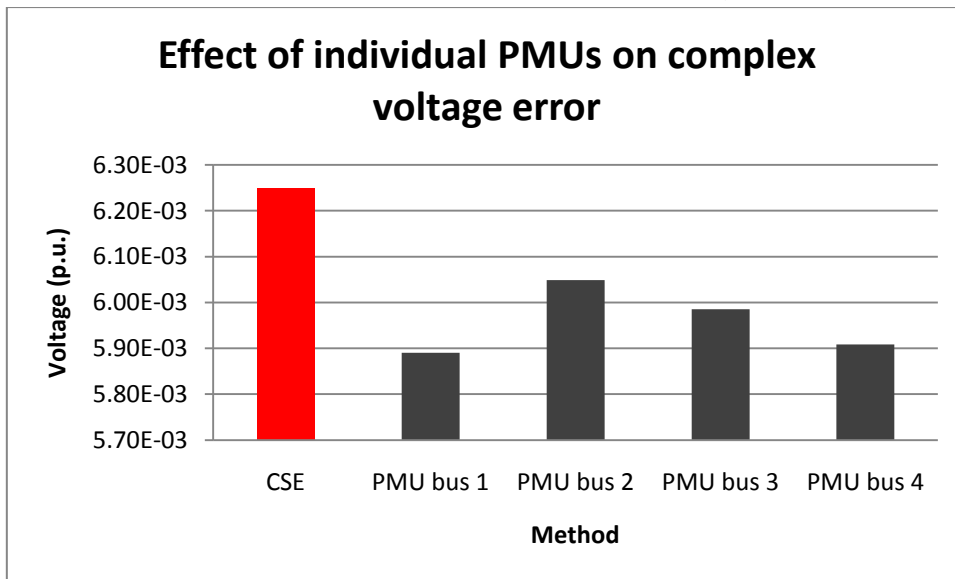
Average	CSE	HSE	LSE
Iterations	3.532	3.532	-
Time taken (s)	2.70E-03	7.20E-03	8.74E-04

Table 29 shows that LSE executes the fastest, followed by CSE, then HSE. This is expected due to the linear non-iterative nature of the LSE. HSE will always be slower than CSE due to the fact that HSE uses the CSE solution and an added linear step to arrive at a solution. The HSE is slower than CSE but produces a more accurate result.

Graph 3 and Graph 4 show the individual effects that PMUs have on the complex PFEs and complex VEs when placed at specific system buses. The errors are computed individually by running a HSE and executing the post-processing linear step of the algorithm with one PMU at a time. This was achieved by modifying the HSE algorithm. Every PMU is considered as a stand-alone device in the system, and each execution is run on the same CSE solution to ensure the results are correlated. Due to the nature of the problem and associated noise added as a random variable, it is necessary to have a large enough sample size in order to obtain a mean that does not vary significantly from run to run. The base CSE errors are always of the same magnitude, ensuring a strong correlation between the cumulative and individual effects.



Graph 3: Effect of individual PMUs on complex power flow error for 4 bus system



Graph 4: Effect of individual PMUs on complex voltage error for IEEE 14 bus system

Graph 3 and Graph 4 indicate that the most significant impact in terms of improving PFE and VE errors can be gained by placing PMUs at buses 1 and 4. The ILP algorithm outputted buses 1 and 4 as optimal placement locations based only on observability rules. The fact that they are located at the buses best suited to improving state estimation in terms of PFE and VE is purely coincidental in this case.

## 5. Chapter 5: Results of state estimation using optimal placement positions from ILP algorithm

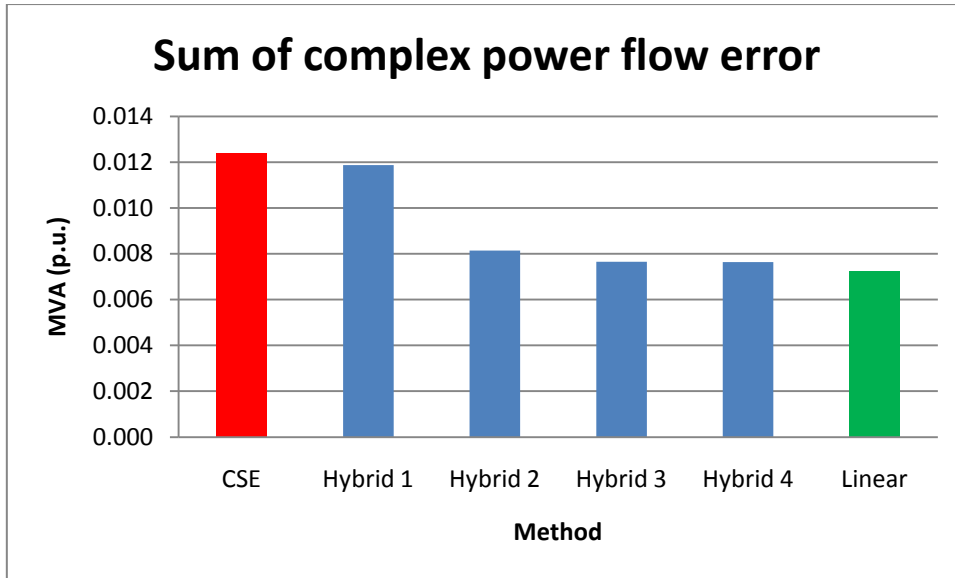
This section analyzes how the accuracy of state estimation is affected by the incorporation of PMU measurement data. Equations (72) and (73) are used to determine the error between the true and estimated complex power flows and true and estimated complex bus voltages respectively. Complex power flow error (PFE) and complex voltage error (VE) have been defined previously in this work. However, they will be referred to using those defined acronyms extensively in these results. The results in this chapter follow the theme of presentation as in the previous chapter. Firstly the cumulative effects of adding PMUs into an IEEE bus system are investigated, followed by an investigation into the impact of individual PMUs.

### 5.1. Algorithm applied to the IEEE 14 bus system

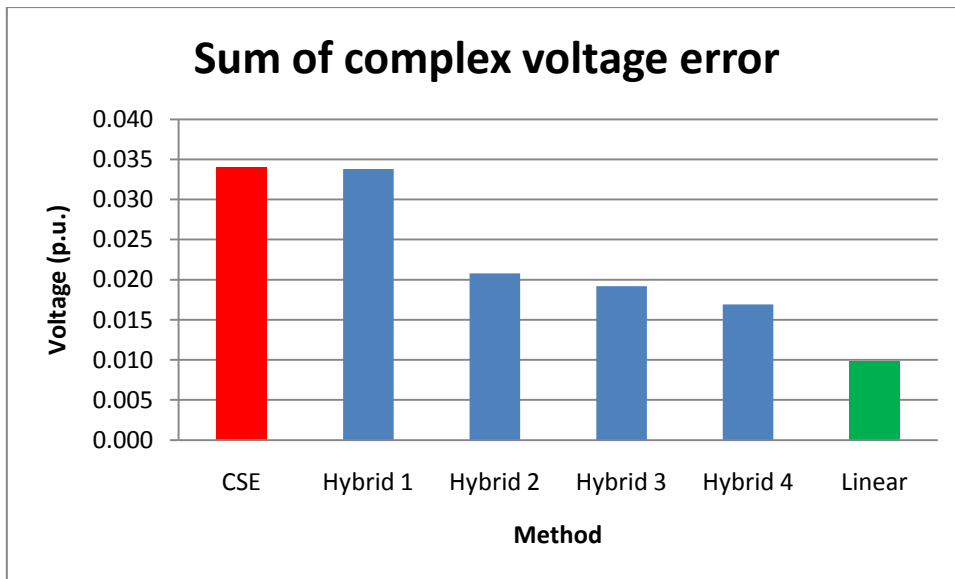
This system has 14 buses with 20 lines. In order to make the system observable by conventional measurements it is assumed that there are 11 flow measurements, 10 power injection measurements and 5 bus voltage magnitude measurements. 4 PMUs are placed at buses 2, 6, 7 and 9 for both hybrid and linear state estimators. In the case of the hybrid state estimator Graph 5 and Graph 6 are plotted with the assumption that PMUs are phased into the system in the order 2→6→7→9. Graph 7 and Graph 8 show the impact of individual PMUs on PFE and VE respectively.

Table 30: 14-bus system properties

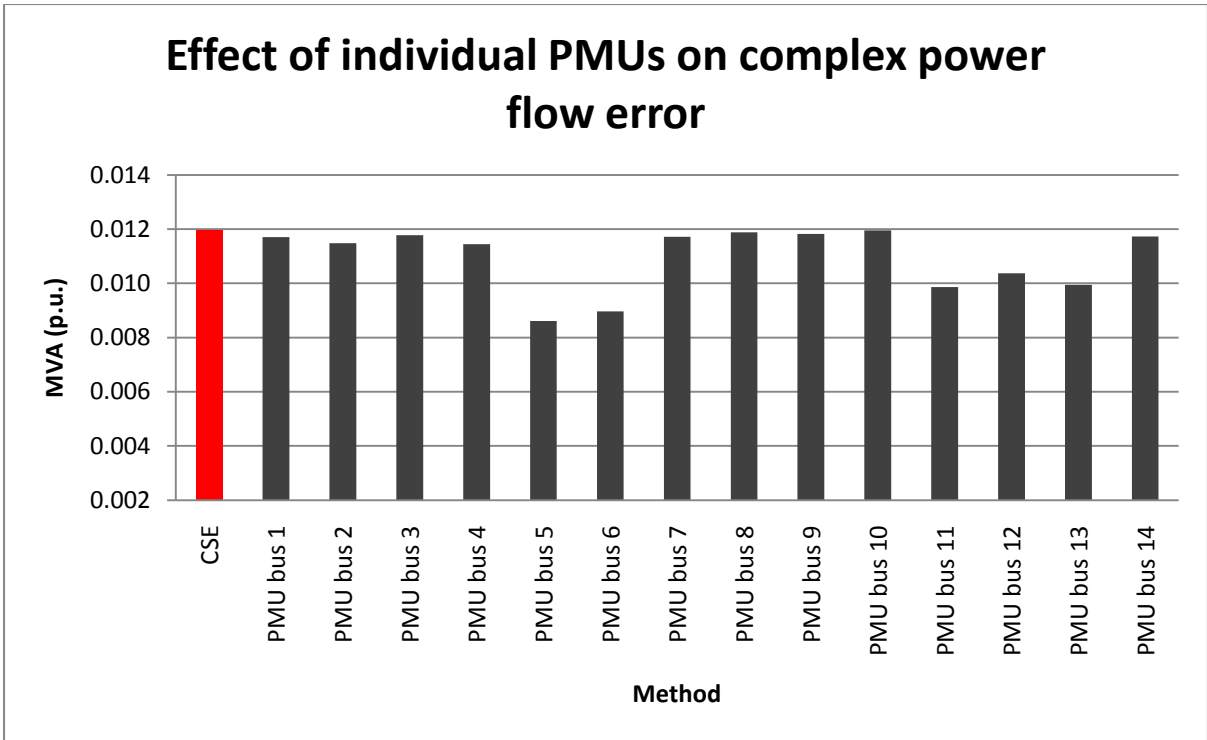
IEEE 14 bus (20 lines)		
Measurement	Number	Buses
PMU	4	2,6,7,9
Power flow	11	1-2,1-5,2-4,3-4,4-5,4-7,6-12,7-8,9-14,12-13,13-14
Power injection	10	1,2,3,4,8,9,10,11,12,14
Voltage measurements	5	1,3,4,5,14
Zero-injections	1	7



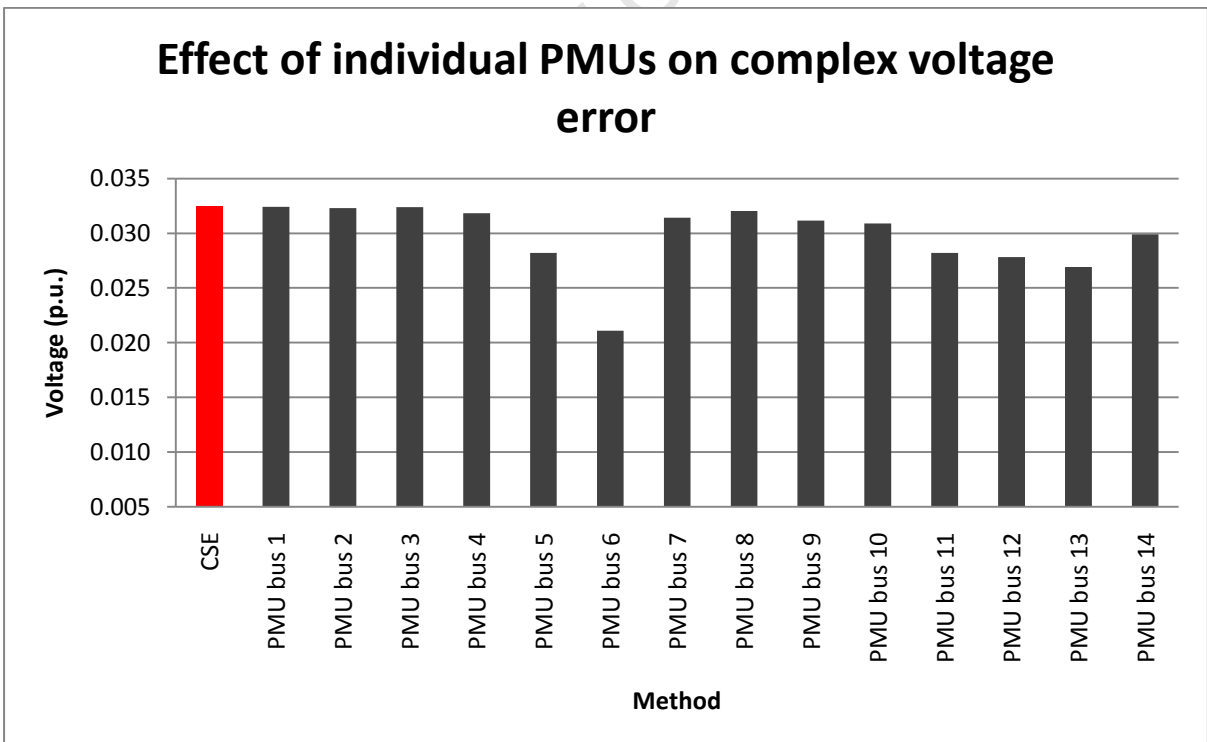
Graph 5: Sum of complex power flow error for IEEE 14 bus system



Graph 6: Sum of complex voltage error for IEEE 14 bus system



Graph 7: Effect of individual PMUs on complex power flow error for IEEE 14 bus system



Graph 8: Effect of individual PMUs on complex voltage error for IEEE 14 bus system

The average iteration number and time taken for the IEEE 14 bus algorithm to converge to a solution are shown in Table 31.

Table 31: Iteration number and time taken for convergence for 14-bus system

Average	CSE	HSE	LSE
Iterations	4.170	4.170	-
Time taken (s)	2.24E-02	2.74E-02	3.40E-03

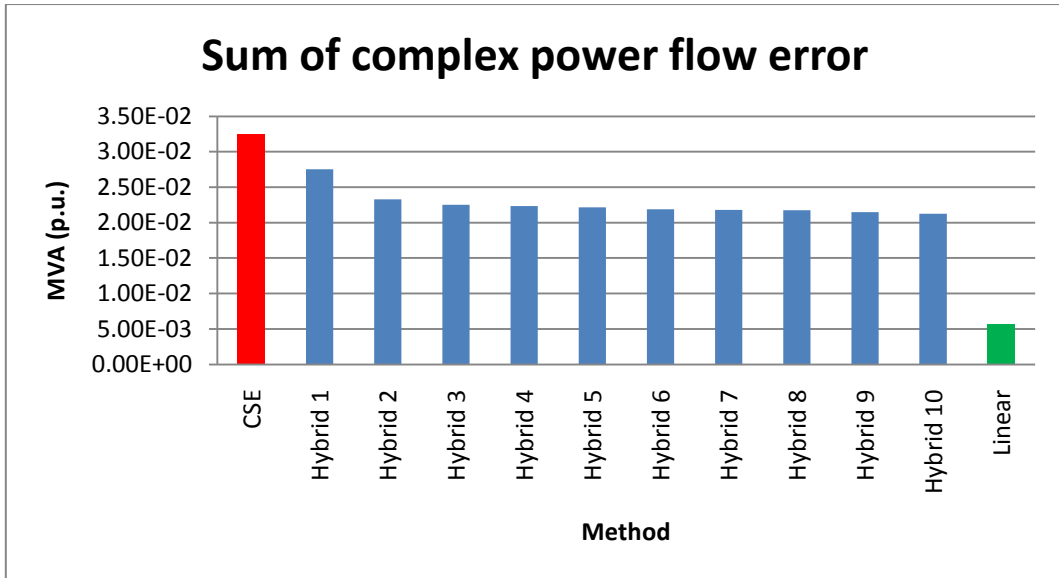
Graph 5 and Graph 6 indicate that the PFE and VE decrease with increasing PMU placement for the HSE resulting in a PFE and VE that are lower than CSE for all cases of PMU placement. The most significant decrease in PFE and VE is obtained by the addition of a PMU at bus 6 in the system. The LSE gives the lowest PFE and VE and executes approximately 7 times faster than CSE. Graph 7 and Graph 8 support the findings in the previous graphs by indicating that an individually placed PMU at bus 6 has the most significant reduction to PFE and VE. Other notable individual PMU placement buses that effect PFE and VE are buses 5, 11, 12 and 13.

## 5.2. Algorithm applied to the IEEE 30 bus system

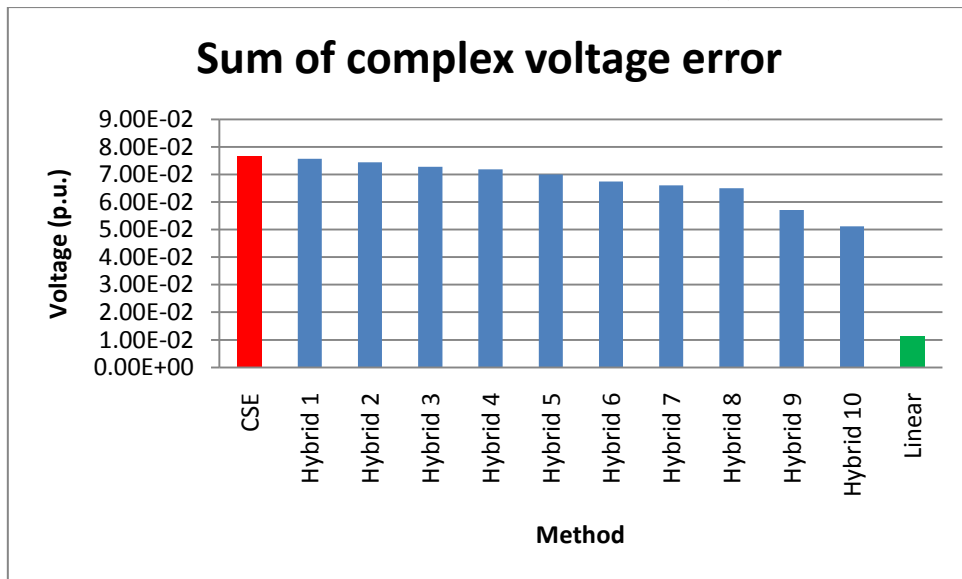
This system has 30 buses with 41 lines. In order to make the system observable by conventional measurements it is assumed that there are 18 flow measurements, 13 power injection measurements and 13 bus voltage magnitude measurements. 10 PMUs are placed at buses 1, 2, 6, 9, 10, 12, 15, 18, 25 and 27 for both hybrid and linear state estimators. In the case of the hybrid state estimator Graph 9 and Graph 10 are plotted with the assumption that PMUs are phased into the system in the order 1→2→6→9→10→12→15→18→25→27. Graph 11 and Graph 12 show the impact of individual PMUs on PFE and VE respectively.

Table 32: 30-bus system properties

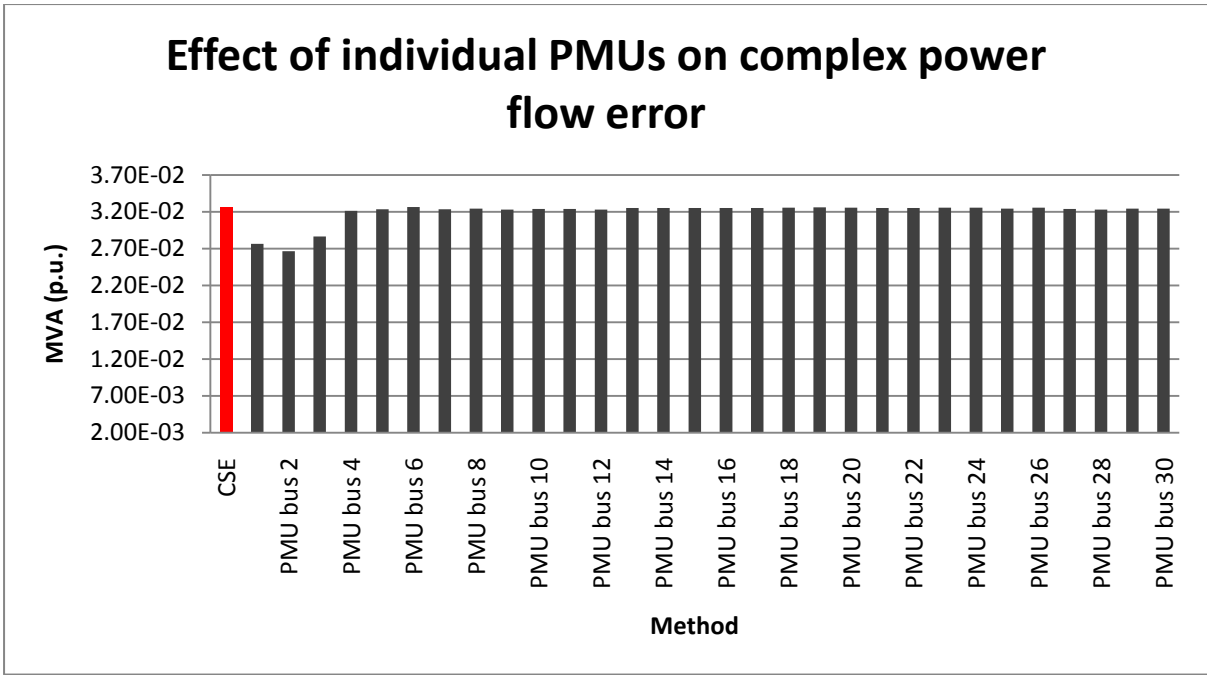
IEEE 30 bus (41 lines)		
Measurement	Number	Buses
PMU	10	1,2,6,9,10,12,15,18,25,27
Power flow	18	3-4,4-6,4-12,5-7,6-7,6-9,6-10,6-28,9-10,9-11,10-21,10-22,12-15,18-19,22-24,25-27,27-28,27-29
Power injection	13	2,5,8,11,12,13,14,17,18,20,23,26,30
Voltage measurements	13	1,3,9,10,11,13,15,16,19,22,24,28,29
Zero-injections	6	6,9,22,25,27,28



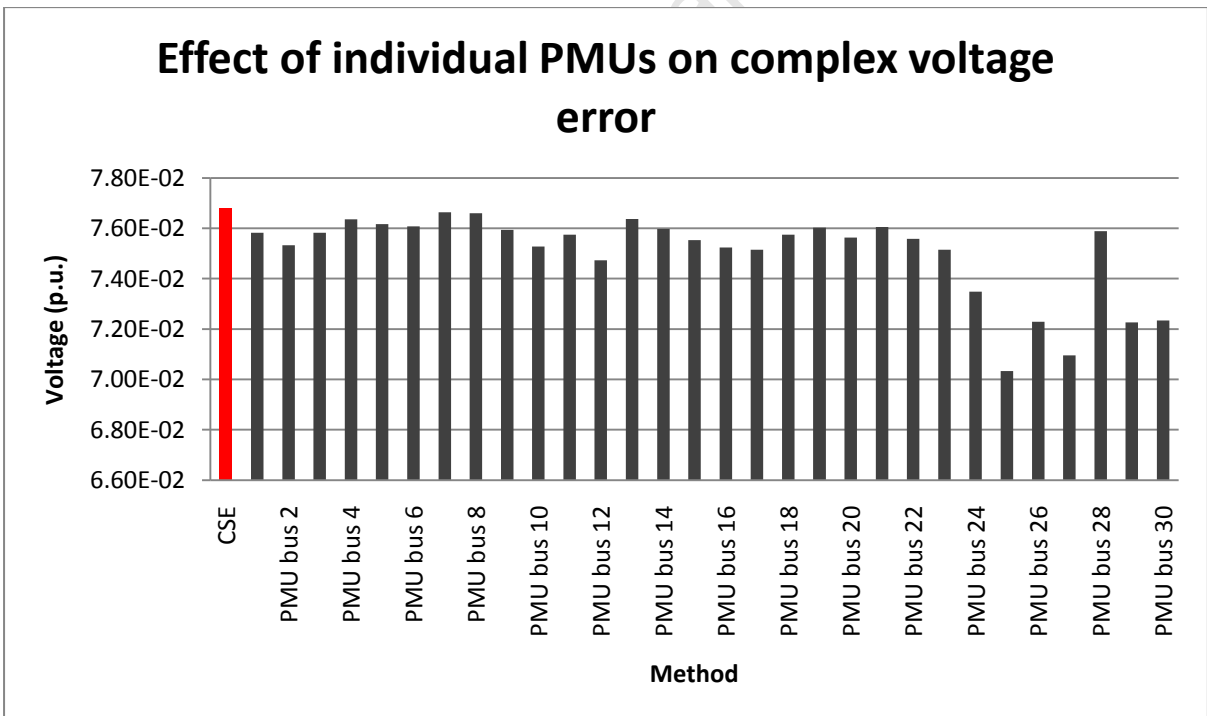
Graph 9: Sum of complex power flow error for IEEE 30 bus system



Graph 10: Sum of complex voltage error for IEEE 30 bus system



Graph 11: Effect of individual PMUs on complex power flow error for IEEE 30 bus system



Graph 12: Effect of individual PMUs on complex voltage error for IEEE 30 bus system

The average iteration number and time taken for the IEEE 30 bus algorithm to converge to a solution are shown in Table 33.

Table 33: Iteration number and time taken for convergence for 30-bus system

Average	CSE	HSE	LSE
Iterations	4.169	4.169	-
Time taken (s)	4.02E-02	5.03E-02	6.30E-03

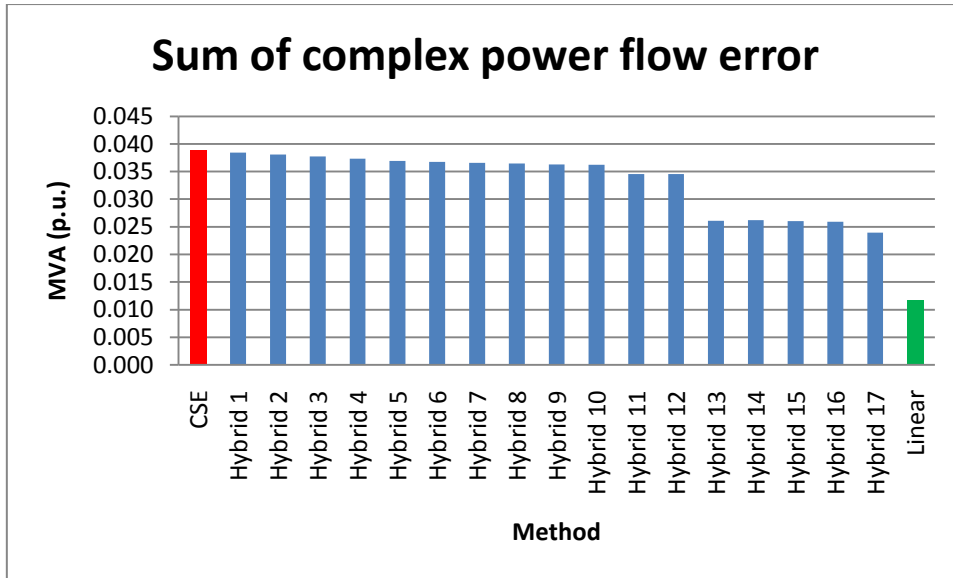
Graph 9 shows that the PFE decreases substantially with the addition of only one PMU in the HSE, then plateaus as the number of PMUs increases. The decrease and levelling out of the PFE is correlated to the phasing scheme, as the PMUs with the most significant PFE reduction effects are added to the HSE first. Graph 10 confirms that the most significant decrease occurs for an individual PMU placed at bus 2 followed closely by bus 1. Graph 9 shows that the VE decreases steadily as the number of PMUs in the HSE are increased. There is a more significant decrease in the last two bars labelled 'hybrid 9 and hybrid 10'. The results in Graph 12 indicate that the most significant decreases in VE are from buses placed at 25 and 27. The PMU phasing scheme adds these two buses in last and explains why the last two bars in Graph 9 show a slightly sharper decrease in VE. The LSE gives the lowest PFE and VE and executes approximately 6 times faster than CSE. Buses with the most notable VE decrease are 24, 25, 27, 26, 29 and 30.

### 5.3. Algorithm applied to the IEEE 57 bus system

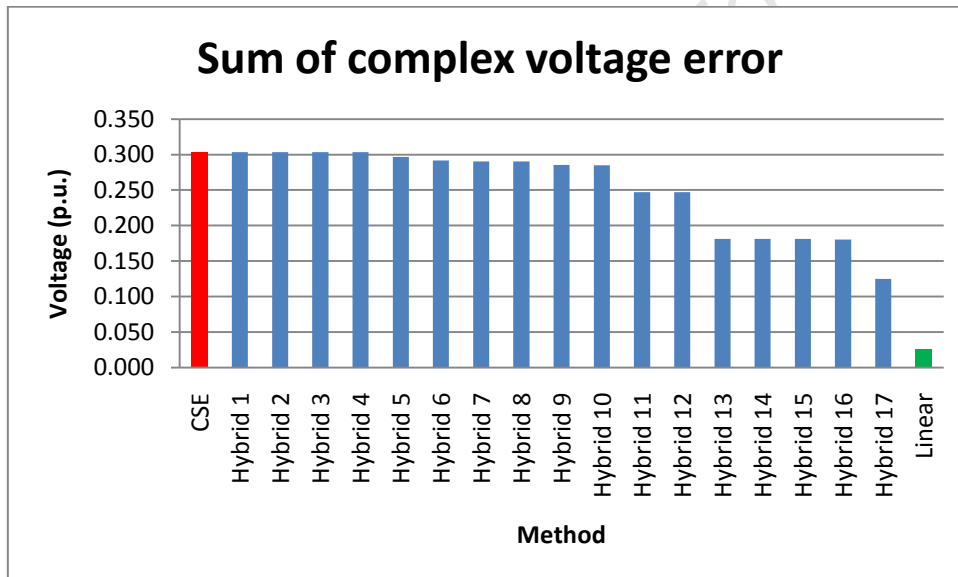
This system has 57 buses with 78 lines. In order to make the system observable by conventional measurements it is assumed that there are 36 flow measurements, 32 power injection measurements and 11 bus voltage magnitude measurements. 17 PMUs are placed at buses 1, 6, 9, 15, 19, 22, 24, 28, 30, 32, 36, 39, 41, 47, 51, 53 and 57 for both hybrid and linear state estimators. In the case of the hybrid state estimator Graph 13 and Graph 14 are plotted with the assumption that PMUs are phased into the system in the order 1→6→9→15→19→22→24→28→30→32→36→39→41→47→51→53→57. Graph 15 and Graph 16 show the impact of individual PMUs on PFE and VE respectively.

Table 34: 57-bus system properties

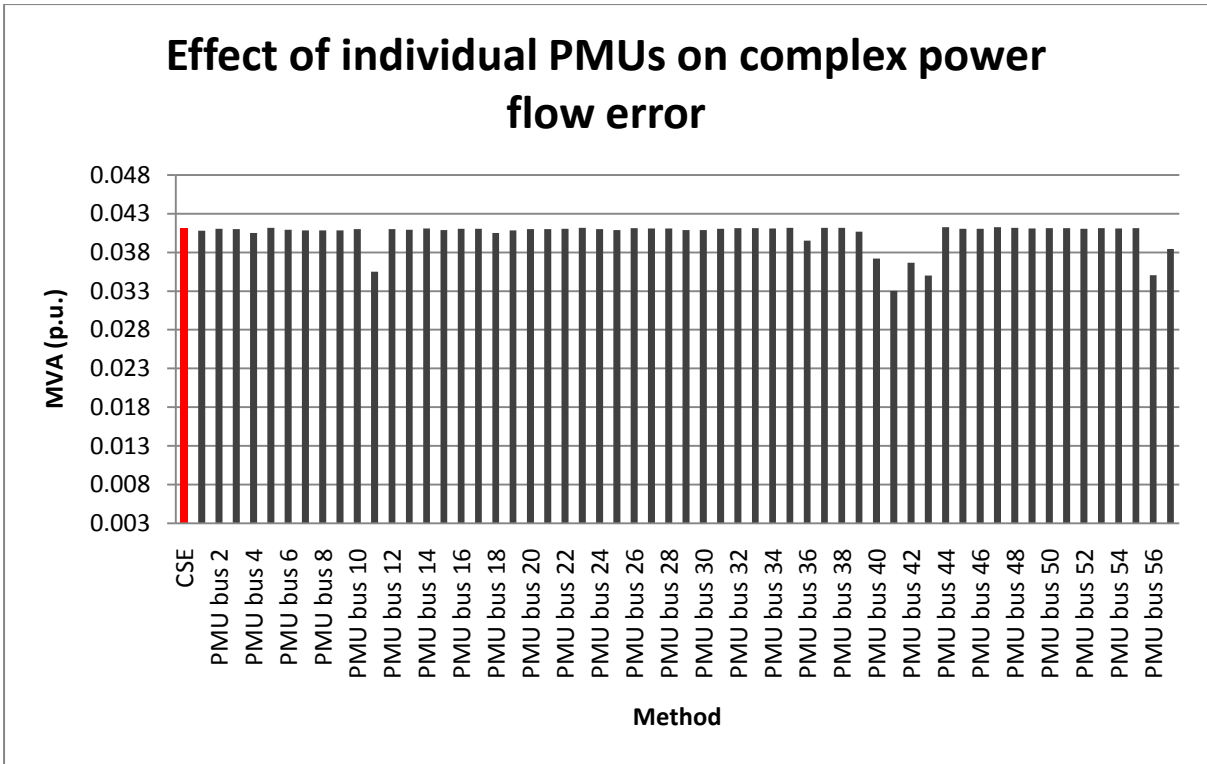
IEEE 57 bus (78 lines)		
Measurement	Number	Buses
PMU	17	1,6,9,15,19,22,24,28,30,32,36,39,41,47,51,53,57
Power flow	36	2-3,3-4,3-15,4-5,6-7,6-8,9-11,9-13,9-55,11-13,14-15,14-46,15-45,18-19,19-20,20-21,22-23,22-38,23-24,24-26,25-30,26-27,27-28,31-32,32-33,34-35,35-36,36-37,37-38,38-49,40-56,41-42,41-43,48-49,49-50,50-51,53-54
Power injection	32	1,3,5,6,8,9,10,12,13,14,16,17,18,20,23,25,27,29,30,31,33,35,38,39,41,44,47,49,50,52,54,55,57
Voltage measurements	11	1,6,15,22,25,29,36,42,47,51,57
Zero-injections	15	4,7,11,21,22,24,26,34,36,37,39,40,45,46,48



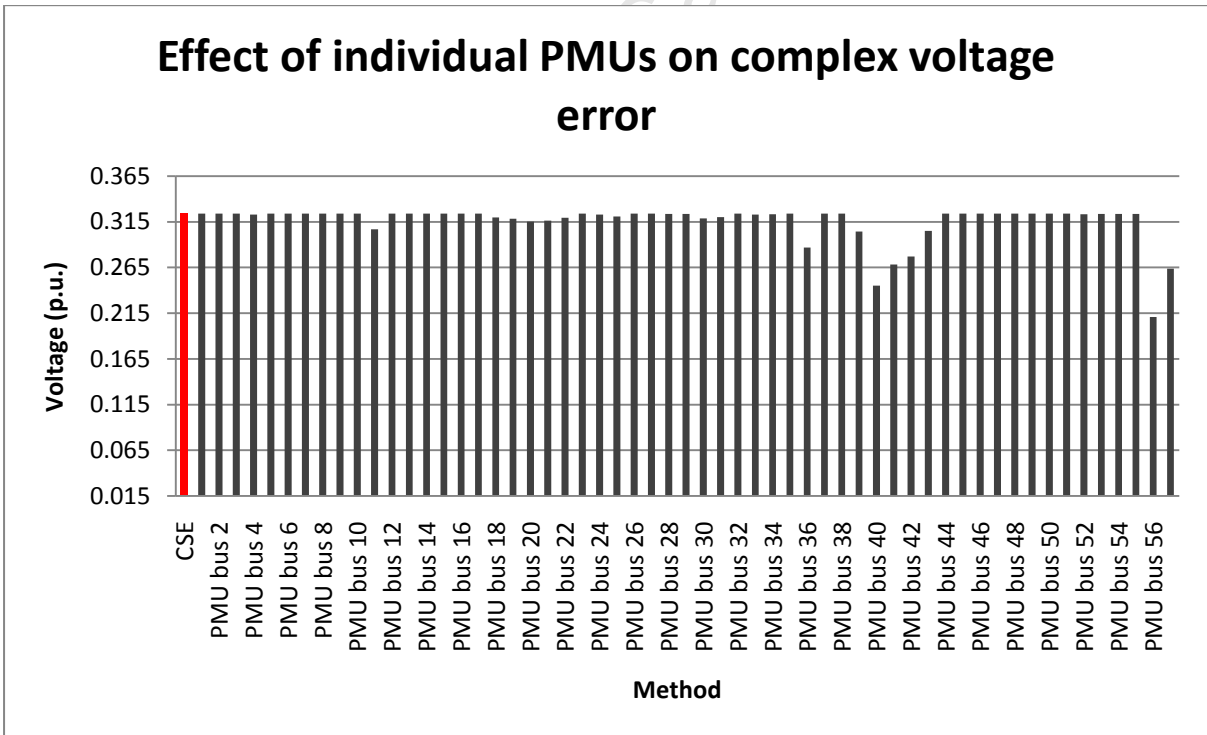
Graph 13: Sum of complex power flow error for IEEE 57 bus system



Graph 14: Sum of complex voltage error for IEEE 57 bus system



Graph 15: Effect of individual PMUs on complex power flow error for IEEE 57 bus system



Graph 16: Effect of individual PMUs on complex voltage error for IEEE 57 bus system

The average iteration number and time taken for the IEEE 57 bus algorithm to converge to a solution are shown in Table 35.

Table 35: Iteration number and time taken for convergence for 57-bus system

Average	CSE	HSE	LSE
Iterations	4.352	4.352	-
Time taken (s)	1.34E-01	1.61E-01	9.30E-03

Graph 13 indicates that the PFE decreases slowly with the addition of PMUs up until the total of PMUs in the system is 12. Then there is a sharp decrease in the PFE with the addition the 13<sup>th</sup> PMU. The 13<sup>th</sup> PMU is placed at bus 41. Graph 15 indicates that a PMU placed at bus 41 has the most significant effect on the PFE. Graph 14 shows a similar trend to the PFE graph, with the VE decreasing drastically when the 13<sup>th</sup> PMU is installed in the system. The VE reaches the lowest point when the 17<sup>th</sup> PMU is installed in the system at bus 57. Graph 16 indicates that the positions that contribute to the most significant decrease in VE are buses 56, 40, 41, 42, 57 and 36. The positions that contribute to the most significant PFE decrease are buses 41, 43, 56, 11, 40 and 42. LSE gives the lowest PFE and VE errors and executes approximately 14 times faster than CSE.

#### 5.4. Comparison of computational time for CSE, HSE and LSE

Table 36 shows the time taken for each respective state estimator to reach a solution. As the system size increases from the 14 bus to 30 bus systems the methods increase in time taken to reach solutions all increase by approximately 1.8 times the original value. However, the move from the 30 bus systems to the 57 bus systems indicate that CSE and HSE computational times increase by approximately 3.2 times, whilst the LSE computational time increases by only 1.5 times.

Table 36: Comparison of computational time for CSE, HSE and LSE

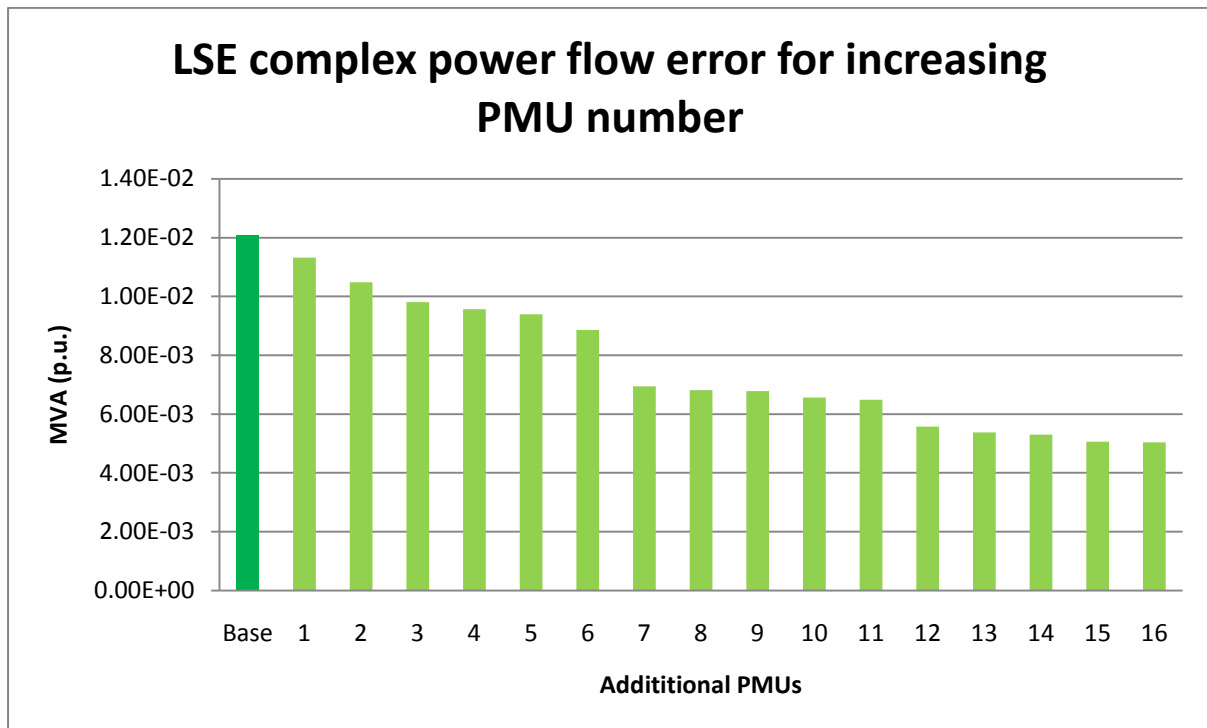
Average	CSE	HSE	LSE
IEEE 14	2.24E-02	2.74E-02	3.40E-03
IEEE 30	4.02E-02	5.03E-02	6.30E-03
IEEE 57	1.34E-01	1.61E-01	9.30E-03

#### 5.5. Linear state estimator applied to IEEE 57 bus system

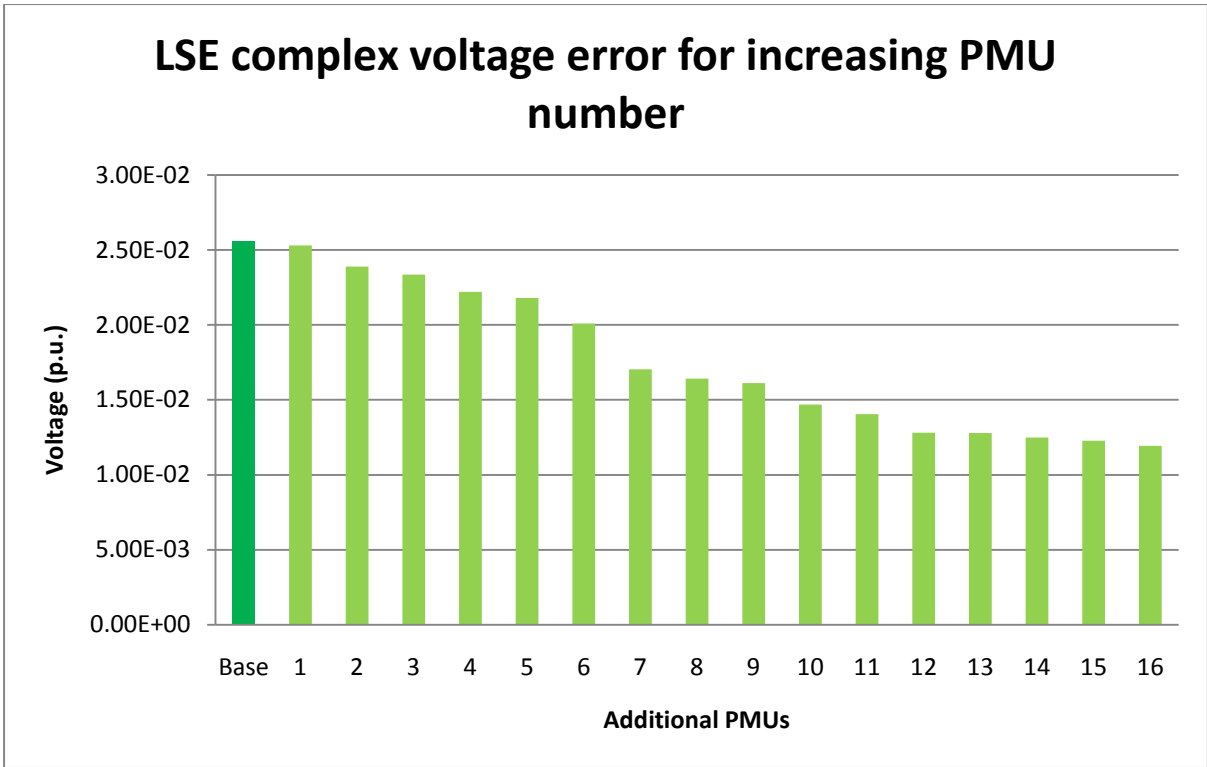
South Africa's national utility is very interested in utilising LSE. The research in this work shows that the linear state estimator output is more accurate than CSE and HSE with smaller complex PFEs and VEs. In addition it converges to a solution significantly faster than CSE and HSE. Therefore it is of interest to take a closer look at LSE and examine the accuracy improvements that additional PMUs will have on the PFE and VE errors.

It was noted in chapter 1 that the national utility is looking to procure an additional 15 PMUs, taking the total up to 19 PMUs. The optimal placement ILP method in this work indicates that 17 PMUs are required for full observability of the IEEE 57 bus system, however, this number decreases to 11 when the zero-injection buses are considered. However, the nature of the Eskom system and the number of zero-injection buses present are unknown at this time. Therefore it will be assumed 19 PMUs will be used for a test system of approximately the same size as the IEEE 57 bus system.

This section analyses the LSE applied to the IEEE 57 bus system. In order to measure each bus voltage in a bus system by linear measurements all the system buses must be made observable. Therefore the initial LSE must be run with 17 PMUs for full observability. These PMUs are placed at the buses 1, 6, 9, 15, 19, 22, 24, 28, 30, 32, 36, 38, 41, 47, 51, 53, 57. For demonstrative purposes the number of PMUs is increased from 17 to 33. This placement represents a worst case scenario whereby there are no zero-injection measurements in the system and 33 PMUs are required to give a redundancy of two or more at every bus in the system. A redundancy level of two is assumed in order to give a utility the security of continued measurements which would result in a LSE solution in the event of a line loss or loss of measurement. The additional considered PMU placement sites are obtained from the ILP algorithm from Table 19 and are 2, 4, 12, 20, 25, 26, 29, 31, 33, 35, 43, 44, 46, 50, 54, and 56.

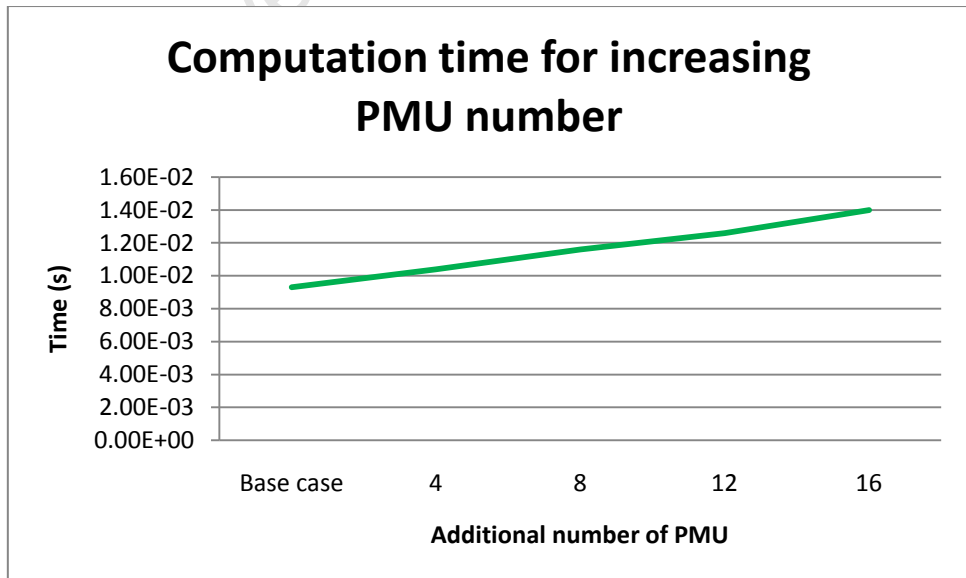


Graph 17: Effect that an increasing number of PMUs have on the LSE complex power flow error



Graph 18: Effect that an increasing number of PMUs have on the LSE complex voltage error

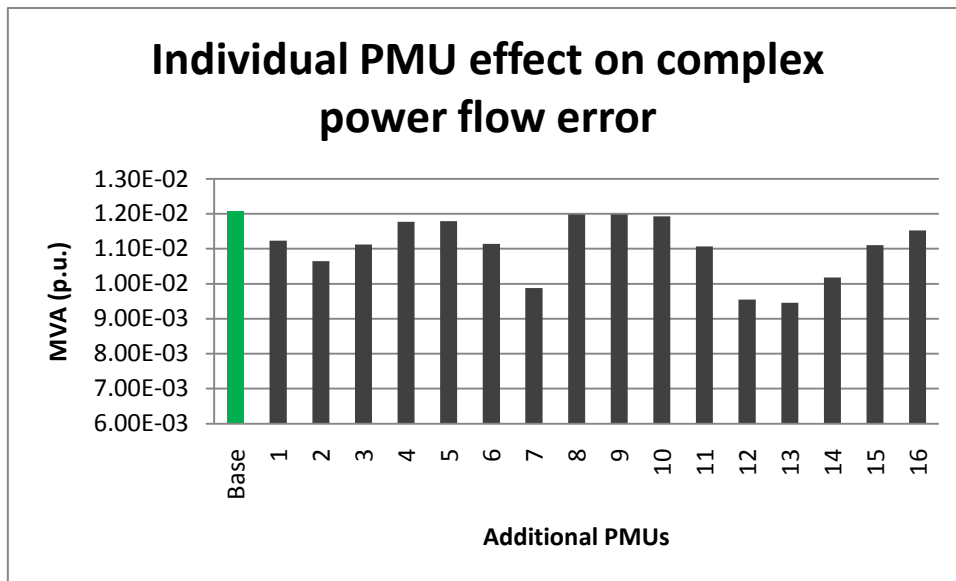
Graph 17 and Graph 18 give the PFE and VE respectively for an increasing number of PMUs utilised for LSE. The dark green bar represents the error of the LSE with 17 PMUs. In both graphs the errors decrease as the amount of PMUs increase. The PFE and VE of the LSE with an additional 16 PMUs installed are approximately two times better than the PFE and VE of the base LSE. Graph 19 shows the computation time for an increasing number of PMUs.



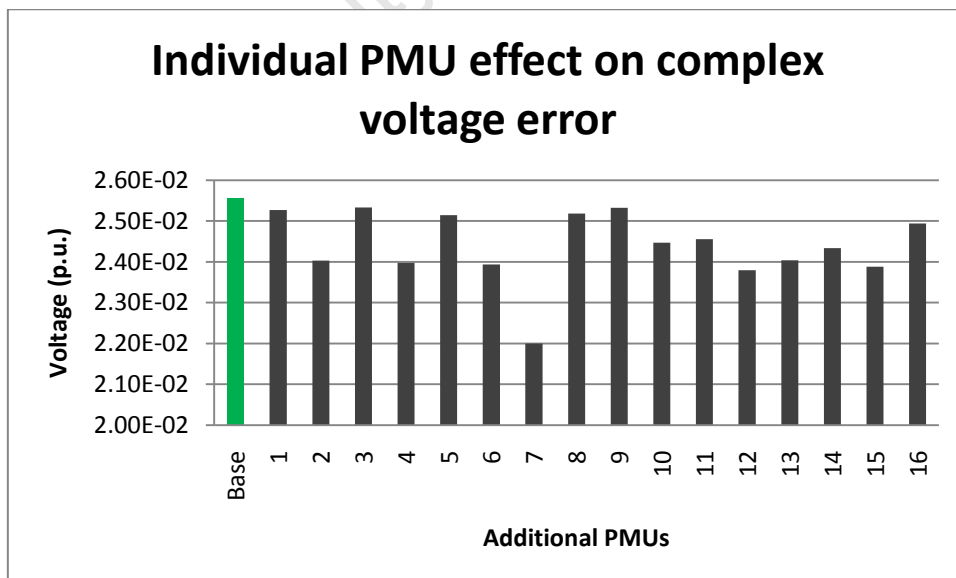
Graph 19: LSE computation time for an increasing number of PMU

Intuitively the computation time needed to reach a solution increases for an increasing number of PMU, due to the additional measurement data that is incorporated into the system. The time increased from approximately 0.009 seconds for the base LSE to 0.014 seconds for an additional 16 PMUs.

Graph 20 and Graph 21 show the effect that each individual PMU has on PFE and VE respectively. As previously mentioned it is assumed that the PMUs are assessed in the order of 2, 4, 12, 20, 25, 26, 29, 31, 33, 35, 43, 44, 46, 50, 54, and 56. Therefore in the graphs, '1' and '16' on the x-axis represent a PMU at bus '2' and '56' respectively.



Graph 20: Effect of individual PMUs on complex power flow error for IEEE 57 bus system



Graph 21: Effect of individual PMUs on complex voltage error for IEEE 57 bus system

If the PFE and VE are considered to have equal weighting in terms of importance in results, the graphs indicate the best numbers for placement are numbers 7, 12, 2 and 13 which represent PMUs placed at buses 29, 44, 4 and 46 respectively.

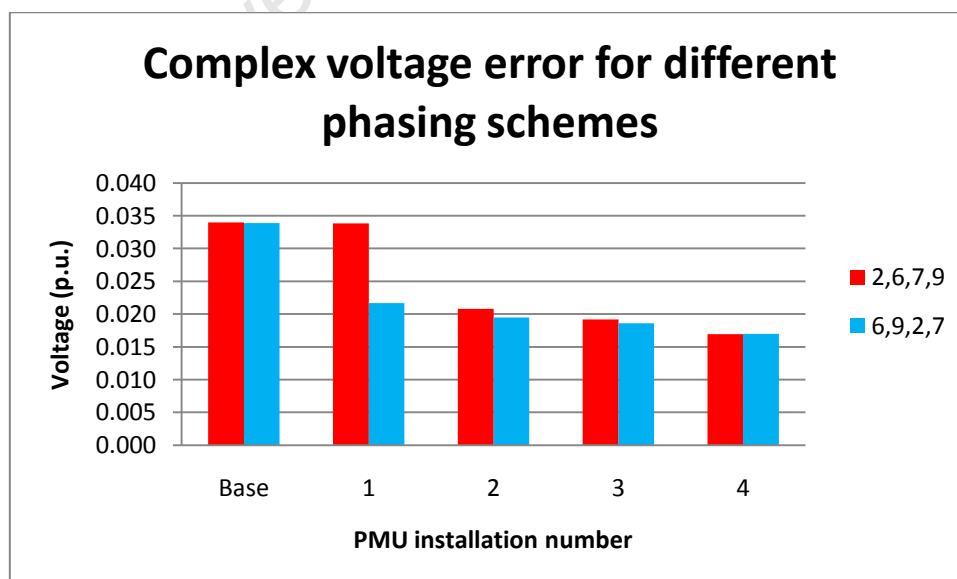
## 5.6. Variation of resulting errors within specific bus test systems

Graphs illustrating the individual PMU effects on the complex power errors and complex voltage errors display a significant amount of variation. This is indicative of the fact that PMUs placed at different buses provide differing levels of error improvements. In all cases, the errors become smaller when a PMU is added. However, these improvements are case-specific and are largely dependent on the positions of the existing PMUs, as well as the system topology and the amount of real and reactive power flow. Consider Graph 20 on the previous page as an illustrative example. This graph is derived from results of a linear state estimator on the IEEE 57 bus system and illustrates how the addition of individual PMUs affects the complex power flow error.

The base complex power flow error is always greater than the resulting error when an additional PMU is added. It is clearly observable that the 7<sup>th</sup>, 12<sup>th</sup> and 13<sup>th</sup> PMU placements corresponding to buses 29, 44 and 46 provide the best complex power flow error reduction effects. The reason for this reduction effect is due to the fact that the additional PMUs are placed in areas where existing PMU measurements do not exist. At these positions the PMUs are able to accurately measure the voltage phasors. In addition, relatively large real and reactive power flows exist on these branches that are now monitored by PMUs. The improvement in the accuracy of the voltage phasors coupled with relatively large real and reactive power flows means that PMUs placed at these buses reduce the complex power flow error to a greater effect than PMUs placed at buses with smaller power flows.

## 5.7. Phasor measurement unit phasing

The results indicate that there is most definitely a decrease in errors for an increasing number of PMUs. However, the rate at which this decrease occurs is not always the same. For example consider two results of different phasing schemes for the IEEE 14 bus system shown below in Graph 22. It is shown that both graphs obtain an identical VE for 4 PMUs installed in the system. However, if PMUs are phased in the order of 2, 6, 7 and 9, the first PMU placement at bus 2 has a minimal effect on decreasing the VE. If the PMUs are phased in the order of 6, 9, 2 and 7 the effects of the first PMU are far more noticeable.



Graph 22: Complex voltage error for different phasing schemes

The results from the above graph are expected due to the fact that a PMU placed at bus 6 gave the best reduction of the VE based on Graph 8. Therefore this work proposes that the phasing schemes be ranked by an analysis of the gradient between the resulting PFE and VE and the different placement sets so that the maximum rate of change can be obtained for a specified PMU phasing scheme.

The optimal phasing schemes determined by the highest rate of error improvement per installation are shown below in Table 37.

Table 37: Optimal phasing schemes for best PFE and VE

Bus type	Best phasing scheme for PFE	Best phasing scheme for VE
IEEE 14	6,2,7,9	6,9,7,2
IEEE 30	2,1,9,12,10,25,27,15,6,18	25,27,12,2,10,15,18,1,9,6
IEEE 57	41,57,36,39,19,1,15,9,6,24,53,51,32,28,22,47	57,41,36,39,19,22,30,24,1,6,7,15,28,32,47,51,53

These phasing schemes indicate that the phasing scheme for the lowest rate of change of PFE is not necessarily the best phasing scheme for the lowest rate of change of VE and vice versa. This difference is due to the topology of the system, the line properties and the amount of load or generation that is present at each individual bus.

## 6. Chapter 6: Conclusions and future work

### 6.1. Conclusions

The literature review of PMU placement methods identified integer linear programming (ILP) as the most versatile algorithm that gave the lowest minimum number of PMUs needed for full observability of the IEEE test bus systems. The versatility of integer linear programming is due to the fact that the underlying concepts can be easily understood and modeled using Matlab. The ILP method developed in this work achieves the optimal minimum number of PMUs to be placed for full system observability for the IEEE 14, 30 and 57 bus systems for the base cases and cases considering zero-injection buses. The optimal number of phasor measurement units needed for the IEEE 14, 30 and 57 bus systems considering zero-injection buses are 3, 7 and 11 respectively. The method is easily adapted and has the ability to optimally place phasor measurement units in a test system to provide a utility with security of continued monitoring in the event of a measure device failure or a loss of line.

PMUs are to be utilised extensively by South Africa's national utility as a backbone device for improving operation, monitoring and control of the power system. The role of PMUs, the incorporating of phasor measurement data as well as the effects that their phasor data have on the accuracy of state estimation was studied in this work. For these reasons a conventional state estimator was modeled and tested on the IEEE 14, 30 and 57 bus systems and the converged solution was assessed in terms of the accuracy criteria of complex power flow and voltage errors. The initial system was considered to be fully observed by conventional measurements. A two stage hybrid state estimator was built using the conventional state estimator as a base, with the appendage of a linear state estimator as a post-processing step that incorporated phasor measurements of complex current and voltage phasors. The PMUs were phased in, one at a time, and the results are evidence to the fact that an increasing number of phasor measurement units in a power system decrease the total complex power flow and voltage errors effectively. The positions of placement were utilised from the optimal output of the ILP method. The appendage of the linear post-processing step added time to the estimation process, but this time was negligible as the accuracy of the state estimate was improved. However, the effects of zero-injection buses were not incorporated into the state estimator model. The inclusion of zero-injection buses into the state estimator model is to be incorporated in future work.

The goal of South Africa's national utility is to ultimately utilise a linear state estimator that incorporates only PMU measurements. Therefore the hybrid state estimator serves as a stepping stone between the conventional state estimator and the linear state estimator. This work designed a linear state estimator that used only phasor measurement data. The linear state estimator achieved the lowest estimated complex power flow and voltage errors for the IEEE 14, 30 and 57 bus systems. It can be concluded that as the system size grows, the linear state estimator benefits become more apparent due to the fact that the voltages and currents have a linear relation to the state vector and the process is non-iterative. Therefore the computational time will not be a burden for larger systems.

This work is unique in the fact that it analyses the individual effects of phasor measurement units to discover the optimal phasing placement schemes for devices for the IEEE 14, 30 and 57 bus systems based on the rate of improvement of the complex power flow and voltage errors. It is found that the

phasing scheme for best improving the power flow error is not necessarily the same as the scheme for best improving the voltage error. Although the accuracy of a predicted power flow is dependent on the accuracy of the voltage, the amount of current flowing through the branches and the impedance of every line are not the same. This is the reason pertaining to the fact that the phasing scheme with the lowest voltage error does not guarantee the lowest power flow error.

This work has provided a platform for assessing future phasor measurement unit positions based on their individual influence to the power flow and voltage error for linear state estimation. Although the error differences between devices are small, they all have a cumulative effect. Assessing a phasor measurement unit bus position helps to serve as a guide as to where to next place a measurement device that will have the most impact on state estimation accuracy.

## 6.2. Future work

### 6.2.1. Bettering the ILP placement algorithm

The ILP algorithm has been used extensively in the literature as a realistic placement method that incorporates many contingencies. A critical factor to be addressed is the limit on the communications channel number available to a phasor measurement unit, as well as the number of concurrent line measurements that can be made. It is suggested that the ILP algorithm is made more eloquent and that these factors be incorporated and utilised for practical placement.

### 6.2.2. Synergy of theory and implementation

To incorporate phasor measurement units into the South African power network requires extensive knowledge of the network topology as well as the deployment level of the measurement device, and its technical specifications such as sampling rate and defined angle accuracy. The theory is more applicable when it is aided by a practical scenario and vice versa. Therefore researchers need an indication as to the benefits that the utilities are expecting phasor measurement to offer, and the assessment criteria that local utilities use to benchmark the accuracy of the state estimator. An interesting study could be done in order to quantify the cost benefits that phasor measurement units are able to offer to a utility. Phasor measurement units are not just placed for improving state estimation or improving observability. There is an approach for choosing placement sites based on the weighting of numerous factors developed by utilities to optimize the benefits of phasor measurement unit placement. The generality of this approach is beyond the scope of this work, but the improvement of state estimation is an element that is considered as a weighted factor. Therefore anyone reading this thesis should be tempted to read [58] to for interest purposes and to broaden the context of this work.

### 6.2.3. Improvement of the state estimator

Currently this state estimator does not include the effects of zero-injection buses. Therefore in this work the number of phasor measurement units used for the linear state estimator will decrease. The inclusion of zero-injection buses will be done in the near future. In addition bad data detection and state estimator robustness with the increasing effects of phasor measurement number can be studied now that there is a base hybrid and linear state estimator in place. Additional accuracy criteria of the state estimator solution could be assessed in future work. In terms of the hybrid state estimator, there is a co-existence of conventionally metered data and PMU data. In order to incorporate the post-processing linear step the system was considered to be fully observed by conventional measurements. Practically this may not be the case. The presence of unmetered,

unobserved buses and lines and their effects on the estimator model workings and solution should be considered for future work.

#### 6.2.4. Theoretical system shortcomings

In the literature there are specific IEEE test bus cases that optimal placement problem algorithms are developed and tested on. These systems are assumed to be closed systems with known generation and loads at their end points. Practically, buses with generation and loads present outside the defined system may alter voltage and current phasors within the defined system. Although this does not have a dramatic effect on PMU placement in terms of maximising observability and redundancy levels, it will affect state estimation, especially when considering the move towards a linear state estimator. Therefore the interfacing of systems monitored by phasor measurement units and systems monitored by conventional measurements should be earmarked as an area of study.

University of Cape Town

## References

- [1] Horowitz S. H., Phadke A. G., Renz B. A., "The Future of Power Transmission", IEEE Power and Energy Magazine, vol. 8, Issue 2 , pp. 34-40, March-April 2010.
- [2] Van Der Merwe C., "Better visibility", Engineering News, vol. 30, no. 45, pp. 31, 19-25 November 2010.
- [3] S. Skok, I. Ivankovic, Z. Cerina, "Applications based on PMU technology for improved power system utilization", Power Engineering Society General Meeting, pp. 1-8, 2007.
- [4] Phadke, A. G., Thorp, J.S., and Adamiak, M.G., "A new measurement technique for tracking voltage phasors, local system frequency, and rate of change of frequency", IEEE Transactions on Power Apparatus and Systems, vol. 102, No. 5, pp 1025-1038, May 1983.
- [5] IEEE Standard for Synchrophasors for Power Systems, IEEE Standard C37.118-2005, 2005.
- [6] "Standard PMU definition", MidwestIS, Version 6.3, accessed 16 June 2011, Available online: <https://www.midwestiso.org/Library/Repository/Project%20Material/Project%20Documentation/Synchrophasor%20Project/Standard%20PMU%20Definition.pdf>
- [7] Phadke A.G., Thorp J.S., "Synchronized Phasor Measurements and Their Applications", Power Electronics and Power Systems Book Series, Springer, 2008.
- [8] Avila-Rosales R., Rice M.J., Giri J., AREVA T&D Inc., Beard L., TVA, Galvan F., Entergy, "Recent Experience with a Hybrid SCADA/PMU On-line State Estimator", IEEE Power and Energy General Meeting, pp. 1-8, July 2009.
- [9] Glover J.D., Sarma M.S., Overbye T.J., "Power System Analysis and Design (Fourth Edition)", Thomas Learning, 2008.
- [10] Novosel D., "Tutorial on PMU Technology and Applications", International Conference on Synchrophasor Measurement Applications, Brasil, 5 June 2006. Available online: [http://www.ceb5.cepel.br/arquivos/artigos\\_e\\_documentos/med\\_fasorial/Damir.pdf](http://www.ceb5.cepel.br/arquivos/artigos_e_documentos/med_fasorial/Damir.pdf)
- [11] Nuqui R.F., "State Estimation and Voltage Security Monitoring Using Synchronized Phasor Measurements", Ph.D. dissertation, Department of Electrical and Computer Engineering, Virginia Polytechnic Institute and State University, Blacksburg, VA, 2001.
- [12] "Power Systems Test Case Archive", Available online at: <http://www.ee.washington.edu/research/pstca/>
- [13] Marin F.J., Garcia-Lagos F., Joya G., and Sandoval F., "Genetic algorithms for optimal placement of phasor measurement units in electric networks", Electronics Letters, vol. 39, no. 19, pp. 1403-1405, September 2003.
- [14] Aminifar F., Lucas C., Khodaei A., and Fotuhi-Firuzabad M., "Optimal placement of phasor measurement units using immunity genetic algorithm", IEEE Transactions on Power Systems , vol. 24, no. 3, pp.1014-1020, July 2009.
- [15] Milosevic B. and Begovic M., "Nondominated sorting genetic algorithms for optimal phasor measurement placement", IEEE Transactions on Power Systems, vol. 18, no. 1, pp. 69-75, February 2003.
- [16] Nuqui R. F., Phadke A. G., "Hybrid Linear State Estimation Utilizing Synchronized Phasor Measurements", IEEE Lausanne PowerTech, pp. 1665-1669, 2007.
- [17] Baldwin T. L., Mili , M. B. Boisen M. B. Jr. and Adapa R., "Power system observability with minimal phasor measurement placement", IEEE Transactions on Power Systems ,vol. 8, no. 2, pp. 707-715, May 1993.
- [18] Peng J., Sun Y., and Wang H. F., "Optimal PMU placement for full network observability using Tabu search algorithm", International Journal of Electrical Power and Energy Systems, vol. 28, no. 4, pp. 223-231, May 2006.
- [19] Rakpenthai C., Premrudeepreechacharn S., Uatrongjit S., and Watson N. R., "An optimal PMU placement method against measurement loss and branch outage", IEEE Transactions on Power Delivery, vol. 22, no. 1, pp. 101-107, January 2007.
- [20] Kennedy J. and Eberhart E., "A discrete binary version of particle swarm algorithm", Proceedings of IEEE Computational Cybernetics and Simulation Conference, vol. 5, pp. 4104-

- 4109, 1997.
- [21] Hajain M., Ranjbar A. M., Amraee T., and Shirani A. R., "Optimal placement of phasor measurement units: Particle swarm optimization approach", *Proceedings of Intelligent Systems Applications to Power Systems*, pp. 1-6, November 2007.
  - [22] Su C. and Chen Z., "Optimal placement of phasor measurement units with new considerations", *Power and Energy Engineering Conference (APPEEC)*, pp. 1-4, April 2010.
  - [23] Peng C., Xu X., "A hybrid algorithm based on immune BPSO and N-1 principle for multi-objective optimization placement", *International Conference Electric Utility Deregulation and Restructuring and Power Technologies*, pp. 610-614, May 2008.
  - [24] Gao Y., Hu Z., He X., Dong L., "Optimal placement of PMUs in power systems based on improved PSO algorithm", *IEEE Conference on Industrial Electronics and Applications*, pp. 2464-2469, June 2008.
  - [25] Chakrabarti S., and Kyriakides E., "Optimal placement of phasor measurement units for power system observability", *IEEE Transactions on Power Systems*, vol. 23, no. 3, pp. 1433-1440, August 2008.
  - [26] TOMLAB Optimisation, "TOMLAB 7.7 CPLEX package", version available 8 June 2011, available online: <http://tomopt.com/tomlab/>
  - [27] Xu B. and Abur A., "Observability analysis and measurement placement for system with PMUs", *Proceedings of IEEE Power System Conference and Exposition.*, vol. 2, pp. 943-946, October 2004.
  - [28] Abur A., Magnago F.H., "Optimal Meter Placement for Maintaining Observability during Single Branch Outages", *IEEE Transactions on Power Systems*, vol. 14, Issue 4, pp. 1273-1278, 1999.
  - [29] Gou B., "Optimal placement of PMUs by integer linear programming", *IEEE Transactions on Power Systems*, vol. 23, no. 3, pp. 1525-1526, August 2008.
  - [30] Gou B., "Generalized integer linear programming formulation for optimal PMU placement", *IEEE Transactions on Power Systems*, vol. 23, no. 3, pp. 1099-1104, August 2008.
  - [31] Dua D., Dambhare S., Gajbhiye R. K., and Soman S. A., "Optimal multistage scheduling of PMU placement: An ILP approach", *IEEE Transactions on Power Delivery*, vol. 23, no. 4, pp. 1812-1820, October 2008.
  - [32] Aminifar F., Khodaei A., Fotuhi-Firuzabad M., and Shahidehpour M., "Contingency-constrained PMU placement in power networks", *IEEE Transactions on Power Systems*, vol. 25, no. 1, pp. 516-523, February 2010.
  - [33] Schweppe F.C. and Wildes J., "Power System Static-State Estimation, Part I: Exact Model", *IEEE Transactions on Power Apparatus and Systems*, Vol.PAS-89, pp. 120-125, January 1970.
  - [34] Schweppe F.C. and Rom D.B., "Power System Static-State Estimation, Part II: Approximate Model", *IEEE Transactions on Power Apparatus and Systems*, Vol.PAS-89, pp.125-130, January 1970.
  - [35] Schweppe F.C., "Power System Static-State Estimation, Part III: Implementation", *IEEE Transactions on Power Apparatus and Systems*, Vol.PAS-89, pp. 130-135, January 1970.
  - [36] Abur A., Exposito A.G., "Power System State Estimation: Theory and Implementation", *Power Engineering (Willis)*, March 2004.
  - [37] Phadke A. G., Thorp J. S., Karimi K. I., "State estimation with phasor measurements", *IEEE Transactions on Power Systems*, vol. 1, no. 1, pp. 233-241, February 1986.
  - [38] Dy Liacco T.E., "Real-Time Computer Control of Power Systems", *Proceedings of the IEEE*, vol. 62, no.7, pp.884-891, , July 1974.
  - [39] Zivanovi R., Cairns C., "Implementation of PMU technology in state estimation: An Overview", *IEEE AFRICON*, vol.2, pp. 1006 – 1011, 24-27 Sep 1996.
  - [40] MATPOWER, Available online: <http://www.pserc.cornell.edu/matpower/>
  - [41] Gonen G., "Electric Power Transmission System Engineering: Analysis and Design", John Wiley & Sons, 1988.

- [42] Baltensperger R., Loosli A., Sauvain H., Zima M., Andersson G., Nuqui R., "An implementation of two-stage hybrid state estimation with limited number of PMU", *Developments in Power System Protection*, pp. 1-5, 2010.
- [43] Ebrahimian R., Baldick R., "State Estimator Condition Number Analysis", *IEEE Transactions on Power Systems*, vol. 16, issue 2, 2001.
- [44] Eastern Interconnection Phasor Project, "Metrics for Determining the Impact of Phasor Measurements on Power System State Estimation", March 2006.
- [45] Phadke A.G., "Power system monitoring with state vector measurements", 2<sup>nd</sup> International Conference on Power System Monitoring and Control, Durham, U.K., June 1986.
- [46] Jiang W., Vittal V., Heydt G.T., "A distributed state estimator utilizing synchronized phasor measurements", *IEEE transactions on Power Systems*, vol. 22, no. 2, May 2007.
- [47] Cheng Y., Hu X., Gou B., "A new state estimation using synchronized phasor measurements", *IEEE Circuits and Systems*, pp. 2817-2820, 2008.
- [48] Qin X., Bi T., Yang Q., "Hybrid Non-linear State Estimation with Voltage Phasor Measurements", *IEEE Power Engineering Society General Meeting*, pp. 1-6, 2007.
- [49] Yang T., Sun H., Bose A., "Two-level PMU-based Linear State Estimator", *Power systems conference and exposition*, pp. 1-6, 2009.
- [50] Zhao H., "A new state estimation model utilizing PMU measurements", *International Conference on Power System Technology*, pp. 1-5, 2006.
- [51] Zhou M., Centeno V. A., Thorp J. S., Phadke A. G., "An Alternative for Including Phasor Measurements in State Estimators", *IEEE Transactions on Power Systems*, vol. 21, no. 4, pp. 1930-1937, November 2006.
- [52] Shiroie M., Hosseini S.H., "Observability and Estimation of Transformer Tap Setting with Minimal PMU Placement", *IEEE Power and Energy Society General Meeting*, pp. 1-4, July 2008.
- [53] Sangrody H.A., Ameli M.T., "The Effect of Phasor Measurement Units on the Accuracy of the Network Estimated Variables", *Conference on Developments in eSystems Engineering*, pp. 66-71, December 2009.
- [54] Jamuna K., Swarup K.S., "Two Stage State Estimator with Phasor Measurements", *International Conference on Power Systems*, pp. 1-5, 2009.
- [55] Valverde G., Charkrabarti S., Kyriakides E., Terzija V., "A Constrained Formulation for Hybrid State Estimation", *IEEE Transactions on Power Systems*, vol. 26, Issue 3, pp. 1102-1109, 2011.
- [56] Rakpenthai C., Premrudeepreechacharn S., Uatrongjit S., Watson N.R., "PMU-based Two Stages State Estimation for Power System with Nonlinear Devices", *International Power Engineering Conference*, pp. 153-158, 2007.
- [57] Rakpenthai C., Uatrongjit S., "Rectangular Coordinates State Estimation of Electrical Power System Using Singular Value Decomposition", *International Conference on Industrial Technology*, pp. 1-4, 2009.
- [58] Madani. V., Parashar M., Giri J., Durbha S., Rahmatian F., Adamiak M., Sheble G., "PMU Placement Considerations-A Roadmap for Optimal PMU Placement", *IEEE Power Systems Conference and Exposition (PSCE)*, pp. 1-7, March 2011.

## Bibliography

### *Conference papers:*

Yuill W., Kgokong R., Chowdhury S., Chowdhury S.P., "Application of Adaptive Neuro Fuzzy Inference System (ANFIS) based short term load forecasting in South African power networks", International Universities Power Engineering Conference, pp. 1-5, August 2010.

Yuill W., Kgokong R., Chowdhury S., Chowdhury S.P., "Management of short term load forecasting in South African power networks", International Conference on Power System Technology, pp. 1-8, October 2010.

### *Magazine articles:*

Yuill. W., Coppez G., Chowdhury S.P., Chowdhury S., "Green Effect of Clean Energy in minimising Global Warming", SAIEE WattNow magazine, pp.12-17, October 2010.

University of Cape Town

## Appendix A

### A.1) IEEE 14 bus system

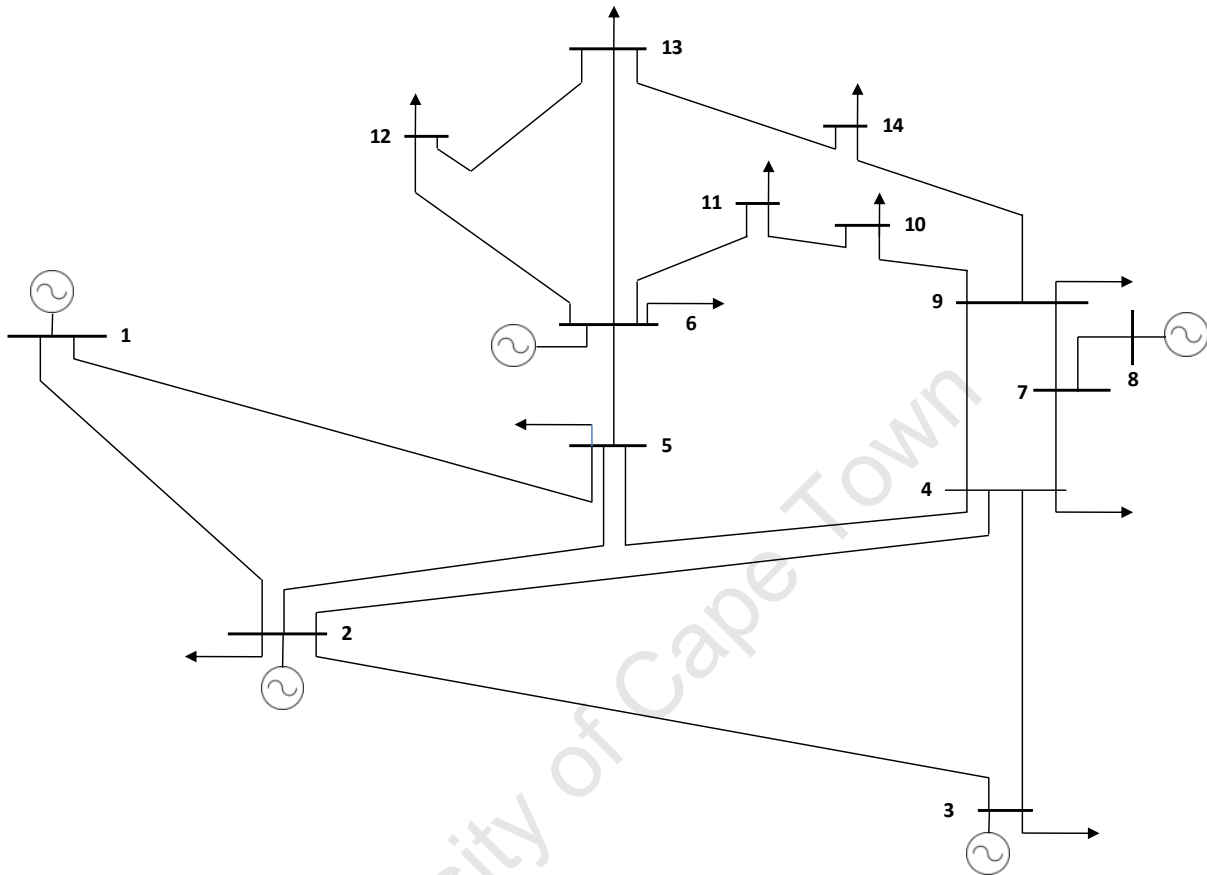


Figure A-1: Line diagram of IEEE 14-bus system

Table A-1: IEEE 14-bus system bus data

Bus	Voltage (p.u.)	Angle (degrees)	Load		Generation	
			Real (MW)	Reactive (Mvar)	Real (MW)	Reactive (Mvar)
1	1.0600	0.0000	0.0000	0.0000	232.3933	-16.5493
2	1.0450	-4.9800	21.7000	12.7000	40.0000	43.5571
3	1.0100	-12.7200	94.2000	19.0000	0.0000	25.0753
4	1.0190	-10.3300	47.8000	-3.9000	0.0000	0.0000
5	1.0200	-8.7800	7.6000	1.6000	0.0000	0.0000
6	1.0700	-14.2200	11.2000	7.5000	0.0000	12.7309
7	1.0620	-13.3700	0.0000	0.0000	0.0000	0.0000
8	1.0900	-13.3600	0.0000	0.0000	0.0000	17.6235
9	1.0560	-14.9400	29.5000	16.6000	0.0000	19.0000
10	1.0510	-15.1000	9.0000	5.8000	0.0000	0.0000
11	1.0570	-14.7900	3.5000	1.8000	0.0000	0.0000

12	1.0550	-15.0700	6.1000	1.6000	0.0000	0.0000
13	1.0500	-15.1600	13.5000	5.8000	0.0000	0.0000
14	1.0360	-16.0400	14.9000	5.0000	0.0000	0.0000

Table A-2: IEEE 14-bus system branch data

Bus direction		Line properties (p.u.)				Power from		Power to	
Bus from	Bus to	R	X	B	Tap	Real (MW)	Reactive (MVar)	Real (MW)	Reactive (MVar)
1	2	0.0194	0.0592	0.0528	1	156.8829	-20.4043	-152.5853	27.6762
1	5	0.0540	0.2230	0.0492	1	75.5104	3.8550	-72.7475	2.2294
2	3	0.0470	0.1980	0.0438	1	73.2376	3.5602	-70.9143	1.6022
2	4	0.0581	0.1763	0.0340	1	56.1315	-1.5504	-54.4548	3.0207
2	5	0.0570	0.1739	0.0346	1	41.5162	1.1710	-40.6125	-2.0990
3	4	0.0670	0.1710	0.0128	1	-23.2857	4.4731	23.6591	-4.8357
4	5	0.0134	0.0421	0.0000	1	-61.1582	15.8236	61.6727	-14.2010
4	7	0.0000	0.2091	0.0000	0.978	28.0742	-9.6811	-28.0742	11.3843
4	9	0.0000	0.5562	0.0000	0.969	16.0798	-0.4276	-16.0798	1.7323
5	6	0.0000	0.2520	0.0000	0.932	44.0873	12.4707	-44.0873	-8.0495
6	11	0.0950	0.1989	0.0000	1	7.3533	3.5605	-7.2979	-3.4445
6	12	0.1229	0.2558	0.0000	1	7.7861	2.5034	-7.7143	-2.3540
6	13	0.0662	0.1303	0.0000	1	17.7480	7.2166	-17.5359	-6.7989
7	8	0.0000	0.1762	0.0000	1	0.0000	-17.1630	0.0000	17.6235
7	9	0.0000	0.1100	0.0000	1	28.0742	5.7787	-28.0742	-4.9766
9	10	0.0318	0.0845	0.0000	1	5.2276	4.2191	-5.2147	-4.1849
9	14	0.1271	0.2704	0.0000	1	9.4264	3.6100	-9.3102	-3.3629
10	11	0.0821	0.1921	0.0000	1	-3.7853	-1.6151	3.7979	1.6445
12	13	0.2209	0.1999	0.0000	1	1.6143	0.7540	-1.6080	-0.7483
13	14	0.1709	0.3480	0.0000	1	5.6439	1.7472	-5.5898	-1.6371

## A.2) IEEE 30 bus system

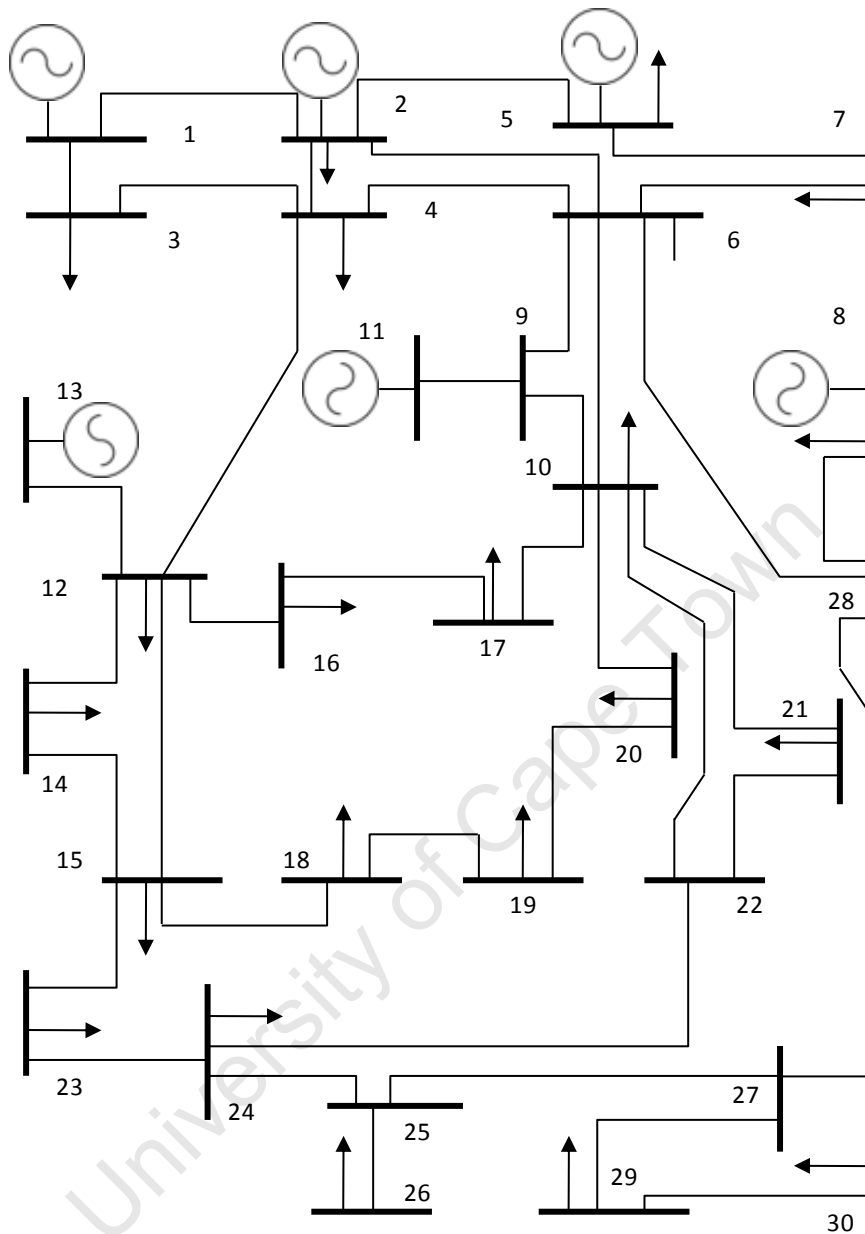


Figure A-2: Line diagram of IEEE 30-bus system

Table A-3: IEEE 30-bus system bus data

Bus	Voltage (p.u.)	Angle (degrees)	Load		Generation	
			Real (MW)	Reactive (Mvar)	Real (MW)	Reactive (Mvar)
1	1.0600	0.0000	0.0000	0.0000	260.9569	-20.4179
2	1.0430	-5.4800	21.7000	12.7000	40.0000	56.0695
3	1.0210	-7.9600	2.4000	1.2000	0.0000	0.0000
4	1.0120	-9.6200	7.6000	1.6000	0.0000	0.0000
5	1.0100	-14.3700	94.2000	19.0000	0.0000	35.6588

6	1.0100	-11.3400	0.0000	0.0000	0.0000	0.0000
7	1.0020	-13.1200	22.8000	10.9000	0.0000	0.0000
8	1.0100	-12.1000	30.0000	30.0000	0.0000	36.1113
9	1.0510	-14.3800	0.0000	0.0000	0.0000	0.0000
10	1.0450	-15.9700	5.8000	2.0000	0.0000	0.0000
11	1.0820	-14.3900	0.0000	0.0000	0.0000	16.0574
12	1.0570	-15.2400	11.2000	7.5000	0.0000	0.0000
13	1.0710	-15.2400	0.0000	0.0000	0.0000	10.4507
14	1.0420	-16.1300	6.2000	1.6000	0.0000	0.0000
15	1.0380	-16.2200	8.2000	2.5000	0.0000	0.0000
16	1.0450	-15.8300	3.5000	1.8000	0.0000	0.0000
17	1.0400	-16.1400	9.0000	5.8000	0.0000	0.0000
18	1.0280	-16.8200	3.2000	0.9000	0.0000	0.0000
19	1.0260	-17.0000	9.5000	3.4000	0.0000	0.0000
20	1.0300	-16.8000	2.2000	0.7000	0.0000	0.0000
21	1.0330	-16.4200	17.5000	11.2000	0.0000	0.0000
22	1.0330	-16.4100	0.0000	0.0000	0.0000	0.0000
23	1.0270	-16.6100	3.2000	1.6000	0.0000	0.0000
24	1.0210	-16.7800	8.7000	6.7000	0.0000	0.0000
25	1.0170	-16.3500	0.0000	0.0000	0.0000	0.0000
26	1.0000	-16.7700	3.5000	2.3000	0.0000	0.0000
27	1.0230	-15.8200	0.0000	0.0000	0.0000	0.0000
28	1.0070	-11.9700	0.0000	0.0000	0.0000	0.0000
29	1.0030	-17.0600	2.4000	0.9000	0.0000	0.0000
30	0.9920	-17.9400	10.6000	1.9000	0.0000	0.0000

Table A-4: IEEE 30-bus system branch data

Bus direction		Line properties (p.u.)				Power from		Power to	
Bus from	Bus to	R	X	B	Tap	Real (MW)	Reactive (MVar)	Real (MW)	Reactive (MVar)
1	2	0.0192	0.0575	0.0528	1	173.3071	-24.7028	-168.0940	34.4658
1	3	0.0452	0.1652	0.0408	1	87.6498	4.2849	-84.5419	2.6546
2	4	0.0570	0.1737	0.0368	1	43.6527	4.7496	-42.6342	-5.5408
2	5	0.0472	0.1983	0.0418	1	82.3613	2.7817	-79.4183	5.1685
2	6	0.0581	0.1763	0.0374	1	60.3800	1.3724	-58.4341	0.5802
3	4	0.0132	0.0379	0.0084	1	82.1419	-3.8546	-81.2863	5.4427
4	6	0.0119	0.0414	0.0090	1	72.1273	-15.9120	-71.4955	17.1894
4	12	0.0000	0.2560	0.0000	0.932	44.1932	14.4100	-44.1932	-9.7214
5	7	0.0460	0.1160	0.0204	1	-14.7817	11.4903	14.9510	-13.1291
6	7	0.0267	0.0820	0.0170	1	38.1321	-2.7814	-37.7510	2.2291
6	8	0.0120	0.0420	0.0090	1	29.5631	-7.1965	-29.4550	6.6559
6	9	0.0000	0.2080	0.0000	0.978	27.7212	-8.0930	-27.7212	9.7174
6	10	0.0000	0.5560	0.0000	0.969	15.8397	0.1865	-15.8397	1.0961
6	28	0.0169	0.0599	0.0130	1	18.6735	0.1147	-18.6157	-1.2330

8	28	0.0636	0.2000	0.0428	1	-0.5450	-0.5446	0.5468	-3.8030
9	11	0.0000	0.2080	0.0000	1	0.0000	-15.5993	0.0000	16.0574
9	10	0.0000	0.1100	0.0000	1	27.7212	5.8819	-27.7212	-5.0824
10	20	0.0936	0.2090	0.0000	1	9.0254	3.7096	-8.9438	-3.5275
10	17	0.0324	0.0845	0.0000	1	5.3317	4.4294	-5.3174	-4.3923
10	21	0.0348	0.0749	0.0000	1	15.7856	10.0109	-15.6743	-9.7714
10	22	0.0727	0.1499	0.0000	1	7.6183	4.6000	-7.5656	-4.4914
12	13	0.0000	0.1400	0.0000	1	0.0000	-10.3174	0.0000	10.4507
12	14	0.1231	0.2559	0.0000	1	7.8575	2.4003	-7.7832	-2.2458
12	15	0.0662	0.1304	0.0000	1	17.8918	6.7899	-17.6749	-6.3628
12	16	0.0945	0.1987	0.0000	1	7.2439	3.3486	-7.1901	-3.2354
14	15	0.2210	0.1997	0.0000	1	1.5832	0.6458	-1.5772	-0.6404
15	18	0.1073	0.2185	0.0000	1	6.0168	1.5953	-5.9782	-1.5167
15	23	0.1000	0.2020	0.0000	1	5.0353	2.9079	-5.0039	-2.8445
16	17	0.0524	0.1923	0.0000	1	3.6901	1.4354	-3.6826	-1.4077
18	19	0.0639	0.1292	0.0000	1	2.7782	0.6167	-2.7733	-0.6068
19	20	0.0340	0.0680	0.0000	1	-6.7267	-2.7932	6.7438	2.8275
21	22	0.0116	0.0236	0.0000	1	-1.8257	-1.4286	1.8263	1.4298
22	24	0.1150	0.1790	0.0000	1	5.7393	3.0616	-5.6938	-2.9907
23	24	0.1320	0.2700	0.0000	1	1.8039	1.2445	-1.7979	-1.2322
24	25	0.1885	0.3292	0.0000	1	-1.2083	2.0128	1.2182	-1.9954
25	26	0.2544	0.3800	0.0000	1	3.5446	2.3667	-3.5000	-2.3000
25	27	0.1093	0.2087	0.0000	1	-4.7628	-0.3712	4.7869	0.4172
27	29	0.2198	0.4153	0.0000	1	6.1899	1.6688	-6.1037	-1.5059
27	30	0.3202	0.6027	0.0000	1	7.0920	1.6628	-6.9298	-1.3575
28	27	0.0000	0.3960	0.0000	0.968	18.0689	5.0360	-18.0689	-3.7488
29	30	0.2399	0.4533	0.0000	1	3.7037	0.6059	-3.6702	-0.5425

### A.3) IEEE 57 bus system

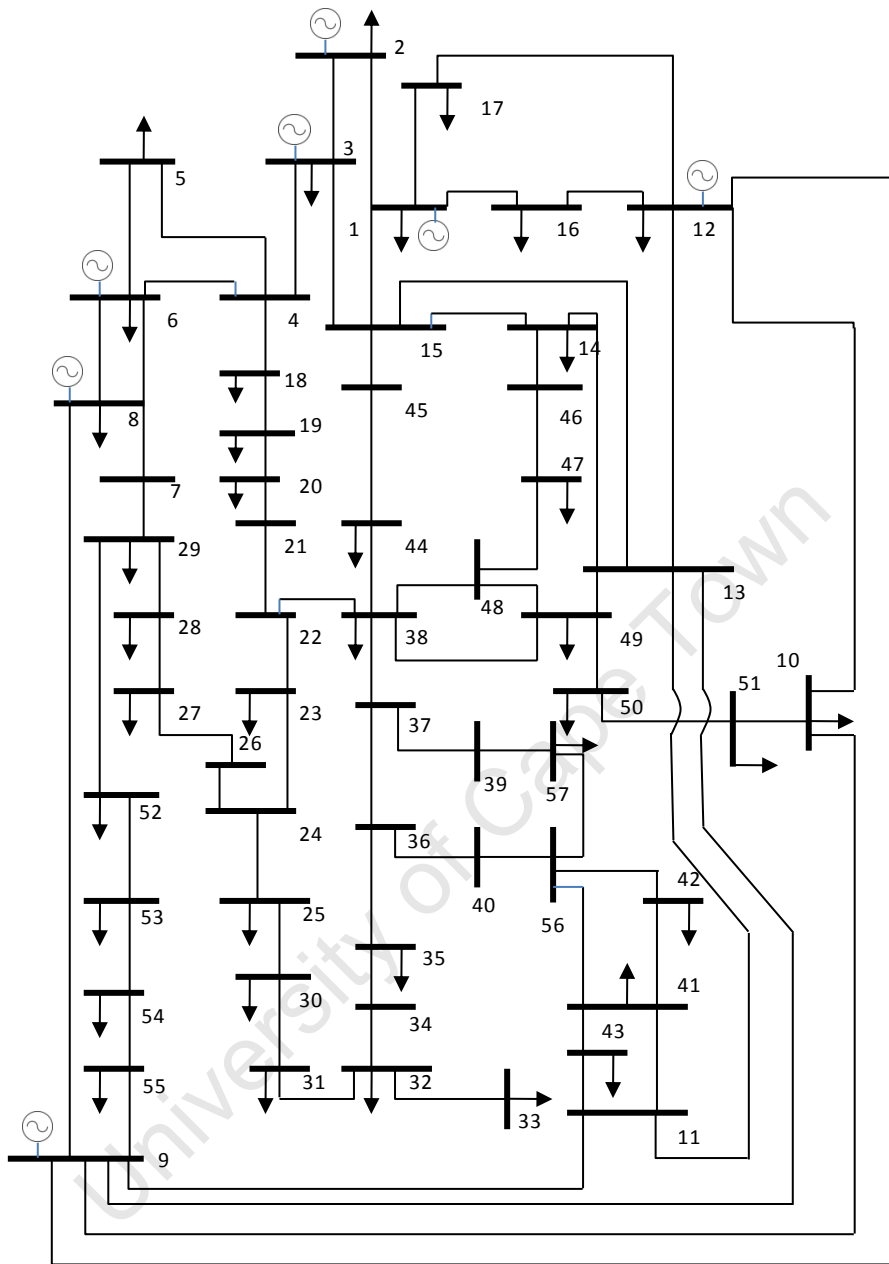


Figure A-3: Line diagram of IEEE 57 bus system

Table A-5: IEEE 57-bus system bus data

Bus	Voltage (p.u.)	Angle (degrees)	Load		Generation	
			Real (MW)	Reactive (Mvar)	Real (MW)	Reactive (Mvar)
1	1.0400	0.0000	55.0000	17.0000	478.9759	129.4138
2	1.0100	-1.1783	3.0000	88.0000	0.0000	-0.7903
3	0.9850	-5.9466	41.0000	21.0000	40.0000	1.1308
4	0.9802	-7.2265	0.0000	0.0000	0.0000	0.0000

5	0.9763	-8.4764	13.0000	4.0000	0.0000	0.0000
6	0.9800	-8.6236	75.0000	2.0000	0.0000	1.6772
7	0.9841	-7.5747	0.0000	0.0000	0.0000	0.0000
8	1.0050	-4.4741	150.0000	22.0000	450.0000	62.2241
9	0.9800	-9.6103	121.0000	26.0000	0.0000	3.0985
10	0.9861	-11.4980	5.0000	2.0000	0.0000	0.0000
11	0.9736	-10.2369	0.0000	0.0000	0.0000	0.0000
12	1.0150	-10.5102	377.0000	24.0000	310.0000	129.4634
13	0.9785	-9.8490	18.0000	2.3000	0.0000	0.0000
14	0.9696	-9.4010	10.5000	5.3000	0.0000	0.0000
15	0.9876	-7.2106	22.0000	5.0000	0.0000	0.0000
16	1.0133	-8.8868	43.0000	3.0000	0.0000	0.0000
17	1.0174	-5.4104	42.0000	8.0000	0.0000	0.0000
18	0.9858	-16.3471	27.2000	9.8000	0.0000	10.0000
19	0.9656	-16.2930	3.3000	0.6000	0.0000	0.0000
20	0.9654	-15.4934	2.3000	1.0000	0.0000	0.0000
21	1.0044	-13.3893	0.0000	0.0000	0.0000	0.0000
22	1.0074	-13.0889	0.0000	0.0000	0.0000	0.0000
23	1.0060	-13.1355	6.3000	2.1000	0.0000	0.0000
24	0.9980	-13.1680	0.0000	0.0000	0.0000	0.0000
25	0.9567	-21.6697	6.3000	3.2000	0.0000	5.9000
26	0.9578	-12.8617	0.0000	0.0000	0.0000	0.0000
27	0.9810	-11.4502	9.3000	0.5000	0.0000	0.0000
28	0.9964	-10.4384	4.6000	2.3000	0.0000	0.0000
29	1.0100	-9.7414	17.0000	2.6000	0.0000	0.0000
30	0.9389	-21.9956	3.6000	1.8000	0.0000	0.0000
31	0.9176	-22.0504	5.8000	2.9000	0.0000	0.0000
32	0.9414	-20.1828	1.6000	0.8000	0.0000	0.0000
33	0.9390	-20.2232	3.8000	1.9000	0.0000	0.0000
34	0.9526	-14.6066	0.0000	0.0000	0.0000	0.0000
35	0.9610	-14.2780	6.0000	3.0000	0.0000	0.0000
36	0.9717	-13.9497	0.0000	0.0000	0.0000	0.0000
37	0.9814	-13.7253	0.0000	0.0000	0.0000	0.0000
38	1.0108	-12.9234	14.0000	7.0000	0.0000	0.0000
39	0.9794	-13.7685	0.0000	0.0000	0.0000	0.0000
40	0.9688	-13.9697	0.0000	0.0000	0.0000	0.0000
41	0.9951	-14.1956	6.3000	3.0000	0.0000	0.0000
42	0.9646	-15.6783	7.1000	4.4000	0.0000	0.0000
43	1.0090	-11.4177	2.0000	1.0000	0.0000	0.0000
44	1.0152	-12.0107	12.0000	1.8000	0.0000	0.0000
45	1.0353	-9.3535	0.0000	0.0000	0.0000	0.0000
46	1.0590	-11.2119	0.0000	0.0000	0.0000	0.0000
47	1.0321	-12.6491	29.7000	11.6000	0.0000	0.0000
48	1.0259	-12.7614	0.0000	0.0000	0.0000	0.0000

49	1.0353	-13.0626	18.0000	8.5000	0.0000	0.0000
50	1.0227	-13.5160	21.0000	10.5000	0.0000	0.0000
51	1.0521	-12.5954	18.0000	5.3000	0.0000	0.0000
52	0.9802	-11.4806	4.9000	2.2000	0.0000	0.0000
53	0.9708	-12.2428	20.0000	10.0000	0.0000	6.3000
54	0.9962	-11.7164	4.1000	1.4000	0.0000	0.0000
55	1.0307	-10.8226	6.8000	3.4000	0.0000	0.0000
56	0.9657	-16.2357	7.6000	2.2000	0.0000	0.0000
57	0.9618	-16.7747	6.7000	2.0000	0.0000	0.0000

Table A-6: IEEE 57-bus system branch data

Bus direction		Line properties (p.u.)				Power from		Power to	
Bus from	Bus to	R	X	B	Tap	Real (MW)	Reactive (MVar)	Real (MW)	Reactive (MVar)
1	2	0.0083	0.0280	0.1290	1	101.4902	75.1609	-100.1821	-84.3039
2	3	0.0298	0.0850	0.0818	1	97.1821	-4.4864	-94.4231	4.2156
3	4	0.0112	0.0366	0.0380	1	57.6419	-6.0363	-57.2563	3.6272
4	5	0.0625	0.1320	0.0258	1	14.1150	-4.8318	-13.9770	2.6540
4	6	0.0430	0.1480	0.0348	1	14.6897	-5.5825	-14.5863	2.5953
6	7	0.0200	0.1020	0.0276	1	-17.3867	-1.7269	17.4497	-0.6138
6	8	0.0339	0.1730	0.0470	1	-42.0620	-6.6842	42.6934	5.2760
8	9	0.0099	0.0505	0.0548	1	179.0058	19.7237	-175.8154	-8.8486
9	10	0.0369	0.1679	0.0440	1	17.4014	-9.2093	-17.2657	5.5744
9	11	0.0258	0.0848	0.0218	1	13.3440	2.3647	-13.2930	-4.2773
9	12	0.0648	0.2950	0.0772	1	2.6243	-15.8691	-2.5198	8.6608
9	13	0.0481	0.1580	0.0406	1	2.5778	-1.7894	-2.5744	-2.0929
13	14	0.0132	0.0434	0.0110	1	-10.0552	22.6178	10.1430	-23.3728
13	15	0.0269	0.0869	0.0230	1	-49.2965	5.0213	49.9898	-5.0044
1	15	0.0178	0.0910	0.0988	1	149.4090	34.1907	-145.4780	-24.2561
1	16	0.0454	0.2060	0.0546	1	79.4905	-0.8720	-76.8364	7.1587
1	17	0.0238	0.1080	0.0286	1	93.5863	3.9342	-91.6524	1.8143
3	15	0.0162	0.0530	0.0544	1	35.7812	-18.0484	-35.5278	13.5853
4	18	0.0000	0.5550	0.0000	0.97	28.4516	6.7870	-28.4516	-2.1374
5	6	0.0302	0.0641	0.0124	1	0.9770	-6.6540	-0.9651	5.4930
7	8	0.0139	0.0712	0.0194	1	-77.4209	-12.6365	78.3008	15.2244
10	12	0.0277	0.1262	0.0328	1	-17.7430	-20.1332	17.9306	17.7033
11	13	0.0223	0.0732	0.0188	1	-9.8684	-4.3611	9.8942	2.6546
12	13	0.0178	0.0580	0.0604	1	-0.1032	60.9358	0.8120	-64.6291
12	16	0.0180	0.0813	0.0216	1	-33.6213	8.9083	33.8364	-10.1587
12	17	0.0397	0.1790	0.0476	1	-48.6862	9.2553	49.6524	-9.8143
14	15	0.0171	0.0547	0.0148	1	-69.6966	-9.6084	70.5946	11.0634
18	19	0.4610	0.6850	0.0000	1	1.2516	2.0545	-1.2242	-2.0137
19	20	0.2830	0.4340	0.0000	1	-2.0758	1.4137	2.0950	-1.3844
21	20	0.0000	0.7767	0.0000	1.043	4.3950	-0.2222	-4.3950	0.3844

21	22	0.0736	0.1170	0.0000	1	-4.3950	0.2222	4.4091	-0.1997
22	23	0.0099	0.0152	0.0000	1	7.9020	3.8024	-7.8945	-3.7909
23	24	0.1660	0.2560	0.0084	1	1.5945	1.6909	-1.5830	-2.5165
24	25	0.0000	1.1820	0.0000	1	11.9422	4.3782	-11.9422	-2.4584
24	26	0.0000	0.0473	0.0000	1.043	-10.3592	-1.8617	10.3592	1.9189
26	27	0.1650	0.2540	0.0000	1	-10.3592	-1.9189	10.5588	2.2263
27	28	0.0618	0.0954	0.0000	1	-19.8588	-2.7263	20.1168	3.1245
28	29	0.0418	0.0587	0.0000	1	-24.7168	-5.4245	24.9864	5.8032
7	29	0.0000	0.0648	0.0000	0.967	59.9713	13.2503	-59.9713	-10.8903
25	30	0.1350	0.2020	0.0000	1	5.6422	4.6583	-5.5632	-4.5402
30	31	0.3260	0.4970	0.0000	1	1.9632	2.7402	-1.9212	-2.6761
31	32	0.5070	0.7550	0.0000	1	-3.8788	-0.2239	3.9697	0.3593
32	33	0.0392	0.0360	0.0000	1	3.8080	1.9074	-3.8000	-1.9000
34	32	0.0000	0.9530	0.0000	0.975	9.3777	4.1135	-9.3777	-3.0666
34	35	0.0520	0.0780	0.0032	1	-9.3777	-4.1135	9.4371	3.9097
35	36	0.0430	0.0537	0.0016	1	-15.4371	-6.9097	15.5699	6.9260
36	37	0.0290	0.0366	0.0000	1	-18.8095	-10.8614	18.9544	11.0442
37	38	0.0651	0.1009	0.0020	1	-22.6803	-13.9224	23.1572	14.4630
37	39	0.0239	0.0379	0.0000	1	3.7260	2.8782	-3.7205	-2.8695
36	40	0.0300	0.0466	0.0000	1	3.2396	3.9354	-3.2314	-3.9225
22	38	0.0192	0.0295	0.0000	1	-12.3111	-3.6026	12.3423	3.6505
11	41	0.0000	0.7490	0.0000	0.955	9.3508	3.6390	-9.3508	-2.9134
41	42	0.2070	0.3520	0.0000	1	9.0496	3.3902	-8.8544	-3.0582
41	43	0.0000	0.4120	0.0000	1	-11.8107	-3.0604	11.8107	3.6798
38	44	0.0289	0.0585	0.0020	1	-25.3708	5.0984	25.5605	-4.9196
15	45	0.0000	0.1042	0.0000	0.955	38.4215	-0.3881	-38.4215	1.8265
14	46	0.0000	0.0735	0.0000	0.9	49.0536	27.6812	-49.0536	-25.6722
46	47	0.0230	0.0680	0.0032	1	49.0536	25.6722	-48.4230	-24.1577
47	48	0.0182	0.0233	0.0000	1	18.7230	12.5577	-18.6362	-12.4466
48	49	0.0834	0.1290	0.0048	1	-0.3384	-7.4701	0.3798	7.0242
49	50	0.0801	0.1280	0.0000	1	9.3054	4.4109	-9.2262	-4.2843
50	51	0.1386	0.2200	0.0000	1	-11.7738	-6.2157	12.0087	6.5886
10	51	0.0000	0.0712	0.0000	0.93	30.0087	12.5587	-30.0087	-11.8886
13	49	0.0000	0.1910	0.0000	0.895	33.2200	34.1283	-33.2200	-30.5036
29	52	0.1442	0.1870	0.0000	1	17.9848	2.4872	-17.5189	-1.8829
52	53	0.0762	0.0984	0.0000	1	12.6189	-0.3171	-12.4925	0.4803
53	54	0.1878	0.2320	0.0000	1	-7.5075	-4.5433	7.6610	4.7329
54	55	0.1732	0.2265	0.0000	1	-11.7610	-6.1329	12.0680	6.5344
11	43	0.0000	0.1530	0.0000	0.958	13.8107	4.9994	-13.8107	-4.6798
44	45	0.0624	0.1242	0.0040	1	-37.5605	3.1196	38.4215	-1.8265
40	56	0.0000	1.1950	0.0000	0.958	3.2314	3.9225	-3.2314	-3.6208
56	41	0.5530	0.5490	0.0000	1	-5.6223	0.6045	5.8119	-0.4163
56	42	0.2125	0.3540	0.0000	1	-1.7432	1.3603	1.7544	-1.3418
39	57	0.0000	1.3550	0.0000	0.98	3.7205	2.8695	-3.7205	-2.5700

57	56	0.1740	0.2600	0.0000	1	-2.9795	0.5700	2.9968	-0.5441
38	49	0.1150	0.1770	0.0030	1	-5.3784	-10.6417	5.5348	10.5684
38	48	0.0312	0.0482	0.0000	1	-18.7503	-19.5701	18.9746	19.9166
9	55	0.0000	0.1205	0.0000	0.94	18.8680	10.4501	-18.8680	-9.9344

University of Cape Town